Eur. Phys. J. C 55, 199–236 (2008)
DOI 10.1140/epjc/s10052-008-0586-6

THE EUROPEAN PHYSICAL JOURNAL C

Regular Article – Theoretical Physics

The dipion mass spectrum in e^+e^- annihilation and τ decay: a dynamical (ρ, ω, ϕ) mixing approach

M. Benayoun[1,a], P. David[1], L. DelBuono[1], O. Leitner[1,2], H.B. O'Connell[3]

[1] LPNHE Paris VI/VII, IN2P3/CNRS, 4 place Jussieu, Tour 33 RdC, 75252 Paris Cedex 05, France
[2] Laboratori Nazionali di Frascati, INFN, 00044 Frascati (Roma), Italy
[3] Fermilab, Batavia IL 60510, USA

Received: 3 December 2007 / Revised version: 21 February 2008 /
Published online: 25 April 2008 –

Abstract. We readdress the problem of finding a simultaneous description of the pion form factor data in e^+e^- annihilations and in τ decays. For this purpose, we work in the framework of the hidden local symmetry Lagrangian and modify the vector meson mass term by including the pion and kaon loop contributions. This leads us to define the physical ρ, ω and ϕ fields as linear combinations of their ideal partners, with coefficients being meromorphic functions of s, the square of the four-momentum flowing into the vector meson lines. This allows us to define a dynamical, i.e. s-dependent, vector meson mixing scheme. The model is overconstrained by extending the framework in order to include the description of all meson radiative ($VP\gamma$ and $P\gamma\gamma$ couplings) and leptonic (Ve^+e^- couplings) decays and also the isospin breaking ($\omega/\phi \to \pi^+\pi^-$) decay modes. The model provides a simultaneous, consistent and good description of the e^+e^- and τ dipion spectra. The expression for the pion form factor in the latter case is derived from those in the former case by switching off the isospin breaking effects specific to e^+e^- and switching on those for τ decays. Besides, the model also provides a good account of all decay modes of the form $VP\gamma$ and $P\gamma\gamma$ as well as the isospin breaking decay modes. It leads us to propose new reference values for the $\rho^0 \to e^+e^-$ and $\omega \to \pi^+\pi^-$ partial widths, which are part of our description of the pion form factor. Other topics ($\phi \to K\overline{K}$, the ρ meson mass and width parameters) are briefly discussed. As the e^+e^- data are found to be perfectly consistent with τ data up to identified isospin breaking effects, one finds no reason to cast any doubt on them and, therefore, on the theoretical estimate of the muon anomalous moment a_μ derived from them. Therefore, our work turns out to confirm the relevance of the reported 3.3σ discrepancy between this theoretical estimate of a_μ and its direct BNL measurement.

1 Introduction

In order to study the phenomenology of light flavor mesons below 1 GeV, like partial decay widths or meson form factors, one needs a framework that includes in a well defined manner the lowest mass nonets of pseudoscalar (P) and vector (V) mesons. Such a framework is well represented by the hidden local symmetry (HLS) model [1, 2]. In this approach, vector mesons are gauge bosons of a spontaneously broken hidden local symmetry that generates their Higgs–Kibble (HK) masses. Besides the non-anomalous sector, this model has an anomalous sector, hereafter called FKTUY Lagrangian [3], which aims at describing the couplings of the form VVP, $VP\gamma$ $P\gamma\gamma$, $VPPP$ for the light flavor mesons.

In its original form, the full (non-anomalous and anomalous) bare HLS Lagrangian obeys the U(3) symmetry, as it possesses both nonet symmetry and SU(3) flavor symmetry. As such, the HLS model covers a limited phenomenological scope. In order to broaden this scope, especially in order to account for $VP\gamma$ and $P\gamma\gamma$ couplings as derived from measured partial widths, the original HLS model should be supplemented with symmetry breaking mechanisms.

Several SU(3) symmetry breaking schemes have been proposed [4–6] following the original idea of Bando, Kugo and Yamawaki (BKY) [7]. It has been shown [8, 9] that the most successful variant is the so-called "new scheme" of [6] briefly recalled in Appendix C. However, breaking only the SU(3) symmetry is insufficient [8, 9] for reaching a satisfactory description of the data on $VP\gamma$ and $P\gamma\gamma$ couplings, which requires one to also break nonet symmetry. This was first performed in an ad hoc manner in [8] with the aim of recovering the radiative decay couplings of O'Donnell [10], which is the most general set fulfilling only SU(3) symmetry; therefore, the model developed in [8] was indeed in agreement with general group theoretical considerations with additionally a mechanism smoothly breaking SU(3) flavor symmetry.

Slightly later, it was shown [9, 11] that an appropriate mechanism for nonet symmetry breaking can be produced

[a] e-mail: benayoun@in2p3.fr

by adding determinant terms [12] to the HLS Lagrangian; the result was shown to meet all properties of extended chiral perturbation theory (EChPT) [13–15] at leading order in the breaking parameters. In addition, it was also proved [11] that the nonet symmetry breaking mechanism proposed in [8] was indeed an appropriate approximation of the (rigorous) mechanism derived from adding the determinant terms to the bare HLS Lagrangian.

However, breaking SU(3) and nonet symmetries is still not enough for fully describing the whole set of radiative decays $VP\gamma$; indeed, a process like $\phi \to \pi^0\gamma$ requires including a ω–ϕ mixing scheme; additionally, any global fit of all available $VP\gamma$ transitions cannot be successful without introducing such a mixing. Traditionally, the ω–ϕ mixing is described [8,9] by rotating the fields ω_I and ϕ_I, which are the entries of the bare vector field matrix, generally called ideal fields. An angle involving the mixing of the η and η' mesons is also required, which has been shown [11] to vanish in the limit of exact SU(3) symmetry of the HLS Lagrangian.

A brief account of the HLS model in its anomalous (FKTUY) and non-anomalous sectors is given in Appendices A and B, mostly focused on the subject of this work. Appendix C gives a brief but complete description of the various symmetry breaking procedures and the field renormalization scheme, except for the SU(2) breaking mechanism, which is the main subject of this paper. Appendix D deals with some specific features of the Yang–Mills piece of the HLS Lagrangian that provides the kinetic energy part of the vector meson fields and should also undergo SU(3) symmetry breaking.

These appendices illustrate that the model depends on very few free parameters as is clear from Appendix E, where they all appear. Among these free parameters, some are specific to our HLS based model, but some others are constrained. For instance, one of the two SU(3) breaking parameters is the ratio of the decay constants f_K/f_π and can be constrained by the corresponding measured value.

On the other hand, decay processes like $\omega/\phi \to \pi^+\pi^-$ can hardly be understood without some scheme for ρ^0–ω and ρ^0–ϕ mixings. Moreover, the decay behavior of ρ^0 and $\rho^\pm$ cannot differ at the coupling constant level. It so happens that the HLS model at one-loop order provides a mechanism that allows us to perform a full ρ^0–ω–ϕ mixing starting from the corresponding ideal (bare) fields. Within the non-anomalous HLS Lagrangian, the precise mechanism, kaon loop contributions, has already been described in [16]. However, we shall see that the (FKTUY) anomalous sector provides K^*K loops as additional mechanism and that another one ($K^*\overline{K}^*$ loops) is provided by the Yang–Mills piece.

Within the HLS model, as recalled below, $V_i \leftrightarrow V_j$ transitions among the ideal ρ^0_I, ω_I and ϕ_I fields are generated by loop effects; these transitions generally do not have a constant amplitude but rather depend on the squared four-momentum flowing through the V_i (and V_j) line(s). We show in Sect. 4 that the loops of the charged and neutral kaon, K^*K and $K^*\overline{K}^*$, enter through their sum in the $\omega_I \leftrightarrow \phi_I$ amplitude, while they enter through their difference in the $\rho^0_I \leftrightarrow \phi_I$ and $\rho^0_I \leftrightarrow \omega_I$ amplitudes. This also means that the ω–ϕ mixing proceeds from quantum effects rather than symmetry breaking effects, in contrast with the ρ^0–ω or ρ^0–ϕ mixings. These transition amplitudes are given by dispersion relations which should be subtracted in order to make the integral convergent (see, for instance, Appendix A in [9]). This gives rise to polynomials with real coefficients to be fixed using external renormalization conditions.

In the exact SU(3) symmetry limit, charged and neutral kaons carry the same mass and one can expect (or require) the polynomials associated with the charged and neutral kaon loops to coincide. Likewise, the charged and neutral K^*K loop functions can be made equal. In this case, the $\omega_I \leftrightarrow \phi_I$ amplitude survives with its renormalization polynomial, while the $\rho^0_I \leftrightarrow \phi_I$ and $\rho^0_I \leftrightarrow \omega_I$ transition amplitudes exactly vanish. If one breaks the SU(3) flavor symmetry leaving conserved the (u,d) quark sector, the same conclusion holds. However, if one introduces a breaking of SU(2) flavor symmetry, the mass difference beween the u and d quarks generates a mass difference between the charged and neutral kaons (and the K^*). Then the three possible transition amplitudes do not identically vanish any longer and, moreover, they depend on the invariant mass associated by the four-momentum flowing through the vector meson lines. Stated otherwise: the ρ^0_I, ω_I and ϕ_I mixing into the physical ρ^0, ω and ϕ fields should also be invariant mass dependent. As already noted in [9,16] this implies that the vector squared mass matrix, which has to be diagonalized in order to define the physical fields, is also invariant mass dependent and that the notion of mass for the physical vector fields becomes unclear as soon as one goes beyond tree level.

The property that ρ^0–ω mixing should be invariant mass dependent has been the subject of several studies in the framework of general local effective field theories [17], and subsequently in vector dominance models [18,19] where it was pointed out that the mixing amplitude should vanish at $s=0$, as the ρ^0 and ω self-masses, in order to preserve gauge invariance. One may also quote other studies going in the same direction [20,21] attributing the mixing to finite width effects, or quark loops (and pion loops). Using only the pion form factor data available at that time, [22] derived an approximate expression for the ρ^0–ω mixing amplitude; however, limiting that much the kind of data used, one cannot really observe a clear mass dependence effect. On the other hand, one should also note that [23] proved that isospin violation effects describing the ρ^0–ω mixing are not accounted for by the low energy constants (LEC) of chiral perturbation theory (ChPT) but are generated near threshold by the difference between charged and neutral kaon loops; it was also shown that these effects are tiny at the two-pion threshold (10^{-4}), while they are known to be at the percent level in the resonance peak region. This illustrates the invariant mass dependence of the ρ^0–ω mixing. However, one should note that the absence of the LECs in this calculation suggests that a one-loop result may be unreliable.

Therefore, the question we address is to consider the effects of loops on ρ^0, ω, ϕ mixing. However, in order to have some chance to single out the mass dependent behav-

ior, one clearly has to treat simultaneously the pion form factor data in the spacelike and timelike regions together with the largest possible set of light meson decays (radiative, leptonic and isospin violating strong decays) within a single framework. As argued above, the HLS model, equipped with suitable symmetry breaking mechanisms, seems able to provide such a framework. We shall not try to include isospin symmetry breaking effects into the coupling constants, which would help by providing more parameter freedom in the fit procedures. If really needed, it can certainly be done along the lines of the BKY breaking scheme [6, 7] as illustrated by [24].

The question of having a unified description of the largest possible set of low energy data is by itself interesting. However, this also addresses the puzzling and long-standing problem of the difference between the (estimated) isospin 1 part of the pion form factor in e^+e^- annihilations and in τ decays, which are related through the conserved vector current assumption (CVC). The importance of the problem is enhanced by its implication for the predicted value of the muon anomalous magnetic moment a_μ to be compared with the direct BNL measurement [25]; referring to the latest account by Davier [26] the estimate of the hadronic vacuum polarization (which enters the theoretical estimate) derived from e^+e^- data provides a 3.3σ disagreement between the theoretical estimation of a_μ and the BNL direct measurement [25]; moreover, the τ data estimate of the hadronic vacuum polarization provides a value of a_μ very close to its direct measurement [26].

Except for an experimental problem with e^+e^- annihilation data (which seems by now unlikely) in the data recently collected at Novosibirsk [27–30], or some new (or unidentified) physics effect, the disagreement between e^+e^- and τ data [31–33] is hard to explain. Indeed, a priori the single difference between these two channels should be due to isospin symmetry breaking (IB) effects. However, the comparison has already been performed with IB effects accounted for in both e^+e^- and τ data. This includes [34–36] pion mass values in kinematical factors, (a parametrization of the) ρ–ω mixing, charged and neutral ρ mass and width differences, short range [37] and long range [38–43] IB effects in the τ partial decay width to two pions.

This persistent disagreement may point towards new physics effects [44]; however, one should also note that the way some IB effects are accounted for has been questioned several times. For instance, effects due to the charged and neutral ρ pole positions [45, 46] were considered, but they have not been found sufficient in order to solve the observed discrepancy [35, 36]; ρ–ω mixing effects may also have been poorly estimated [47]. However, based on sum rules derived using an OPE input, Maltman [48, 49] concluded that there is inconsistency of the (presently) estimated isospin 1 part of the e^+e^- data with expectation, while the τ data provide a nice agreement.

We plan to address this question once again by building an effective model relying on the (symmetry broken) HLS model. In this approach, we plan to use a framework giving simultaneously an account of the partial decay widths of light mesons decays (radiative, leptonic, isospin breaking decay modes), of the pion form factor in e^+e^- data (both timelike and close spacelike regions) and in τ decay. By construction, the corresponding expressions of the pion form factor will be such that they will solely differ from each other by isospin symmetry breaking effects, mostly located in the (ρ, ω, ϕ) mixing scheme, which, of course, has no counterpart in τ decay. Stated otherwise, our model is built in such a way that going from the pion form factor expression in e^+e^- annihilations to the expression valid for τ decays is performed by switching off IB effects specific to e^+e^- and switching on those specific to τ decays.

At the start, the model we built is rendered complicated by the large number of possible loops involved. Fortunately, it can be somewhat simplified without loosing too much physics insight. Of course, this model depends on some parameters to be fixed in a fitting procedure; we should define a fitting procedure flexible enough that τ decay data can be removed or kept. Stated otherwise, the light mesons decays and the pion form factor in the e^+e^- data are expected to fix practically the U(3)/SU(3)/SU(2) breaking model. In this approach, we may get a prediction of the τ decay two-pion spectrum, which can be compared with the existing measurements. Including τ decay data should only refine the values of the fit parameters.

The paper is organized as follows: In Sect. 2, we derive the Lagrangian pieces of relevance in order to deal with the pion form factor in e^+e^- annihilations and τ decays, while in Sect. 3 we give the pion form factor expressions without loop corrections and symmetry breaking effects, mostly for illustration. In Sect. 4 we discuss the loop corrections that modify the vector meson mass matrix and perform already some simplifications. The modified vector meson squared mass matrix we propose is given in Sect. 5 with the diagonalization procedure and the relation between physical and ideal vector meson fields. The method used in order to renormalize the loop functions defining the self-energies and the transition amplitudes is sketched in Sect. 6. The form factor functions used for τ decays and e^+e^- annihilations are given in respectively Sects. 7 and 8. A necessary ingredient affecting the pion form factor in e^+e^- annihilations is the photon vacuum polarization (VP), which is discussed in Sect. 9. Fitting with the partial width expressions is briefly discussed in Sect. 10; more details can be found in [16], where a practically identical method is used with constant mixing functions, however. The way to deal with the various kinds of data used in the fit procedures is described in Sect. 11, with a special emphasis on our dealing with some correlation phenomena present in the existing data. In Sect. 12, we fully describe the fit procedures we worked out under various conditions and the results and conclusions we reach; we also comment on the numerical and physical properties of our model. Finally, Sect. 13 is devoted to a summary of our conclusions.

As already commented upon in the introduction, several appendices gather results of ours or others already published. They are given in an attempt to be as self-contained as possible; they are placed outside the main text in the interest of clarity and ease of reading. However, Appendix D contains new results concerning the Yang–Mills piece of the HLS Lagrangian.

2 The HLS Lagrangian model

We outline in the appendices the main features of the HLS model in both the non-anomalous (Appendix A) and anomalous (Appendix B) sectors. This allows us to derive the leading terms of the non-anomalous Lagrangian of interest for the present paper by expanding the exponentials defining the ξ fields. The breaking of flavor symmetries, SU(3) and the nonet symmetry is sketched in Appendix C.

Several pieces of the HLS Lagrangian of relevance for our problem will be given explicitly in the main text; first, the part describing the photon sector (traditional VMD) is

$$\begin{aligned}\mathcal{L}_{\rm VMD} &= {\rm i}e\left(1-\frac{a}{2}\right)A\pi^-\overleftrightarrow{\partial}\pi^+ + {\rm i}\frac{e}{z_A}\left(z_A-\frac{a}{2}-b\right)A\\ &\times K^-\overleftrightarrow{\partial}K^+ + {\rm i}\frac{e}{z_A}bAK^0\overleftrightarrow{\partial}\overline{K}^0 + \frac{{\rm i}ag}{2}\rho_{\rm I}^0\pi^-\overleftrightarrow{\partial}\pi^+\\ &+\frac{{\rm i}ag}{4z_A}\left(\rho_{\rm I}^0+\omega_{\rm I}-\sqrt{2}z_V\phi_{\rm I}\right)K^-\overleftrightarrow{\partial}K^+\\ &+\frac{{\rm i}ag}{4z_A}\left(\rho_{\rm I}^0-\omega_{\rm I}+\sqrt{2}z_V\phi_{\rm I}\right)K^0\overleftrightarrow{\partial}\overline{K}^0\\ &-eagf_\pi^2\left[\rho_{\rm I}^0+\frac{1}{3}\omega_{\rm I}-\frac{\sqrt{2}}{3}z_V\phi_{\rm I}\right]A\\ &+\frac{1}{9}af_\pi^2e^2(5+z_V)A^2\\ &+\frac{af_\pi^2g^2}{2}\left[\left(\rho_{\rm I}^0\right)^2+\omega_{\rm I}^2+z_V\phi_{\rm I}^2\right], \end{aligned}\tag{1}$$

limiting oneself to vector mesons, pion and kaon fields. Flavor symmetries have been broken and, as noted in [6, 7], this implies a pseudoscalar field renormalization. The pseudoscalar field renormalization has been performed (following the prescription given by (C.3) or, rather, by (C.7), which includes nonet symmetry breaking). The free Lagrangian of the vector meson fields is standard [1, 2], as well as the (canonical) pseudoscalar kinetic energy piece, the leptonic (see (A.11)) and the photonic free Lagrangian pieces.

The parameter g is the traditional universal vector meson coupling constant. On the other hand, the parameter a is specific for the HLS model and fulfills $a = 2$ in the standard VMD approaches; however such a stringent condition is not mandatory and several phenomenological studies involving pion form factor data on the one hand [50, 51] and light meson decays on the other hand [8, 9] concluded that a much better favored value is $a \simeq 2.4$–2.5. This opens a way to a direct coupling of photons to pseudoscalar pairs within VMD-like approaches. One should note the presence of a photon mass term of order e^2, which is traditionally removed by a field redefinition [2, 52] (see also [53] and the discussion concerning the photon pole position). It can also be removed by renormalization conditions at one loop order.

The parameter b in (1) is $b = a(z_V - 1)/6$, where z_V is the SU(3) breaking parameter of the $\mathcal{L}_V$ part of the HLS Lagrangian, while $z_A = [f_K/f_\pi]^2 = 1.495 \pm 0.031$ [54] is the SU(3) breaking parameter of its $\mathcal{L}_A$ part [1, 2]. z_A is almost fixed numerically, while z_V is the major origin of the HK mass difference between the ϕ meson and the (ω, ρ^0) system; it has to be fit as the relation between vector meson masses determined experimentally and the (Higgs–Kibble) masses occurring in the Lagrangians is unclear [9, 52]. On the other hand, the value for f_K/f_π provided by the review of particle properties (RPP) [54] can be added to the set of measurements to be fit.

The subscript I on the fields, standing for "ideal", affects the neutral vector meson fields. It indicates that the corresponding fields occurring in the Lagrangian are not the physical fields.

One should note [6] that the SU(3) breaking of the HLS Lagrangian generates a non-resonant coupling of the photon to neutral kaon pairs; this is a property common to all breaking procedures of the HLS Lagrangian proposed so far [4–7].

On the other hand, still limiting oneself to pions and kaon terms, the Lagrangian piece of relevance for τ decay after symmetry breaking and field renormalization is given by

$$\begin{aligned}\mathcal{L}_\tau &= -\frac{{\rm i}g_2}{2}V_{ud}W^+\\ &\times\left[\left(1-\frac{a}{2}\right)\pi^-\overleftrightarrow{\partial}\pi^0+\left(z_A-\frac{a}{2}\right)\frac{1}{z_A\sqrt{2}}K^0\overleftrightarrow{\partial}K^-\right]\\ &-\frac{af_\pi^2gg_2}{2}V_{ud}W^+\rho^- - \frac{{\rm i}ag}{2}\rho^-\left[\pi^0\overleftrightarrow{\partial}\pi^+ - \frac{1}{z_A\sqrt{2}}\overline{K}^0\overleftrightarrow{\partial}K^+\right]\\ &+f_\pi^2g_2^2\left\{\frac{1+a}{4}\left[z_A|V_{us}|^2+|V_{ud}|^2\right]+\frac{a}{4}[\sqrt{z_V}-z_A]|V_{us}|^2\right\}\\ &\times W^+W^- + af_\pi^2g^2\rho^+\rho^-, \end{aligned}\tag{2}$$

plus the conjugate of the interaction term (the W^- term, not displayed). This Lagrangian piece depends on g_2 (which is fixed by its relation with the Fermi constant (see (A.12)), on the CKM matrix element $V_{ud} = 0.97377 \pm 0.00027$ [54], on the universal coupling g and on the breaking parameters z_A and z_V already defined. One should note, balancing the photon mass term in $\mathcal{L}_{\rm VMD}$, a small mass term complementing the W mass of the standard model, which could be removed by appropriate field redefinitions.

Finally, the effective Lagrangian of the model we use in order to describe low energy physics is

$$\mathcal{L} = \mathcal{L}_{\rm VMD} + \mathcal{L}_\tau + \mathcal{L}_{\rm anomalous} + \mathcal{L}_{\rm YM}, \tag{3}$$

where $\mathcal{L}_{\rm anomalous}$ is given by (C.10). Its VVP part is not given in the appendices but can be found fully expanded in the appendices of [8]. The last term is the Yang–Mills piece given by (D.1), which undergoes SU(3) symmetry breaking as depicted in Appendix D; the main effect of this on the low energy phenomenology we deal with concerns the K^* radiative decay widths (see the discussion around (C.10)).

The first two terms in (3) allow us to build up the pion form factor in the e^+e^- interactions and τ decay and the leptonic widths of neutral vector mesons, while the anomalous decays will be dealt with starting from the third piece. All breaking parameters are common to all pieces of our $\mathcal{L}$; more precisely, all parameters of our model, except those of the vector meson mixing, could be fixed from only $\mathcal{L}_{\rm anomalous}$ and the leptonic decays of vector mesons. This was proved in [8, 9, 16] by adding various (ρ, ω, ϕ) mixing schemes including the most traditional (ω, ϕ) mixing in isolation [8].

The case of the parameter z_T, which is important only for K^* radiative decays, is special; this enters as the SU(3) breaking parameter of $\mathcal{L}_{\rm YM}$, which shows up in the anomalous Lagrangian of (C.10) when replacing there the bare vector field matrix by its renormalized partner (see Appendix D).

3 The pion form factor without symmetry breaking

The Lagrangian given in (3) allows us to construct the pion form factor in e^+e^- annihilation and in τ decay. One has ($m_\pi \equiv m_{\pi^\pm}$)

$$F_\pi(s) = \left(1-\frac{a}{2}\right) - \frac{a^2 g^2 f_\pi^2}{2}\frac{1}{D_V(s)}\,, \tag{4}$$

for both processes involving an intermediate photon and a W boson. We also have

$$\begin{cases} \sigma(e^+e^-\to\pi^+\pi^-) = \dfrac{8\pi\alpha^2}{3s^{5/2}}|F_\pi(s)|^2 q_\pi^3\,, \\ \dfrac{{\rm d}\Gamma}{{\rm d}s}(s) = \dfrac{|V_{ud}|^2 G_{\rm F}^2}{64\pi^3 m_\tau^3}|F_\pi(s)|^2\left[G_0(s)+\epsilon^2 G_2(s)\right]\,, \end{cases} \tag{5}$$

with[1]

$$\begin{cases} G_0(s) = \dfrac{4}{3}\dfrac{\left(m_\tau^2-s\right)^2\left(m_\tau^2+2s\right)}{s^{3/2}}Q_\pi^3\,, \\ G_2(s) = -\dfrac{\left(m_\tau^2-s\right)^2\left(4s-m_\tau^2\right)}{s^{5/2}}m_\pi^4 Q_\pi\,, \end{cases} \tag{6}$$

and

$$\begin{cases} \epsilon = \dfrac{m_{\pi^0}^2-m_{\pi^+}^2}{m_{\pi^+}^2} \simeq -0.06455 \quad (m_\pi \equiv m_{\pi^+})\,, \\ q_\pi = \dfrac{1}{2}\sqrt{s-4m_\pi^2}\,, \\ Q_\pi = \dfrac{\sqrt{\left[s-\left(m_{\pi^0}+m_{\pi^+}\right)^2\right]\left[s-\left(m_{\pi^0}-m_{\pi^+}\right)^2\right]}}{2\sqrt{s}}\,, \end{cases} \tag{7}$$

factor and will be cancelled out from now on. The bare inverse propagator $D_V = s - m_\rho^2$ has to be modified for self-mass effects, which fortunately shift the ρ meson pole off the physical region by giving it an imaginary part. At this stage, there is also no inclusion of loop effects in $\gamma\rho$ or $W\rho$ transition amplitudes in the expression for the pion form factor itself.

In addition, there is clearly no interplay of the ω or ϕ mesons as can be seen from inspecting the various pieces of the full Lagrangian in (3); this should come from isospin symmetry breaking.

Including self-mass effects for the ρ (and adding the ω/ϕ meson contributions for e^+e^- annihilation), these expressions provide the usual HLS based framework for pion form factor fitting of the e^+e^- data [50, 51]. Even if omitting this, in principle, (4) applies to the τ data, again after shifting the $\rho^\pm$ singularity off the physical region by means of a varying width Breit–Wigner amplitude, for instance.

4 Including one-loop effects in the HLS Lagrangian

From the expressions given in the previous section, the ρ meson occurs as a pole on the physical region; this is moved off the real axis by self-mass (loop) effects, which essentially turn out to provide a width to the ρ through the imaginary part of the pion loop. However, besides this effect, a closer look at our $\mathcal{L}$ allows us to see that loop effects contribute to the generation of self-masses to all vector mesons, *and* transition amplitudes among all neutral vector mesons. Assuming from now on SU(3) and SU(2) breaking effects, the charged and neutral pion and kaon masses become different. One can see that kaon loops and the anomalous VVP piece of the Lagrangian give the following transition amplitudes for neutral vector mesons (ideal fields are understood, i.e. $\Pi_{\rho\rho}(s)$ should be understood as $\Pi_{\rho_{\rm I}\rho_{\rm I}}(s)$, for instance):

$$\begin{cases} \Pi_{\rho\rho}(s) = g_{\rho\pi\pi}^2\Pi'(s) + g_{\rho KK}^2(\Pi_+(s)+\Pi_0(s)) & + \left[g_{\rho\omega\pi}^2\Pi_{\omega\pi}(s)+\cdots\right], \\ \Pi_{\omega\omega}(s) = g_{\omega KK}^2(\Pi_+(s)+\Pi_0(s)) & + \left[g_{\rho\omega\pi}^2\Pi_{\rho\pi}(s)+\cdots\right], \\ \Pi_{\phi\phi}(s) = g_{\phi KK}^2(\Pi_+(s)+\Pi_0(s)) & + \left[g_{\phi K^*K}^2\Pi_{K^{*+}K^-}(s)+\cdots\right], \\ \Pi_{\omega\phi}(s) = -g_{\omega KK}g_{\phi KK}(\Pi_+(s)+\Pi_0(s)) & + \left[2g_{\phi K^*K}g_{\omega K^*K}\left(\Pi_{K^{*\pm}K^\mp}(s)+\Pi_{K^{*0}K^0}(s)\right)\right], \\ \Pi_{\rho\omega}(s) = g_{\rho KK}g_{\omega KK}(\Pi_+(s)-\Pi_0(s)) & + \left[2g_{\omega K^*K}g_{\rho K^*K}\left(\Pi_{K^{*\pm}K^\mp}(s)-\Pi_{K^{*0}K^0}(s)\right)\right], \\ \Pi_{\rho\phi}(s) = -g_{\rho KK}g_{\phi KK}(\Pi_+(s)-\Pi_0(s)) & + \left[2g_{\phi K^*K}g_{\rho K^*K}\left(\Pi_{K^{*\pm}K^\mp}(s)-\Pi_{K^{*0}K^0}(s)\right)\right], \end{cases} \tag{8}$$

where one accounts for the pion mass difference. The $G_2(s)$ term gives a completely negligible contribution to the form

where we have defined $g_{\rho\pi\pi} = ag/2$, $g_{\rho KK} = g_{\omega KK} = ag/(4z_A)$ and $g_{\phi KK} = \sqrt{2}agz_V/(4z_A)$. $\Pi'(s)$ is the charged pion loop, while $\Pi_+(s)$ and $\Pi_0(s)$ are the charged and neutral kaon loops, each amputated from their couplings to vector mesons (i.e. loops carrying unit coupling constants).

[1] Of course, in the SU(2) symmetry limit, we have $\epsilon = 0$ and $q_\pi = Q_\pi$.

The contributions of the anomalous loops have been displayed in square brackets. The anomalous FKTUY Lagrangian gives several terms contributing to the self-masses $\Pi_{\rho\rho}(s)$, $\Pi_{\omega\omega}(s)$ and $\Pi_{\phi\phi}(s)$. They can easily be constructed from the VVP Lagrangian given in Appendix 4 of [8]; for these, we have displayed in (8) only one representative of the full list, which always includes $K^{*\pm}K^{\mp}$, $K^{*0}\overline{K}^0$,$\overline{K}^{*0}K^0$ and, depending on the particular self-mass considered, contributions from $\omega\pi^0$, $\rho\pi^0$, $\omega\eta$, $\rho\eta$, $\phi\eta$, $\omega\eta'$, $\rho\eta'$ or $\phi\eta'$ loops.

The anomalous parts of all transition amplitudes have been entirely displayed, as they exhibit an interesting correspondence with the non-anomalous contributions. We have identified to each other both $K^{*\pm}K^{\mp}$ loops on the one hand, and $K^{*0}\overline{K}^0$ with $\overline{K}^{*0}K^0$ on the other hand. Using the present set of notations, we have defined $g_{\rho K^*K} = g_{\omega K^*K} = \sqrt{z_T/z_A}G_{\rm anom}/2$ and $g_{\phi K^*K} = G_{\rm anom}/\sqrt{2z_A\,z_T}$ with [8] $G_{\rm anom} = -3g^2/\left(8\pi^2 f_\pi\right)$. We have also denoted by $\Pi_{K^{*\pm}K^{\mp}}(s)$ and $\Pi_{K^{*0}K^0}(s)$ the amputated $K^{*\pm}K^{\mp}$ and $K^{*0}K^0$ loop functions.

In the exact isospin symmetry limit, one has $\Pi_+(s) = \Pi_0(s)$ on the one hand, and $\Pi_{K^{*\pm}K^{\mp}}(s) = \Pi_{K^{*0}K^0}(s)$ on the other hand. Then, all transition amplitudes vanish except for $\omega\phi$.

Therefore, within the HLS model, the $\omega\phi$ mixing is a natural feature generated by loop effects and not from some breaking mechanism. In contrast, the $\rho\phi$ mixing and the prominent $\rho\omega$ mixing are fully due to isospin symmetry breaking. Including the anomalous sector does not change the picture.

Actually, as emphasized in Appendix D, the Yang–Mills sector of the HLS Lagrangian [2] provides a further mechanism, which comes in supplementing the kaon and K^*K loop mechanism just described. This additional mechanism is produced by charged and neutral $K^*\overline{K}^*$ loops; these still come in by their sum in the $\omega\phi$ transition amplitude, while it is their difference that occurs in the $\rho\omega$ and $\rho\phi$ transition amplitudes.

One may wonder that, within the VMD-like approaches, all mechanisms contributing to the vector meson mixing at order g^2 always involve loops with a pair of mesons carrying open strangeness. This was true for the non-anomalous HLS Lagrangian ($K\overline{K}$) and for the anomalous HLS Lagrangian (K^*K); we also find it to be true for the Yang–Mills piece ($K^*\overline{K}^*$).

If one denotes by $\Pi_{+/0}(s)$ the amputated K^+K^0 loop and by $\Pi''(s)$ the amputated $\pi^\pm\pi^0$ loop, the charged ρ self-mass reads

$$\Pi'_{\rho\rho}(s) = g^2_{\rho\pi\pi}\Pi''(s) + 2g^2_{\rho KK}\Pi_{+/0}(s) + \left[g^2_{\rho^\pm\omega\pi^\pm}\Pi_{\omega\pi}(s) + \cdots\right], \qquad (9)$$

with a partial display of the anomalous loop contributions between the square brackets. The Yang–Mills term introduces also $\rho\rho$ loops (not displayed as they are of little importance at our energies). This expression actually differs little from the neutral ρ self-mass; indeed, the effect of having different masses for the neutral and charged particles in these loop computations is tiny. Of course, in the isospin symmetry limit, we have $\Pi'_{\rho\rho}(s) = \Pi_{\rho\rho}(s)$ and then the ρ^0 and $\rho^\pm$ propagators (and their poles) coincide.

As is clear from the Lagrangian pieces given by (1) and (2), the fields $\rho^{\rm I}$, $\omega^{\rm I}$, and $\phi^{\rm I}$ as well as $\rho^\pm$ are certainly mass eigenstates at tree level. This statement remains true for $\rho^\pm$ at one-loop order as there is no transition loop from this meson to any other one. This is, however, clearly not true for the $\rho^{\rm I}$, $\omega^{\rm I}$ and $\phi^{\rm I}$ fields, which undergo mixing with each other, as can be seen from (8). Moreover, as for the self-masses, these transition amplitudes are invariant mass dependent as already noted [9, 16]!

This implies that physical fields associated with the ρ^0, ω and ϕ mesons do not coincide with their ideal combinations as soon as one-loop corrections are considered. Moreover, the precise content of the physical fields in terms of ideal fields varies with s, or more precisely with the invariant mass flowing through the physical field under consideration. This does not prevent in standard approaches the use of $\rho^{\rm I}$, $\omega^{\rm I}$ and $\phi^{\rm I}$ in the physical amplitudes [55]. However, as one-loop effects have certainly to be considered even only in order to shift the vector meson poles off the physical region, they should legitimately be considered also for field mixing.

We raise the question of taking these loop effects properly into account and proceeding to the appropriate field redefinition to physical fields. In order to deal with this problem, let us define as effective Lagrangian the Lagrangian in (3) supplemented with the self-masses and transition terms occurring at one-loop order; this turns out to replace the simple vector meson mass term in the HLS Lagrangian by ($m^2 = ag^2f_\pi^2$)

$$\mathcal{L}_{\rm mass} = \left\{ \begin{array}{l} \frac{1}{2}\Big\{ \left[m^2 + \Pi_{\rho\rho}(s)\right]\rho_{\rm I}^2 + \left[m^2 + \Pi_{\omega\omega}(s)\right]\omega_{\rm I}^2 \\ \quad + \left[z_V m^2 + \Pi_{\phi\phi}(s)\right]\phi_{\rm I}^2 + 2\Pi_{\rho\omega}(s)\rho_{\rm I}\omega_{\rm I} \\ \quad + 2\Pi_{\rho\phi}(s)\rho_{\rm I}\phi_{\rm I} + 2\Pi_{\omega\phi}(s)\omega_{\rm I}\phi_{\rm I}\Big\} \\ \quad + \left[m^2 + \Pi'_{\rho\rho}(s)\right]\rho^+\rho^- \end{array} \right. . \qquad (10)$$

The K^* mass term, which should also be modified correspondingly, is not shown as it plays no role in the present problem.

Even if anomalous VP contributions seem to play some role visible [51] (and, nevertheless, marginal) in the pion form factor data, qualitatively their explicit form is really active only above the $\omega\pi$ threshold, which is the lowest mass VP threshold; all others are far above the GeV region[2]. Below the threshold, the main effect is due to their subtraction polynomials, which can be well absorbed in the subtraction polynomials of the accompanying pion and kaon loops in order to put the poles of the ρ propagator at the place requested by the data.

Beside the (non-anomalous) pion and kaon loops, all transition amplitudes involve K^*K and $K^*\overline{K}^*$ loops, the thresholds of which respectively are at $\simeq 1.4$ GeV and $\simeq$

[2] Their threshold masses are spread out between $\simeq 1.3$ GeV and $\simeq 2$ GeV. The situation is similar for the loops generated by the Yang–Mills term.

1.8 GeV. This means that, besides their subtraction polynomials (minimally of degree 2), in the region below the GeV, their behavior [9] is a real logarithmic function (below $\sqrt{s} \simeq 0.4\,\mathrm{GeV}$) or an arctangent function ($0.4 \leq \sqrt{s} \leq 1.4\,\mathrm{GeV}$). This also can be numerically absorbed in a fit subtraction polynomial.

Therefore, there is some sense in neglecting the (explicit) contributions of the anomalous and Yang–Mills loops, it being understood that their effect is mostly concentrated in their subtraction polynomials. Moreover, as these come always together with pion and kaon loops, they can be accounted for by simply letting the (free) pion and kaon loop subtraction polynomials be of second degree. Therefore, we shall neglect their (explicit) contributions, pointing at the appropriate places to their possible influence. Thus, from now on, the self-energies and transition amplitudes should be understood as (8)–(9) amputated from the square bracket terms and without the Yang–Mills contributions depicted in Appendix D.

The use of the modified HLS Lagrangian has already been discussed in [9], where it was shown, for instance, that this method allows one to recover vector meson propagators usually derived through the Schwinger–Dyson resummation procedure, which turns out to sum up an infinite series, which is not necessarily convergent. However, we shortly show that introducing this modified mass term allows us to also account for the other transition effects, which would be more difficult to derive from the Schwinger–Dyson resummation procedure (of course, this should be possible but is merely tedious).

5 Mass matrix diagonalization and physical fields

As is clear from (10), at one-loop order, the mass term is diagonal in the charged vector meson sector and will not be discussed any longer. In the neutral vector meson sector, however, the mass matrix is not diagonal and the effective Lagrangian mass term is

$$\mathcal{L}_{\mathrm{mass}} = \frac{1}{2}\widetilde{U}M^2(s)U\,, \quad \widetilde{U} = (\rho^{\mathrm{I}}, \omega^{\mathrm{I}}, \phi^{\mathrm{I}}) \tag{11}$$

(the ideal fields being supposed real) and[3]

$$M^2(s) = \begin{pmatrix} m^2 + \Pi_{\pi\pi}(s) + \epsilon_2 & \epsilon_1 & -\mu\epsilon_1 \\ \epsilon_1 & m^2 + \epsilon_2 & -\mu\epsilon_2 \\ -\mu\epsilon_1 & -\mu\epsilon_2 & z_V m^2 + \mu^2\epsilon_2 \end{pmatrix}, \quad (\mu \equiv z_V\sqrt{2})\,, \tag{12}$$

where we have defined

$$\begin{cases} \epsilon_1 = g^2_{\rho KK}(\Pi_+(s) - \Pi_0(s))\,, \\ \epsilon_2 = g^2_{\rho KK}(\Pi_+(s) + \Pi_0(s))\,, \\ \Pi_{\pi\pi}(s) = g^2_{\rho\pi\pi}\Pi'(s)\,. \end{cases} \tag{13}$$

In the region where we work – invariant masses bounded essentially by the two-pion threshold and the ϕ mass – the functions ϵ_1 and ϵ_2 are small and can be treated as perturbation parameters[4]; moreover, they are real for real s up to the two-kaon threshold region. In contrast, $\Pi_{\pi\pi}(s)$ is complex starting from the two-pion production threshold and is not expected to be small enough to be consistently treated as a perturbation parameter.

The physical vector meson mass eigenstates are the (s-dependent) eigenvectors of $M^2(s)$ and their masses are the corresponding eigenvalues, which are also s-dependent! Expressed in this way, the notion of vector meson mass looks a little bit paradoxical; however, it is not really new: writing, as usual, the inverse ρ dressed propagator $D_V(s) = s - m^2 - \Pi_{\rho\rho}(s)$ can be interpreted as stating that the ρ mass squared is $m^2 + \Pi_{\rho\rho}(s)$ and includes an imaginary part. From the physical point of view, what is important is that the pole position associated with the ρ is always a zero of $s - m^2 - \Pi_{\rho\rho}(s)$ located on the unphysical sheet, close to the physical region[5]. The ρ pole position has been fit long ago by [56] in the e^+e^- data, and more recent fit values can be found in [57]; this piece of information is actually highly model independent, in contrast with any other definition [53]. We shall revisit this issue with our fit results.

One may wonder about the hermiticity properties of the Lagrangian modified as proposed. As below the two-pion threshold, the loops defined above are all real for real s; we still indeed have $\mathcal{L}(s) = \mathcal{L}^\dagger(s)$; however, above this point, the hermiticity should be redefined as $\mathcal{L}(s) = \mathcal{L}^\dagger(s^*)$. This property known as hermitian analyticity [58] is fulfilled by our modified Lagrangian as it is already fulfilled by the loop functions.

Now, in order to define the physical ρ, ω and ϕ in terms of their ideal partners, one has to find the eigenstates of the squared mass matrix given by (12). Let us take advantage of the smallness of ϵ_1 and ϵ_2 to solve the problem perturbatively in order to avoid dealing with intractable expressions. Let us split up the squared mass matrix into two pieces and write it $M^2 = M_0^2 + \epsilon B$, with

$$M_0^2 = \begin{pmatrix} m^2 + \Pi_{\pi\pi}(s) & 0 & 0 \\ 0 & m^2 + \epsilon_2 & 0 \\ 0 & 0 & z_V m^2 + \mu^2\epsilon_2 \end{pmatrix}, \quad \epsilon B = \begin{pmatrix} \epsilon_2 & \epsilon_1 & -\mu\epsilon_1 \\ \epsilon_1 & 0 & -\mu\epsilon_2 \\ -\mu\epsilon_1 & -\mu\epsilon_2 & 0 \end{pmatrix}. \tag{14}$$

In this splitting up, we have found it appropriate to leave a part of the actual perturbation inside M_0^2. In this way, we avoid to some extent the problem of having the unperturbed eigenvalues degenerated twice or even three times

[3] For ease of reading, ϵ_1 and ϵ_2 are not written with their explicit s-dependence, which is (or may be) understood throughout this paper.

[4] Actually, from their very expressions in terms of kaon and K^*K loops, one may expect ϵ_1 to be sensitively smaller than ϵ_2 in absolute magnitude.

[5] The upper lip of the physical region – the $s \geq 4m_\pi^2$ semi-axis – located on the physical sheet is topologically close to the lower lip in the unphysical sheet of the Riemann surface; in contrast, the lower lip in the physical sheet is topologically far from the upper lip in the same sheet.

(when $z_V = 1$) for some values of s and some z_V. However, while assuming that $\Pi_{\pi\pi}(s)$, $\epsilon_1(s)$ and $\epsilon_2(s)$ vanish at the origin, one cannot avoid to have a twofold degeneracy at $s \equiv 0$; this degeneracy is resolved as soon as s departs from zero by an arbitrary small quantity. This issue, which affects strictly the point $s = 0$ (where the exact solution is trivial!), does not raise any problem with our data, which are all at $s \neq 0$, even if close to zero, as the NA7 spacelike form factor data [59]. Another solution to this problem would be that the HK masses for $\rho_{\rm I}$ and $\omega_{\rm I}$ would be slightly different; such a mechanism remains to be found[6].

The unperturbed solution is then trivial, as the eigenvectors are the canonical ideal combinations of the neutral vector meson fields, with eigenvalues as can be read off the diagonal of M_0^2. Then, one has to solve the following system for the perturbations δv_i and $\delta\lambda_i$:

$$\begin{cases} M_0^2 v_i = \lambda_i v_i, \quad \tilde{v_i} v_i = 1 \quad (i = 1,2,3)\,, \\ M^2(v_i + \delta v_i) = (\lambda_i + \delta\lambda_i)(v_i + \delta v_i)\,, \\ \qquad \text{with [60]}\ \tilde{v_i}\delta v_i = 0 \end{cases} \tag{15}$$

for each $i = (\rho, \omega, \phi) = (1,2,3)$. The solution can be written

$$\begin{pmatrix} \rho^0 \\ \omega \\ \phi \end{pmatrix} = R(s) \begin{pmatrix} \rho_{\rm I}^0 \\ \omega_{\rm I} \\ \phi_{\rm I} \end{pmatrix}\,, \quad \begin{pmatrix} \rho_{\rm I}^0 \\ \omega_{\rm I} \\ \phi_{\rm I} \end{pmatrix} = \widetilde{R}(s) \begin{pmatrix} \rho^0 \\ \omega \\ \phi \end{pmatrix}\,, \tag{16}$$

where (recall $\epsilon_i \equiv \epsilon_i(s)$ are analytic functions of s):

$$R = \begin{pmatrix} 1 & \dfrac{\epsilon_1}{\Pi_{\pi\pi}(s) - \epsilon_2} & -\dfrac{\mu\epsilon_1}{(1-z_V)m^2 + \Pi_{\pi\pi}(s) - \mu^2\epsilon_2} \\ -\dfrac{\epsilon_1}{\Pi_{\pi\pi}(s) - \epsilon_2} & 1 & -\dfrac{\mu\epsilon_2}{(1-z_V)m^2 + (1-\mu^2)\epsilon_2} \\ \dfrac{\mu\epsilon_1}{(1-z_V)m^2 + \Pi_{\pi\pi}(s) - \mu^2\epsilon_2} & \dfrac{\mu\epsilon_2}{(1-z_V)m^2 + (1-\mu^2)\epsilon_2} & 1 \end{pmatrix}. \tag{17}$$

The matrix R is orthogonal up to (neglected) second order terms (see Sect. 6 in [16]) and its elements are, actually, meromorphic functions of s; this, for instance, means that one has to check that they do not develop singularities in the region of physical interest for our model.

On the other hand, one may wonder getting $\widetilde{R}(s)$ with no complex conjugation in the field transformation ($\Pi_{\pi\pi}(s)$ is complex and fulfills the real analyticity condition $\Pi_{\pi\pi}(s) = \Pi^*_{\pi\pi}(s^*)$). This is due to the unitarity condition [9]

$$R(s + {\rm i}\varepsilon)R^\dagger((s + {\rm i}\varepsilon)^*) = R(s + {\rm i}\varepsilon)R^\dagger(s - {\rm i}\varepsilon) = 1\,, \tag{18}$$

for real s above threshold and $\varepsilon > 0$. The real analyticity property fulfilled by the matrix function R then gives $R^*(s - {\rm i}\varepsilon) = R(s + {\rm i}\varepsilon)$ and then (18) becomes

$$R(s + {\rm i}\varepsilon)\widetilde{R}(s + {\rm i}\varepsilon) = 1\,, \tag{19}$$

as can be checked directly with the R matrix above.

At first order, the corrections for the eigenvalues are not changed with respect to their unperturbed values for ω and ϕ, while for ρ^0, the first order correction is such that the eigenvalue is restored to $m^2 + \Pi_{\pi\pi}(s) + \epsilon_2$ and is formally identical to the $\rho^\pm$ mass squared[7]. Therefore, in order to deal with the physical eigenstates ρ^0, ω and ϕ, one has to introduce in the Lagrangian (3) above the physical fields as defined by (16) using (17). For the coupling constants, one has to proceed exactly as explained in Sect. 6.3 of [16], using the R matrix above and, where appropriate, the ideal coupling constants given in Appendix E.

In order that this solution should be considered valid, one has to check that the non-diagonal elements of the matrix R are small compared to 1 in the whole range of application of our model. As they depend on the fit parameters, this check can only be performed with the fit solution.

We will not go into more details with expressing the full Lagrangian (3) in the basis of physical neutral vector meson fields, as the formulae become really complicated (even if they can be readily and tediously written down). Let us only give the most interesting piece in terms of physical fields for illustrative purposes:

$$\frac{{\rm i}ag}{2}\rho^{\rm I}\pi^- \overleftrightarrow{\partial} \pi^+ = \frac{{\rm i}ag}{2}\left[\rho^0 - \frac{\epsilon_1}{\Pi_{\pi\pi}(s) - \epsilon_2}\omega + \frac{\mu\epsilon_1}{(1-z_V)m^2 + \Pi_{\pi\pi}(s) - \mu^2\epsilon_2}\phi\right]\pi^- \overleftrightarrow{\partial} \pi^+\,. \tag{20}$$

This clearly shows how kaon loops generate couplings of the *physical* ω and ϕ fields to $\pi^-\pi^+$, which vanish (with ϵ_1) in the isospin symmetry limit. As $\Pi_{\pi\pi}(s)$ has a large imaginary part, it is clear that the phase of the ω coupling compared with ρ^0 will be very large at the ρ peak. It should also be mentioned that the couplings shown here (and the matrix elements of R) all have a finite limit at $s = 0$ even if the loops individually vanish at $s = 0$ as the pseudoscalar pairs couple to conserved currents [17, 52].

The effects of the neglected loops could be briefly mentioned here. The most important effect in the expression for $R(s)$, (17), is on the denominators of $R_{12}(s)$ and $R_{21}(s)$,

[6] A way to get it would have been to use as breaking matrix $X_V = {\rm Diag}(1 + \varepsilon_u, 1 + \varepsilon_d, \sqrt{z_V})$ instead of $X_V = {\rm Diag}(1, 1, \sqrt{z_V})$ while computing $\mathcal{L}_V$ (see Appendix C). This, actually, generates a mass difference between ρ^0 and $\rho^\pm$, but the HK mass for the ω meson remains equal to that of the ρ^0 meson. In addition, the coupling constants of the charged and neutral ρ mesons to a pion pair differ only by terms of order $\varepsilon^2_{u/d}$ and thus can be kept equal.

[7] For $\rho^\pm$, the mass squared value contains what was called $\Pi'_{\pi\pi}(s)$ and $\epsilon_2 \to 2g^2_{\rho KK}\Pi_{+/0}(s)$.

where the difference of the anomalous contributions to the self-energies for the ρ and ω mesons will add to the present $\Pi_{\pi\pi}(s)-\epsilon_2(s)$; this could change a little bit the behavior near $s=0$, where all loops tend to zero.

As stated above, at first order in perturbations, the squared mass eigenvalues are the entries in the diagonal of $M^2(s)$ given in (12). For further use, let us also give the second order corrections to the eigenvalues (and thus to the running squared meson masses):

$$\begin{cases} \delta_2\lambda_\rho = \dfrac{\epsilon_1^2}{\Pi_{\pi\pi}(s)-\epsilon_2} + \dfrac{\mu^2\epsilon_1^2}{(1-z_V)m^2+\Pi_{\pi\pi}(s)-\mu^2\epsilon_2}\,, \\ \delta_2\lambda_\omega = -\dfrac{\epsilon_1^2}{\Pi_{\pi\pi}(s)-\epsilon_2} + \dfrac{\mu^2\epsilon_2^2}{(1-z_V)m^2+(1-\mu^2)\epsilon_2}\,, \\ \delta_2\lambda_\phi = -\dfrac{\mu^2\epsilon_1^2}{(1-z_V)m^2+\Pi_{\pi\pi}(s)-\mu^2\epsilon_2} \\ \qquad\quad -\dfrac{\mu^2\epsilon_2^2}{(1-z_V)m^2+(1-\mu^2)\epsilon_2}\,. \end{cases} \tag{21}$$

In the mass range in which we are working (from the two-pion threshold to the ϕ mass), the mass eigenvalues at first order are real[8] for the ω and ϕ, excluding a width. At second order, one observes that the pion loop generates an imaginary part to these mass eigenvalues. Let us remind the reader that, as the pole positions are the solutions of $s-\lambda_i(s)=0$, one expects to find the ρ pole position close to the value found by [56]. However, there is little chance that the ω width happens to carry the correct width value, as this should be generated by the anomalous $\rho\pi$ loop with additional insertion of a pion loop on the ρ leg (or simply considering the dressed ρ propagator) or directly through a possible $\omega\to 3\pi\to\omega$ (double) loop. Finally, in the model we use, it is only at second order that a difference between neutral and charged ρ propagators (and thus masses) occurs and this is a net (and small) effect of the neutral vector meson mixing. This comes in addition to other sources of the ρ^0–$\rho^\pm$ mass difference (see footnote 6).

6 Renormalization conditions on loops

With the approximations we chose (neglecting the anomalous loop contributions), the loop expressions needed in order to construct the pion form factor $F_\pi(s)$ are only the $\pi\pi$ and $K\overline{K}$ loops. They can be computed by means of dispersion relations [9, 52] and can be derived without explicit integration, relying only on properties of analytic functions, especially the uniqueness property of the analytic continuation (see Appendix A in [9][9]).

From general principles, any loop $\Pi(s)$ is a so-called real analytic function (see the previous section), the imaginary part of which is calculable using the Cutkosky rules, or in the simple case of single loops, using the partial width of the process $V\to PP'$. Indeed

$$\mathrm{Im}\,\Pi(s) = -\sqrt{s}\Gamma(s)\,, \quad s>s_0\,, \tag{22}$$

where s is the pair invariant mass squared, s_0 the threshold mass squared of the pair and Γ the partial width of the decay. With this at hand, the full loop is the solution of the integral equation:

$$\Pi(s) = P_{n-1}(s) + \frac{s^n}{\pi}\int_{s_0}^{\infty}\frac{\mathrm{Im}\,\Pi(z)}{z^n(z-s+\mathrm{i}\epsilon)}\,\mathrm{d}z\,, \tag{23}$$

where $P_{n-1}(s)$ is a polynomial of degree $n-1$ with real coefficients, and the integral runs over the right-hand cut (the physical region). These coefficients should be fixed by means of the conditions to be fulfilled by $\Pi(s)$, the so-called subtraction polynomial, nothing but renormalization conditions chosen externally and depending on the problem at hand.

A priori, the number of subtractions, i.e. the number of conditions, can be arbitrary, however, in order that the integral in (23) converges, there is a minimal number of subtractions to perform: for PP' and VV loops $n\geq 2$, and for VP loops $n\geq 3$.

In the most general form of the pion form factor following from the Lagrangian (3), and using the modified one-loop mass term (10) the relevant basic loops are only the pion loops and the kaon loops. These imply that at least $n=2$; however, the very existence of VP neglected loops implies that we are still minimally subtracting with using $n=3$ for all loop functions in this paper. As discussed in Sect. 4, in this way, the subtraction polynomials carry some (unknown) information on the anomalous loop contribution.

In addition, we require all polynomials $P_{n-1}(s)$ to fulfill $P_{n-1}(0)=0$, reflecting in this way current conservation [17, 51, 52, 61] when needed and an appropriate constraint otherwise[10].

In the usual approaches [52, 57, 61], the renormalization conditions are defined from the start and, then, one leaves free the other parameters like meson mass and width in order to accommodate the experimental data. As already done in [51], we proceed in the opposite way: as masses and couplings are fixed consistently in our Lagrangian, we leave free the subtraction polynomials in the loops $\Pi_{\pi\pi}(s)$, $\epsilon_1(s)$ and $\epsilon_2(s)$. This allows the full data set to contribute to fixing the subtraction constants. The basic (pion and kaon) loop expressions are given in Appendix E and are used only in the form subtracted once (in order that they vanish at $s=0$); they are supplemented with second degree polynomials vanishing at $s=0$ and having coefficients to be fixed by fitting the data.

[8] Actually, near the accepted ϕ mass our perturbation parameters start to carry a tiny imaginary part.

[9] In this reference, the loop expressions for equal mass pseudoscalar meson pairs and vector–pseudoscalar pairs are already given and are correct; the function given for unequal mass pseudoscalar meson pairs is not correct as the contribution of the gauge term has been omitted; we apologize for this error and correct for it in the present paper (see Appendix F).

[10] In this case, the constant term in the ρ propagators is the squared (HK) mass occurring in the Lagrangian with no modification.

7 The model pion form factor in τ decay

Introducing pion and kaon loop effects gives the $\rho^\pm$ a self-mass, but, nevertheless, the $\rho^\pm$ fields remain mass eigenstates. To stay consistent with using the ρ self-mass, one has also to account for loops in the W–ρ transition amplitude. In τ decay the relevant loop effects, while neglecting anomalous VP loops, are the $\pi^\pm\pi^0$ and $K^0K^\pm$ contributions. Accounting for this modifies (4) to

$$F_\pi^\tau(s) = \left[\left(1-\frac{a}{2}\right) - F_\rho^\tau g_{\rho\pi\pi}\frac{1}{D_\rho(s)}\right], \tag{24}$$

with

$$\begin{cases} F_\rho^\tau = f_\rho^\tau - \Pi_W(s)\,, \\ D_\rho(s) = s - m^2 - \Pi'_{\rho\rho}(s)\,, \\ f_\rho^\tau = a g f_\pi^2\,, \end{cases} \tag{25}$$

where $m^2 = a g^2 f_\pi^2$ and the charged ρ self-mass $\Pi'_{\rho\rho}(s)$ has been defined in Sect. 4 by (9) and used in (10) (recall that we neglect VP loops). One should note that (24) and (25) are not affected by any breaking mechanism. The diagrams contributing to the pion form factor in τ decays are sketched in Fig. 1.

Let us denote for a moment the pion and kaon amputated (i.e. computed with unit coupling constants) loops by $\ell_\pi(s)$ and $\ell_K(s)$, assuming that they are already subtracted once in order that they identically vanish at $s=0$ (see Appendix F). The W–ρ transition amplitude and the $\rho^\pm$ self-energy occurring in the pion form factor have the following expressions in terms of pion and kaon amputated loops:

$$\begin{cases} \Pi_W(s) = g_{\rho\pi\pi}\left[\left(1-\frac{a}{2}\right)\ell_\pi(s) + \frac{1}{2z_A^2}\left(z_A - \frac{a}{2}\right)\ell_K(s)\right] \\ \qquad\qquad + P_W(s)\,, \\ \Pi'_{\rho\rho}(s) = g^2_{\rho\pi\pi}\left[\ell_\pi(s) + \frac{1}{2z_A^2}\ell_K(s)\right] + P_\rho(s)\,, \end{cases} \tag{26}$$

where $g_{\rho\pi\pi} = ag/2$ and $P_W(s)$ and $P_\rho(s)$ being subtraction polynomials with real coefficients to be fixed by external renormalization. As emphasized in [51, 61], the polynomials $P_W(s)$ and $P_\rho(s)$ can be chosen independent. Indeed, $\mathrm{Im}\,\Pi_W(s)$ and $\mathrm{Im}\,\Pi'_{\rho\rho}(s)$ are even not proportional as soon as SU(3) is broken ($z_A \neq 1$); moreover, the transition amplitude $\Pi_W(s)$ is non-zero even if $a=2$ as soon as SU(3) symmetry is broken. We choose to constrain $P_W(s)$ and $P_\rho(s)$ to be second degree and vanishing at $s=0$, as discussed in Sect. 6.

For the sake of simplicity, we have also chosen to use the pseudoscalar meson loops assuming $m_{\pi^\pm} = m_{\pi^0}$ and $m_{K^\pm} = m_{K^0}$ after having checked that this is numerically harmless while dealing with all form factor data. Under this approximation[11], we have $\Pi'_{\rho\rho}(s) = \Pi_{\rho\rho}(s)$ (see (8))

[11] This implies that the ρ^0 and $\rho^\pm$ widths do not significantly differ. This statement is supported by the various experimental data collected in [54].

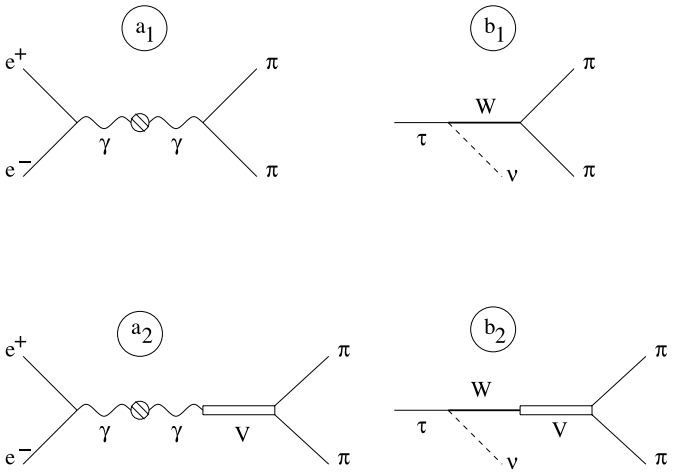

Fig. 1. Schematic representation of the Feynman diagrams contributing to the pion form factor. The *left plots* (referred to as a_1 and a_2) sketch the case of the pion form factor in e^+e^- annihilations, while the *right plots* (referred to as b_1 and b_2) show τ decay. The *upper plots* show the non-resonant HLS specific diagrams, the *lower plots* describe the resonance contributions. The *shaded blobs* represent the photon vacuum polarization. The γV and WV transitions are dressed by s-dependent terms

and all symmetry breaking effects due to the pion mass difference are concentrated in the phase space factors (see (5)–(7)) for cross sections and partial widths where these have a sizable effect.

Therefore, one can rewrite (26) in a form more appropriate for our fitting procedure:

$$\begin{cases} \Pi_W(s) = \frac{1}{g_{\rho\pi\pi}}\left[(1-\frac{a}{2})\Pi^W_{\pi\pi}(s) + (z_A - \frac{a}{2})\epsilon_2(s)\right], \\ \Pi'_{\rho\rho}(s) = \Pi_{\rho\rho}(s) = \Pi^\rho_{\pi\pi}(s) + \epsilon_2(s)\,, \end{cases} \tag{27}$$

where $\epsilon_2(s)$, already defined in (13), carries its own subtraction polynomial, and we have defined

$$\begin{cases} \Pi^W_{\pi\pi}(s) \equiv g^2_{\rho\pi\pi}\ell_\pi(s) + Q_W(s)\,, \\ \Pi^\rho_{\pi\pi}(s) \equiv g^2_{\rho\pi\pi}\ell_\pi(s) + Q_\rho(s)\,, \end{cases} \tag{28}$$

where $Q_W(s)$ and $Q_\rho(s)$ are second degree polynomials[12] (with real coefficients to be fit) and vanishing at the origin. Possible correlations among them, if any, would be an outcome of the fit procedure and can be detected from inspecting the fit error covariance matrix. Finally, one can check that the condition $F_\pi^\tau(0) = 1$ is automatically fulfilled.

Before turning to the pion form factor in e^+e^- annihilations, let us also remind the reader that the τ partial width expression in (5) has to be further corrected for isospin breaking effects by multiplying it by[13] $S_{\mathrm{EW}} =$

[12] We recall here that these polynomials may account for the neglected anomalous loop effects not introduced explicitly.

[13] Actually, this numerical value has been derived for the pion final state; in practical applications, it is usually assumed that this value holds also for the ρ final state – see for instance [34–36].

1.0232, which accounts for short range radiative corrections [37]. Long range radiative corrections have been derived in [38–40] and come as a further factor $G_{\rm EM}(s)$; another estimate taking into account additional Feynman diagrams can be found [41, 42] and a corresponding numerical parametrization of $G_{\rm EM}(s)$ has been provided in [43]. This means that in all our fits we perform the substitution

$$F_\pi^\tau(s) \Longrightarrow S_{\rm EW} G_{\rm EM}(s) F_\pi^\tau(s)\,, \tag{29}$$

which, therefore, accounts for all reported isospin symmetry breaking effects specific to the τ sector. Another isospin breaking effect might have to be considered, namely a ρ^0–$\rho^\pm$ mass difference. This can be generated, for instance, by means of the mechanism sketched in footnote 6. It can be shown that this turns out to modify (25) to

$$\begin{cases} F_\rho^\tau = f_\rho^\tau - \Pi_W(s)\,, \\ D_\rho(s) = s - m^2 - \delta m^2 - \Pi'_{\rho\rho}(s)\,, \\ f_\rho^\tau = agf_\pi^2 + \dfrac{\delta m^2}{g}\,, \end{cases} \tag{30}$$

where δm^2 is left free. The modified (30) allows (24) to still fulfill $F_\pi^\tau(0) = 1$ automatically[14].

8 The model pion form factor in e^+e^- annihilations

In τ decay, the pion form factor, as we have just seen, is free from any vector meson mixing effect. Instead, the expression for the form factor of the pion $F_\pi^e(s)$ is sharply influenced by the vector meson mixing mechanism constructed explicitly in Sect. 5, which leads us to make the transformation from ideal to physical vector meson fields. After this transformation, we get from our effective Lagrangian the diagrams shown in Fig. 1 and the corresponding expression:

$$F_\pi^e(s) = \left[\left(1-\frac{a}{2}\right) - F_\rho^e(s) g_{\rho\pi\pi} \frac{1}{D_\rho(s)} - F_\omega^e(s) g_{\omega\pi\pi} \frac{1}{D_\omega(s)} - F_\phi^e(s) g_{\phi\pi\pi} \frac{1}{D_\phi(s)} \right], \tag{31}$$

where $D_\rho(s)$ (see (25) for its charged partner), $D_\omega(s)$ and $D_\phi(s)$ are the inverse propagators of the corresponding (physical) vector mesons. We now have

$$D_\rho(s) = s - m^2 - \Pi_{\rho\rho}(s) \tag{32}$$

(recall that our assumptions on pseudoscalar meson masses implies $\Pi_{\rho\rho}(s) = \Pi'_{\rho\rho}(s)$, which reduces the number of free parameters in our model). The vector meson couplings to a pion pair after symmetry breaking are

$$\begin{cases} g_{\rho\pi\pi} = \dfrac{ag}{2} \\ g_{\omega\pi\pi} = -\dfrac{ag}{2} \dfrac{\epsilon_1}{\Pi^\rho_{\pi\pi}(s) - \epsilon_2} \\ g_{\phi\pi\pi} = \dfrac{ag}{2} \dfrac{\mu\epsilon_1}{(1-z_V)m^2 + \Pi^\rho_{\pi\pi}(s) - \mu^2\epsilon_2} \end{cases}, \tag{33}$$

where $\Pi^\rho_{\pi\pi}(s)$ has been defined in the previous section. One should note that the quantity called $\Pi_{\pi\pi}(s)$ in the definition of the matrix $R(s)$ (see Sect. 5) coincides with the presently defined $\Pi^\rho_{\pi\pi}(s)$.

The quantities F_V^e can be written

$$F_V^e(s) = f_V^e - \Pi_{V\gamma}(s)\,. \tag{34}$$

Collecting the various couplings of the ideal fields suitably weighted by elements of the matrix transformation $R(s)$ (see (17)), we get

$$\begin{cases} f_\rho^e = agf_\pi^2 \left[1 + \dfrac{1}{3} \dfrac{\epsilon_1}{\Pi^\rho_{\pi\pi}(s) - \epsilon_2} + \dfrac{1}{3} \dfrac{\mu^2\epsilon_1}{(1-z_V)m^2 + \Pi^\rho_{\pi\pi}(s) - \mu^2\epsilon_2} \right] \\ f_\omega^e = agf_\pi^2 \left[\dfrac{1}{3} - \dfrac{\epsilon_1}{\Pi^\rho_{\pi\pi}(s) - \epsilon_2} + \dfrac{1}{3} \dfrac{\mu^2\epsilon_2}{(1-z_V)m^2 + (1-\mu^2)\epsilon_2} \right] \\ f_\phi^e = agf_\pi^2 \left[-\dfrac{\mu}{3} + \dfrac{\mu\epsilon_1}{(1-z_V)m^2 + \Pi^\rho_{\pi\pi}(s) - \mu^2\epsilon_2} + \dfrac{\mu}{3} \dfrac{\epsilon_2}{(1-z_V)m^2 + (1-\mu^2)\epsilon_2} \right] \end{cases} \tag{35}$$

and, keeping only the leading (first order) terms, the loop corrections $\Pi_{V\gamma}(s)$ (see the definitions in (13), and the expression for μ in (12)) are

$$\begin{cases} \Pi_{\rho^0\gamma}(s) = \left(1-\dfrac{a}{2}\right) \dfrac{\Pi^\gamma_{\pi\pi}(s)}{g_{\rho\pi\pi}} + \left(z_A - \dfrac{a}{2} - b\right) \dfrac{\epsilon_1+\epsilon_2}{g_{\rho\pi\pi}} + b\dfrac{\epsilon_2-\epsilon_1}{g_{\rho\pi\pi}} \\ \Pi_{\omega\gamma}(s) = -\left(1-\dfrac{a}{2}\right) \dfrac{\epsilon_1}{\Pi^\rho_{\pi\pi}(s) - \epsilon_2} \dfrac{\Pi^\gamma_{\pi\pi}(s)}{g_{\rho\pi\pi}} + \left(z_A - \dfrac{a}{2} - b\right) \dfrac{\epsilon_1+\epsilon_2}{g_{\rho\pi\pi}} - b\dfrac{\epsilon_2-\epsilon_1}{g_{\rho\pi\pi}} \\ \Pi_{\phi\gamma}(s) = \left(1-\dfrac{a}{2}\right) \dfrac{\mu\epsilon_1}{(1-z_V)m^2 + \Pi^\rho_{\pi\pi}(s) - \mu^2\epsilon_2} \dfrac{\Pi^\gamma_{\pi\pi}(s)}{g_{\rho\pi\pi}} - \left(z_A - \dfrac{a}{2} - b\right) \mu \dfrac{\epsilon_1+\epsilon_2}{g_{\rho\pi\pi}} + b\mu\dfrac{\epsilon_2-\epsilon_1}{g_{\rho\pi\pi}}\,. \end{cases} \tag{36}$$

The first term for each transition loop is the pion loop contribution while the others are respectively the charged and neutral kaon loops. Of course, the functions occurring there are the same as for F_π^τ. We have denoted by $\Pi^\gamma_{\pi\pi}(s)$ the transition amplitude for γ–$\rho^{\rm I}$, which is in correspondence with the W–$\rho^\pm$ transition amplitude introduced in the previous section (see (28)). A priori, the subtraction

[14] Anticipating somewhat the fit results, a possible δm^2 can be detected on ALEPH data [31] (not on CLEO data [33]) and amounts to $\simeq -0.25\ {\rm GeV}^2$. $f_\rho^\tau (\simeq 0.7\ {\rm GeV}^2)$ is then increased by $0.5 \times 10^{-3}\ {\rm GeV}^2$, a quite negligible quantity.

polynomials of $I\!\!\Pi^{\gamma}_{\pi\pi}(s)$ and $I\!\!\Pi^{W}_{\pi\pi}(s)$ might be slightly different. However, in an attempt to reduce further the number of free parameters of the model, we assume that they coincide, which turns out to identify the amputated W–$\rho^{\pm}$ and γ–$\rho^{\rm I}$ transition amplitudes[15]. We shall see that this assumption is well in agreement by the data and, moreover, makes clearer the switching to the expression of the form factor of the τ.

In addition to the explicit dependence of our model on the HLS basic parameters a, g, and on the breaking parameters x, z_A, z_V, z_T and δm^2, there is a further dependence on the subtraction parameters hidden inside $I\!\!\Pi^{\rho}_{\pi\pi}(s)$, $I\!\!\Pi^{W/\gamma}_{\pi\pi}(s)$, $\epsilon_1(s)$ and $\epsilon_2(s)$. Isospin symmetry breaking is reflected in having a non-zero $\epsilon_1(s)$ function. We have

$$\begin{cases} I\!\!\Pi^{W/\gamma}_{\pi\pi}(s) = Q_0(s) + \ell_\pi(s)\,, \\ I\!\!\Pi^{\rho}_{\pi\pi}(s) \;\; = P_0(s) + \ell_\pi(s)\,, \\ \epsilon_1(s) \qquad = P_-(s) + \ell_{K^\pm}(s) - \ell_{K^0}(s)\,, \\ \epsilon_2(s) \qquad = P_+(s) + \ell_{K^\pm}(s) + \ell_{K^0}(s)\,, \end{cases} \tag{37}$$

where $\ell_\pi(s)$, $\ell_{K^\pm}(s)$ and $\ell_{K^0}(s)$ are now the *non-amputated* $\pi^+\pi^-$, K^+K^- and $K^0\overline{K}^0$ loops, subtracted so that these loops vanish at the origin. The parameter polynomials $Q_0(s)$, $P_0(s)$, $P_-(s)$ and $P_+(s)$ are chosen to be of second degree with zero constant terms in order to stay consistent with the node theorem [17, 52].

One can check that $F^e_\pi(0) = 1 + \mathcal{O}(\epsilon_1^2)$, which could have been expected from having neglected terms of order greater than 1 in our diagonalization procedure[16].

As the form factor data collected at the ϕ are not currently available, the last term in (31) could have been removed. However, in order to account for tails effects, we preferred keeping it and use a fixed width Breit–Wigner expression incorporating the mass and width recommended by the Particle Data Group [54]. Due to the narrowness of the ω mass distribution, we also have replaced in our fits the ω propagator by a fixed width Breit–Wigner constructed using the recommended mass and width from [54].

Let us also recall that (31) is our formula for the pion form factor $F^e_\pi(s)$ in both the spacelike and timelike regions. Indeed, for consistency, we will not remove the ω and ϕ meson contributions while going to negative s.

Using the first order correction to the ρ mass eigenvalue, the inverse propagator could have been written $D_{\rho^0}(s) = s - \lambda_\rho(s)$, as the leading order squared mass eigenvalue is

$$\lambda_\rho(s) = m^2 + I\!\!\Pi^{\rho}_{\pi\pi}(s) + \epsilon_2(s)\,. \tag{38}$$

As far as the e^+e^- data are concerned, we shall modify the eigenvalue expression to

$$\lambda_\rho(s) = m^2 + I\!\!\Pi^{\rho}_{\pi\pi}(s) + \epsilon_2(s) + \delta_2\lambda_\rho(s) \tag{39}$$

by adding the second order correction given in (21). This does not add any more freedom in the model, but rather allows for some check of the diagonalization method.

Therefore, the difference between $F^e_\pi(s)$ and $F^\tau_\pi(s)$ is solely concentrated in the coupling changes from ideal to physical fields given by the varying matrix $R(s)$ (see (17)) which only affects $F^e_\pi(s)$. Stated otherwise, modifying the function $F^\tau_\pi(s)$ in order to incorporate isospin breaking effects is strictly equivalent to using our expression for $F^e_\pi(s)$ directly, the factor $S_{\rm EW}G_{\rm EM}(s)$ being removed and δm^2 being made identically zero.

9 The photon vacuum polarization

The raw data on the pion form factor $F^e_\pi(s)$ should be "undressed" by unfolding the contributions due to radiative corrections and to the photon vacuum polarization (VP) before any comparison with the τ data (we refer the reader to [62, 63] for a comprehensive analysis of these factors and for previous references). Quite generally, the available experimental data on $F^e_\pi(s)$ have already been unfolded from radiative corrections [27–30, 59, 64]. All the data sets just referred to are not unfolded from photon vacuum polarization (VP) effects, except for KLOE data [64]. Therefore, one has to account for VP effects by including the corresponding factor when comparing a pion form factor model with the experimental data. Traditionally (see for instance [65] and references quoted therein), this results in the change[17]

$$F^e_\pi(s) \longrightarrow (1 - I\!\!\Pi_{\rm VP}(s))F^e_\pi(s)\,, \tag{40}$$

when comparing with most data sets.

The VP function $I\!\!\Pi_{\rm VP}(s)$ contains two parts. The first one is the sum of the leptonic loops, which can be computed in closed form at leading order. (In Appendix F, we recall the explicit form at order α and give its expression along the real s axis). The second part is the one particle irreducible hadronic contribution to the photon self-energy, which is derived by means of a dispersion relation; at low energy, where non-perturbative effects are dominant, this is estimated using the experimentally measured e^+e^- cross section (see, for instance, [62, 65–67]), while the high energy tail is calculated using perturbative QCD.

For our purpose, we use the sum of the leptonic VP as given in Appendix F for e^+e^-, $\mu^+\mu^-$ and $\tau^+\tau^-$ together with a numerical parametrization of the hadronic contribution. From the two-pion threshold to the ϕ mass, we benefited from a parametrization[18] provided by Davier [68]. Be-

[15] This is nothing but a strong CVC assumption.

[16] Actually, it depends on the (1,2) rotation matrix element: $1 + \mathcal{O}([R_{12}(s=0)]^2)$ and, numerically, the neglected term is $\simeq 1.5 \times 10^{-3}$.

[17] If one denotes by $\Sigma(s)$ the self-mass of the photon, the inverse photon propagator is given by $D^{-1}_\gamma(s) = s - \Sigma(s) = s(1 - \Sigma(s)/s)$. Therefore, compared with traditional notation, we have $I\!\!\Pi_{\rm VP}(s) = -\Sigma(s)/s$. This is not a problem but should be kept in mind.

[18] This parametrization neglects the (very small) imaginary part of the hadronic VP contribution.

low the two-pion threshold and down to $s = -0.25\,\mathrm{GeV}^2$, we use instead the (real valued) parametrization provided by Burkhardt [69].

10 Decay widths of light mesons

In order to compute decay widths and fit data, one has to define the couplings allowing for the decays of the light mesons involved. For the two-photon decays of the η and η' mesons, as well as for the radiative decays of the $\rho^\pm$ and K^* mesons, the couplings defined after SU(3) and nonet symmetry breaking (see (E.2) and (E.5)) are the couplings coming directly in the decay widths formulae (see Appendix E.3), and they do not depend on further isospin symmetry breaking effects other than mass values in phase space factors.

The isospin breaking procedure we presented plays only a role for the ρ^0, ω and ϕ mesons. In order to compute the leptonic decays of these, one has to use the full couplings $F_V^e(s)$ as given by (35) and (36) in (E.9) and computed at the appropriate vector meson masses $F_V^e(m_V^2)$. As the loop functions are slowly varying, one can choose m_V as the Higgs–Kibble masses occurring in the Lagrangian (see (1)), which moreover simplifies the fitting procedure.

For the other (radiative decay) coupling constants one has to combine the ideal coupling constants (given in Appendix E) using the transformation $R(s)$ to derive the physical coupling constants, as was described in [16]; the context, compared to [16], slightly differs due to the fact that, now, the mixing parameters are functions to be computed at the appropriate m_V^2 values in order to go to the vector meson mass shell.

Traditionally, the ρ^0 is decoupled from mixing and is treated as the $\rho^\pm$ and mixing effects are only considered in the (ω–ϕ) sector. In addition, it is usual to treat the (ω–ϕ) mixing angle as a constant to be fit (see [4, 5, 8, 9, 16] and the references quoted therein). The approach in the present study is different: one considers a full (ρ^0–ω–ϕ) mixing scheme (as in [16]), however – for the first time – the mixing parameters are functionally related and the same functions have to be computed at each vector meson mass. For instance, the (ω–ϕ) mixing "angle" has not the same numerical value at the ω mass and at the ϕ mass. This only reflects that the mixing is actually invariant mass dependent. When, as for $\omega \to \pi\pi$ [50] and $\phi \to \pi\pi$ [70, 71] data exist on the phase of the coupling constant, these phases can be introduced in the fit with the same functions, the moduli of which determine the branching fractions.

11 The full set of data submitted to fit

In order to work out the model presented in the sections above, we use several kinds of data sets. In this section, we list them and give some details on the way they are dealt with in our fit procedure.

11.1 Partial width decays

Generally speaking, the decay data submitted to fits have been chosen as the so-called "fit" values recommended by the Particle Data Group (PDG) in the latest (2006) issue of the Review of Particle Properties [54].

This covers, with no exception, the leptonic decay widths of the ρ^0, ω and ϕ mesons, the two-photon decay widths of the η and η' mesons and the $\pi^+\pi^-$ partial width of the ϕ meson. There are two measurements of the phase of the coupling constant $g_{\phi\pi^+\pi^-}$ reported in the literature; the older one [70] is $\psi_\phi = -42^\circ \pm 13^\circ$ and more recently [71] $\psi_\phi = -34^\circ \pm 4^\circ \pm 3^\circ$. Summing up in quadrature the errors, we choose as reference value in our fits $\psi_\phi = -34^\circ \pm 5^\circ$. We could have chosen to include in our fits the two-photon decay width of the π^0; however, we preferred replacing this piece of information by the pion decay constant value $f_\pi = 92.42\,\mathrm{MeV}$ and did not let it vary, as this is supposed to carry a very small error[19] [54].

The RPP pieces of information [54] concerning the ρ and ω decay width to $\pi^+\pi^-$ and the partial width $\rho^0 \to e^+e^-$ are not considered as data to be submitted to fits, as they have all been extracted from fitting the same pion form factor timelike data that we have included in our fit procedure (see the subsection below); this does not prevent us from comparing our results to the RPP available information. This is also true for the relative phase of the couplings $g_{\omega\pi^+\pi^-}$ to $g_{\rho\pi^+\pi^-}$ (the so-called Orsay phase), which has been measured [50] with the result $\psi_\omega = 104.7^\circ \pm 4.1^\circ$.

Instead, it is quite legitimate to include the $\omega \to e^+e^-$ partial width in our fit procedure as, even if this mode could have been marginally influenced by the pion form factor data, it is mostly extracted from the $e^+e^- \to \pi^+\pi^-\pi^0$ data [54]. As the pion form factor spectrum around the ϕ mass is not currently available, the $\phi \to e^+e^-$ partial width is quite legitimately included in our fit data set.

In the present work, as in our previous works on the same subject [8, 9, 16], we do not intend to use the decay widths $K^* \to K\pi$. Actually, as for the width $\rho \to \pi\pi$, which is inherently fit with the pion form factor, the choice of the mass value for a very broad object makes the extraction of coupling constants a delicate matter. It should be more appropriately discussed with the $K\pi$ form factor in τ decays when the corresponding data will become available.

The data on the two kaon partial widths of the ϕ meson are also left outside our fit procedure. In a previous work of some of us [16], as in other works [72] the issue of accommodating the $\phi \to K^+K^-$ partial width was raised. A recent work [73] claims that the ratio of these partial widths can be accommodated by introducing corrections to the decay widths that increase both partial widths as derived from the matrix elements of the transitions. Then the problem may affect both the $\phi \to K^+K^-$ and the $\phi \to K^0\overline{K}^0$ partial widths; therefore, we have preferred leaving both modes outside the fit procedure. We will discuss this issue below in a devoted subsection.

[19] Possible isospin symmetry breaking effects might have to be considered.

We also use all radiative decay partial widths of the light flavor mesons of the form $V \to P\gamma$ or $P \to V\gamma$. As a general rule, we chose as reference data the "fit" values recommended by the PDG as given in the latest RPP issue [54]. There are two exceptions to this statement: the partial widths for $\omega \to \eta\gamma$ and $\omega \to \pi^0\gamma$.

Indeed, as already noted in [16], there is some difficulty in accommodating the present $\omega \to \eta\gamma$ "fit" branching fraction ($(4.9 \pm 0.5) \times 10^{-4}$), while the so-called "average" value [54] ($(6.3 \pm 1.3) \times 10^{-4}$) is much better accepted by our model fitting.

On the other hand, the new "fit" value for the branching fraction $\omega \to \pi^0\gamma$ ($(8.90 \pm 0.25) \times 10^{-2}$) is also hard to accommodate in our model. We show that the previous PDG "fit" value ($[8.50 \pm 0.50] \times 10^{-2}$) seems in better consistency with the rest of the data we handle; we also checked that the value ($[8.39 \pm 0.25] \times 10^{-2}$) produced by a fit [74] performed in a completely different context was also well accepted, pointing to a possible overestimate of the central value for this mode[20]. The questions raised by the values of these two decay widths will be discussed at the appropriate place below.

Finally, we also introduce in the fit procedure the ratio of the kaon to pion decay constants as they are reported in the latest RPP [54]. This actually coincides with our SU(3) breaking parameter ($z_A = [f_K/f_\pi]^2$).

11.2 Timelike form factor data in e^+e^- annihilations

Beside the decay data listed just above, we have included in our fit all data on the pion form factor collected in e^+e^- annihilations by the OLYA and CMD collaborations as tabulated in [75] and the DM1 data [76] collected at ACO (Orsay). These data will be referred to globally as "old timelike data". When included into a χ^2 expression, systematic errors have to be combined with the published statistical errors; they have been first added in quadrature to the statistical errors for the OLYA data (4%) and CMD (2%) following expert advice [77]. However, for the sake of consistency with the new data discussed just below, we preferred extracting the correlated part of the systematic errors, estimated [77] to be 1%, and we have performed the same treatment as for the new data (see below). The accuracy of the DM1 data making the influence of this data set marginal, we did not add any further contribution to the published errors. We only use the data points located below the ϕ meson mass in order to avoid being sensitive to higher mass vector mesons, not included in the present model.

Four additional data sets have been collected later at Novosibirsk on the VEPP2M ring. The first one, covering the region from about 600 to 960 MeV, collected by the CMD2 collaboration [78] and recently corrected [27], is claimed to have the lowest systematic error (0.6%) ever reached in this field.

[20] Looking at [54], the role of the data and analyses for the $e^+e^- \to \pi^0\gamma$ process itself to get the "fit" value for the partial width $\omega \to \pi^0\gamma$ is unclear.

CMD2 has collected in 1998 and recently published two additional data sets; one [28] covering the energy region from 600 to 970 MeV is claimed to reach a systematic error of 0.8%, and a second set [29] covering the threshold region (from 370 to 520 MeV) with an estimated systematic error of 0.7%. On the other hand, the SND collaboration has recently published [30] a new data set covering the invariant mass region from 370 to 970 MeV with a systematic error of 1.3% over the whole data set except for the very low mass region where the (first) two points carry a systematic error of 3.2%.

Concerning these four data sets (which will be referred to globally as "new timelike data"), we could, as per usual, add in quadrature the systematic and statistical errors and then get a diagonal error matrix, which can be used in χ^2 fits in a trivial way.

However, an important part of the systematic uncertainties for these data sets is expected to be a common global scale uncertainty [77], which has been estimated to 0.4% and generates bin to bin correlated errors. In principle, one should take the latter information into account in the fits; this implies dealing with systematic and statistical errors in a way slightly more elaborate than simply adding in quadrature statistical and systematic errors.

First, the (bin per bin) uncorrelated part of the systematic error is derived by subtracting in quadrature 0.4% from the already quoted systematic errors. This uncorrelated part of the systematic error (i.e. $\sqrt{\sigma^2_{\rm syst.} - (0.4\%)^2}$, depending on the data set considered) can certainly be added in quadrature to the statistical error bin per bin, giving a combined standard deviation named σ_i for the measurement m_i in the energy bin i; the σ_i are uncorrelated errors and define a diagonal error matrix. The question then becomes how to redefine the full covariance matrix for each experiment, it being understood that the quantity to be compared with the theoretical pion form factor $f_i^{\rm th}$ for each energy bin i is related with the measurement m_i by

$$f_i^{\rm th} \longmapsto m'_i = (1 + \delta\lambda) m_i \,, \tag{41}$$

where $\delta\lambda$ is considered a Gaussian random variable with zero mean and standard deviation $\lambda = 0.4 \times 10^{-2}$. With this assumption it is possible to model reasonably well the covariance matrix, which is no longer diagonal.

Second, one has to treat these correlations. The quoted correlated systematic error is a conservative estimate of the accuracy of radiative corrections performed on the four data sets using the same Monte Carlo generator [77]. Therefore, the fit parameter introduced in order to optimize the absolute scale should be the same for all data sets; in statistical terms, this fit parameter value can be considered as only *one* sampling of the Gaussian random variable $\delta\lambda$ defined just above and should be valid for all data collected by the CMD2 and SND collaborations.

If the correlated part of the systematic error was strictly zero, the error covariance matrix for each data set would simply be given by

$$V_{ij} = \sigma_i^2 \delta_{ij} \,, \tag{42}$$

where i and j label energy bins in the data set. In the case of existing correlations, having defined σ_i as the sum in quadrature of the statistical error and the uncorrelated systematic error in the ith bin, the error covariance matrix elements can be written

$$V_{ij} = \sum_{k,l} M_{ik} W_{kl} M_{lj} \,, \tag{43}$$

where

$$M_{ij} = \sigma_i \delta_{ij} \,, \quad W_{ij} = \delta_{ij} + \lambda^2 e_i e_j \,, \tag{44}$$

$\lambda = 0.4 \times 10^{-2}$ being the standard deviation of the correlated error function and the vector e being defined by its components on the various energy bins i as the ratio of the corresponding measurement and its uncorrelated error:

$$e_i = m_i/\sigma_i \,, \quad \forall i \in [1, \cdots n_{\text{measur.}}] \,. \tag{45}$$

However, what is relevant for χ^2 fitting is not so much the covariance matrix (44) as its inverse. It so happens that the matrix W can be inverted in closed form:

$$W^{-1}_{ij} = \delta_{ij} - \mu^2 e_i e_j \,, \quad \mu^2 = \frac{\lambda^2}{1 + \lambda^2 \sum_{i=1}^{n_{\text{measur.}}} e_i^2} \,, \tag{46}$$

and the full error covariance matrix is also inverted in closed form:

$$V^{-1}_{ij} = \sum_{k,l} M^{-1}_{ik} W^{-1}_{kl} M^{-1}_{lj} \,. \tag{47}$$

This is, together with the measured values, the main ingredient of the χ^2 calculation, which will be performed with the four new timelike data sets. Finally, while fitting the new data, a term has to be added to the χ^2; calling λ_{fit} the fit parameter for the global scale common to all the new Novosibirsk data sets and $\lambda_{\text{exp}} = 0.4 \times 10^{-2}$ the scale uncertainty on the measured form factor estimated by the experiments, this additional contribution to the χ^2 is simply $[\lambda_{\text{fit}}/\lambda_{\text{exp}}]^2$.

Mutatis mutandis, the same method has been applied to the old Novosibirsk data sets using another global scaling factor λ'_{fit} with $\lambda'_{\text{exp}} = 1.0 \times 10^{-2}$, as recommended by informed people [77], and the same procedure to construct the final inverse covariance matrix to be used in fits.

A new data set has recently been collected by the KLOE collaboration [64] using the radiative return method. Existing analyses (see, for instance, the short account in [26]), however, report a disagreement between KLOE data and the recently collected data sets at Novosibirsk due to some systematic effect presently not understood. A recent study of a parametrization of the pion factor [79] argues for a possible systematic energy shift in the data, which would be detected by fitting the ω mass. In view of this unclear situation, we have found it appropriate to postpone including the existing KLOE set among our fitting data samples.

11.3 Spacelike pion form factor data

In order to further constrain the pion form factor in the timelike region, information on the close spacelike region is valuable. Reliable data on the pion form factor in the negative s region are somewhat old [59, 80]. The Fermilab data set [80] consists of 14 measurements of $|F_\pi(s)|^2$ between $s = -0.039\,\text{GeV}^2/c$ and $s = -0.092\,\text{GeV}^2/c$ with 2%–7% statistical error; an estimated systematic error (overall normalization) of 1% is provided in [80]. The NA7 data cover the region between $s = -0.015\,\text{GeV}^2/c$ and $s = -0.253\,\text{GeV}^2$ with 45 measurement points and an overall statistical precision better than those of the Fermilab data. However, NA7 data are also claimed to undergo an overall scale error of 0.9% rms.

One will use these two data sets and treat these correlated systematic errors exactly as explained above for the timelike pion form factor data.

Data have more recently been collected at the Jefferson Accelerator Facility [81] and reanalyzed in order to optimize the extraction of the pion form factor data in the region for s between -0.60 and $-1.60\,\text{GeV}^2$ with a quoted uncertainty of about 10%. No precise information on the correlated–uncorrelated sharing of the systematic error is reported. Including these data involves some more studies and modeling, which goes beyond the main task of the present work, namely, to check the consistency of the e^+e^- and τ data.

11.4 Phase pion form factor data

There are several data sets available, which provide measurements of the isospin 1 part of the $\pi\pi$ amplitude phase shift. The most precise set is the CERN/Munich one [82], but the older Fermilab data set [83] is still useful. However, systematic errors here are not completely controlled. Moreover, as we neglect vertex corrections at the $\pi\pi$ vertex and t-channel resonance exchanges, one cannot draw firm conclusions when comparing the phase information of our pion form factor with phase shift data. Therefore, we have left these data outside our fitting procedure and limited ourselves to simply comparing graphically with the phase of our pion form factor.

11.5 Pion form factor data from τ decays

There are presently three available data sets concerning the pion form factor. These have been collected at LEP by ALEPH [31] and OPAL [32] collaborations and at much lower energy by the CLEO collaboration [33].

The data provided by the ALEPH collaboration [31] include the covariance matrices for statistical and systematic errors, which should be added before inversion in order to be used in a χ^2 minimization. There is some disagreement between ALEPH [31] and OPAL data [32], which has led most works to discard this data set; we shall do likewise.

The CLEO data [33] on the pion form factor are also provided with their full error matrix, but one that accounts for statistical errors only. Statistical errors dominate most

of the systematic uncertainties except for those contributing to the absolute energy scale for determining $\sqrt{s}$ [84]. These were quantified by CLEO as a systematic uncertainty on the value of the $\rho^\pm$ mass obtained in their fits to form factor models, estimated to be 0.9 MeV. This error, not accounted for by the CLEO error covariance matrix, is a systematic error that correlates the various bin energy values. In contrast with the Novosibirsk data, it is not easy to rigorously account for this correlated systematic error[21]. As an approximation we allow the central bin $\sqrt{s}$ value to vary by some ε MeV and add $[\varepsilon/0.9]^2$ to the CLEO data χ^2. This approach provides a simple and reasonable way to deal with the data and errors [84].

In order to stay consistent with our dealing with e^+e^- data, we have limited our fitting range to the ϕ mass and then removed all points above $s = 0.9\,\mathrm{GeV}^2$. This leaves us with 33 measurements from ALEPH and 25 from CLEO, largely unaffected by higher mass vector meson effects, as will be checked.

12 The main global fit to the data sets

12.1 General comments about the fits

Our global model has seven parameters carrying an obvious physical meaning:

- the universal vector coupling g,
- the SU(3) breaking parameter z_A (expected to coincide with $[f_K/f_\pi]^2$ within errors),
- the nonet symmetry breaking parameter x,
- the basic HLS parameter a (expected close to 2),
- the parameter z_V, which mostly governs the mass difference between the ρ^0–ω system and the ϕ meson but also plays a role in some coupling constants,
- z_T which affects only the K^* radiative decay sector in the data used, and, finally,
- the ρ^0–$\rho^\pm$ squared mass shift δm^2.

These have already been fit in isolation in related previous works [8, 9, 16, 51, 85] and we expect to find fit values close to the already published ones. Within our approach, the pseudoscalar mixing angle is not free but is derived from the previous parameters using (E.7) and is expected to be close to -10.5° from previous fits [8, 16]. This has been found in perfect agreement with the two-angle formulation [11] expressed in the framework of extended chiral perturbation theory [13, 14].

Beside these parameters, carrying a clear physical meaning, one has the subtraction polynomial of the pion loop (mostly associated with the ρ meson self-energy), assumed to be written $c_1 s + c_2 s^2$, with c_1 and c_2 to be fit. Two additional subtraction polynomials carrying the same form and associated with the difference ($\epsilon_1(s)$) and the sum ($\epsilon_2(s)$) of the K^+K^- and $K^0\overline{K}^0$ loops introduce four more parameters[22] to be fit. Finally, two more subtraction parameters come from the specific subtraction of the $\gamma\rho$ (or $W\rho^\pm$) transition amplitude. We thus end up with 15 parameters[23] for a number of data of 344 (18 decay modes, 127 data points from the new timelike pion form factor data, 82 from the old timelike pion form factor data, 59 data points in the spacelike region, 33 data points coming from ALEPH data and 25 from CLEO).

In addition to these parameters, which define our model, we have to account for correlated systematic errors in several experiments by fitting the corresponding scale factors and using the experimental pieces of information as constraints. These additional degrees of freedom are therefore exactly compensated in number by the constraints. This covers the global scale factor of the former Novosibirsk experiments as reported in [75] (estimated to 1.0% rms), the global scale factor of the new Novosibirsk experiments as reported in [27–30] (estimated to be 0.4% rms), the scale factor for the NA7 [59] and Fermilab [80] data (estimated respectively to be 0.9% and 1.0% rms). Finally, the CLEO data set is expected to carry a systematic energy shift, which will be fit and is expected [84] to be of the order 0.9 MeV.

We have performed various kinds of fits. In all of them, as detailed above, we have introduced all usual symmetry breaking effects in the value of meson masses, the prominent effects of ρ^0–ω–ϕ mixing (for the e^+e^- data) and the long and short range [37] IB correction factors (for the τ spectra). We have observed that the two proposed ways to account for long range corrections by either of the [38–40] and [41–43] approaches provide quite similar effects and that, on the basis of probabilities, the difference was never observed significant in any of our fits. For definiteness, we choose to use the function of [38–40] for all results presented here.

On the other hand, it was useful to check the effect of excluding the photon vacuum polarization (VP), by fixing the corresponding factor to 1. We also found it of interest to perform fits by excluding either the τ data or the spacelike data; this gives information on the effect of these on the global fit quality and on the stability of the fit parameter values. Finally, it has also been of interest to check the mass shift effect between the ρ^0 and the $\rho^\pm$ mesons, by fixing the corresponding parameter to zero. The results summarizing the statistical qualities are gathered in Table 1 and the fit parameter values can be found in the appropriate data column of Tables 2 and 3.

12.2 Discussion of the fit information

Table 1 reports the statistical information on our fits under various conditions. Generally speaking, the fit quality is al-

[21] It affects the position of the measurement, not the measured value itself.

[22] We note that we approximate the $K^\pm K^0$ loop by the average value of the K^+K^- and $K^0\overline{K}^0$ loops in order to limit the number of free parameters.

[23] It will be emphasized later on that one among these subtraction parameters does not influence the fit and can be safely fixed to zero.

Table 1. The first column lists the subset named as defined in the text together with its number of measurements and condition(s) if any. Each row displays the corresponding χ^2 contribution under the condition quoted in the heading of the data column. The last row gives the total χ^2/(number of degree of freedom), followed by the fit probability. Information written boldface indicates the χ^2 distance of the fit function to a data set left outside from the fit procedure together with its number of data points. In this case, the condition parameter associated with the corresponding data set (scale or mass shift) is fixed at the value returned by the full global fit reported in the second data column and given in Table 2

Data Set	Without VP	with vacuum poliarisation (VP)			
# (data + conditions)	Full fit	Full fit	No τ	No spacelike	No ρ mass shift
Decays (18 + 1)	11.46	11.13	11.52	11.48	11.25
New timelike (127 + 1)	132.81	128.10	122.02	125.76	132.23
Old timelike (82 + 1)	62.22	59.05	54.68	55.20	60.15
Spacelike (59 + 2)	68.53	65.70	55.20	**89.82/(59)**	65.13
τ ALEPH (33)	27.06	23.86	**42.27/(33)**	20.80	24.48
τ CLEO (25 + 1)	25.53	26.06	**26.16/(25)**	29.72	28.55
χ^2/dof	327.40/331	313.83/331	257.73/274	238.81/272	321.75/332
Probability	54.6%	74.3%	75.2%	92.7%	64.7%

Table 2. Parameter values in fits performed including the photon VP. Three data columns are associated with all data (first data column), removing only the τ data (second data column) and removing only the spacelike data (third data column). The last data column reports parameter values returned while fitting all data sets by fixing $\delta m^2 \equiv 0$. Information written boldface displays values not allowed to vary in the fit procedure

Parameter	Full fit	No τ	No spacelike	No ρ mass shift
Scale new timelike	1.006 ± 0.004	1.000 ± 0.003	1.004 ± 0.003	1.007 ± 0.003
Scale old timelike	1.012 ± 0.009	1.010 ± 0.009	1.011 ± 0.009	1.013 ± 0.009
Scale NA7	1.008 ± 0.007	1.008 ± 0.007	**1.008**	1.011 ± 0.006
Scale Fermilab	1.006 ± 0.007	1.006 ± 0.008	**1.006**	1.008 ± 0.007
CLEO shift (MeV)	0.40 ± 0.52	**0.40**	0.36 ± 0.52	1.37 ± 0.39
δm^2 (10^2 GeV^2)	-0.268 ± 0.095	**−0.268**	-0.285 ± 0.096	**0**
a	2.303 ± 0.012	2.297 ± 0.012	2.292 ± 0.012	2.306 ± 0.012
g	5.576 ± 0.015	5.578 ± 0.017	5.597 ± 0.016	5.573 ± 0.015
x	0.903 ± 0.013	0.902 ± 0.013	0.902 ± 0.013	0.903 ± 0.013
z_A	1.503 ± 0.010	1.505 ± 0.010	1.507 ± 0.010	1.503 ± 0.010
z_V	1.459 ± 0.014	1.466 ± 0.014	1.453 ± 0.014	1.460 ± 0.014
z_T	1.246 ± 0.049	1.245 ± 0.049	1.243 ± 0.049	1.246 ± 0.049

Table 3. Parameter values under various strategies (cont'd). Boldface parameters are not allowed to vary. Each subtraction polynomial is supposed to be written $c_1 s + c_2 s^2$

Parameter	Full fit	No τ	No spacelike	No ρ mass shift
Subtraction Polynomial: $\Pi^{\rho}_{\pi\pi}(s)$				
c_1	**0**	**0**	**0**	**0**
c_2	-0.467 ± 0.013	-0.463 ± 0.014	-0.472 ± 0.013	-0.470 ± 0.013
Subtraction polynomial: $\epsilon_2(s)$				
c_1	-0.071 ± 0.003	-0.071 ± 0.003	-0.072 ± 0.003	-0.072 ± 0.003
c_2	0.045 ± 0.004	0.045 ± 0.004	0.046 ± 0.004	0.045 ± 0.004
Subtraction polynomial: $\epsilon_1(s)$				
c_1	-0.017 ± 0.001	-0.017 ± 0.001	-0.017 ± 0.001	-0.017 ± 0.001
c_2	0.020 ± 0.001	0.020 ± 0.001	0.020 ± 0.001	0.020 ± 0.001
Subtraction polynomial $\Pi^{W/\gamma}_{\pi\pi}(s)$				
c_1	0.918 ± 0.061	0.944 ± 0.068	0.727 ± 0.074	0.915 ± 0.060
c_2	0.433 ± 0.106	0.361 ± 0.115	0.831 ± 0.145	0.440 ± 0.105

ways either reasonable or very good, as is clear from the last row in Table 1.

As a first remark, neglecting to account for photon vacuum polarization effects does not end up with a dramatic failure; however, there is a general improvement, while introducing the corresponding function. The negligible degradation observed for CLEO data is entirely produced by the value found for the CLEO mass shift param-

eter (which contributes to the χ^2, as explained above) will be discussed below. This statement clearly follows from comparing the two data columns called "full fit" in Table 1.

The gain in χ^2, while including the photon VP, is 13.5 units without any additional parameter freedom and, in terms of the fit probability, one wins 20%. Therefore, one may conclude that the data description prefers including explicitly the photon VP, while fitting the e^+e^- data. Under realistic conditions, the fit probability is then always of the order 75% or better.

The fits have always been performed using the package MINUIT [86] and the errors quoted are always the improved errors returned by the routine MINOS. This has allowed us to check that the minimum χ^2 was always locally parabolic, which provides symmetric errors.

Tables 2 and 3 display the fit parameter values as returned by the fit under the conditions defined by the various titles of the data columns. We only provide results including the photon VP inside the definition of the pion form factor for e^+e^- annihilations. Comparing the various data columns in Tables 2 and 3 clearly illustrates that the fit parameter values stay close together, and generally widely within their (MINOS) errors. The single exception is obtained while removing the spacelike data; in this case, the coefficients for the subtraction polynomial $\Pi^{W/\gamma}_{\pi\pi}$ differ significantly from all other cases. This could have influenced the predicted values for the $V \to e^+e^-$ partial widths; however, we have checked that this is not the case numerically.

Among the fit parameter values given in Table 2, the most interesting are clearly the fit values for the scale factors, which are nicely consistent with the corresponding experimental information recalled at the beginning of this section.

The single exception is the CLEO global invariant mass shift, which is found to be consistent with zero. Taking into account the way the 0.9 MeV expected shift has been determined[24] [84], this information is interesting. It will be discussed again when examining the fit residuals, which provides additional important information.

The third and fourth data columns in Table 1 provide further information.

i/ Removing the τ data from the fit sample, one can construct the *predicted* distributions for the ALEPH and CLEO data, which are fully derived using our model together with only light meson partial width decays and the e^+e^- data. The predicted χ^2 distance to the CLEO data is practically unchanged with respect to fitting with them, while the prediction for the ALEPH data is not as good even if it remains reasonable[25]. This indicates that CLEO data are in such a nice agreement with the predictions (especially the e^+e^- data) that they do not really constrain the fit! In this respect, the ALEPH data, while introduced in the fit data set, clearly influence the procedure.

ii/ Removing only the spacelike data looks a little bit more appealing. The χ^2 distance of the NA7 and Fermilab data altogether is degraded by $\simeq 24$ units, and the fit probability grows from 74% to 93%, pointing to some slight difficulty in accommodating these data sets. However, this result is by no way problematic enough to either force us to remove the spacelike data or to deeply question their quality.

In order to compute the χ^2 distance of the data samples left out from the fit, one had to choose either the CLEO energy shift or the NA7 and Fermilab scale factors, as they can no longer be fit. We choose to fix them to their fit value as given in the first data column in Table 2.

Tables 2 and 3 mostly illustrate that, whatever the fit conditions examined, the location of the minimum in the fit parameter space remains practically unchanged (with the exception mentioned above). The results obtained by removing the τ data from the fit sample, those by removing the spacelike data, those corresponding to removing the photon VP function (not shown) ... are consistent with each other. Let us note that the fit parameter c_1 in the $\Pi^{\rho}_{\pi\pi}(s)$ function (i.e. essentially the ρ self-mass function) has been fixed to zero, as it was not found to sensitively affect the fits in the energy range we are fitting. The various fit conditions only affect the fit quality, which varies from good to very good, while including the photon VP.

Figure 2 shows the fit with the e^+e^- data in the timelike region superimposed. The global scale factor effects are accounted for. In the ϕ mass region, the line shape is a prediction essentially derived from the phase and branching fraction of the $\phi \to \pi^+\pi^-$ decay mode as measured by the SND collaboration [71]. Information on the full (local) invariant mass spectrum (when available) would certainly improve this prediction.

Likewise, Fig. 3 shows the fit function and the ALEPH [31] and CLEO [33] data superimposed. One may note that the highest data point from the CLEO data lies at $\simeq 2\sigma$ of the fitting curve. Actually, the line shape of the CLEO data in the neighborhood of the maximum raises some difficulty while fitting, as will be seen shortly with the fit residuals.

The left-hand side of Fig. 4 shows the spacelike data [59, 80] together with the fit function. One may note a small but systematic upwards shift of the fit compared with the NA7 data, which certainly explains the jump in the fit probability while removing this data sample from the fit.

One may conclude from Figs. 2–4 and the fit probabilities that the agreement of the data with the model functions is good and that no obvious drawback shows up.

In order to refine this statement, we have had a closer look at the fit residual plots. The fit residuals for the new Novosibirsk data are shown in Fig. 5. The plotted experimental errors do not take into account the bin-to-bin correlations generated by the global scale error common to all data sets. As the difference between our pion form factor functions $F^e_\pi(s)$ and $F^\tau_\pi(s)$ essentially lies in the

[24] This is in order to make consistent the ρ parameters derived from fits to the ALEPH and CLEO data.

[25] The χ^2 distance for the fit part of the ALEPH spectrum corresponds to an average χ^2 per point of 1.28 and thus to an average distance of 1.13σ per data point. As a prediction, it is already a good starting point, which is improved by the global fit to an average distance of 0.90σ per data point.

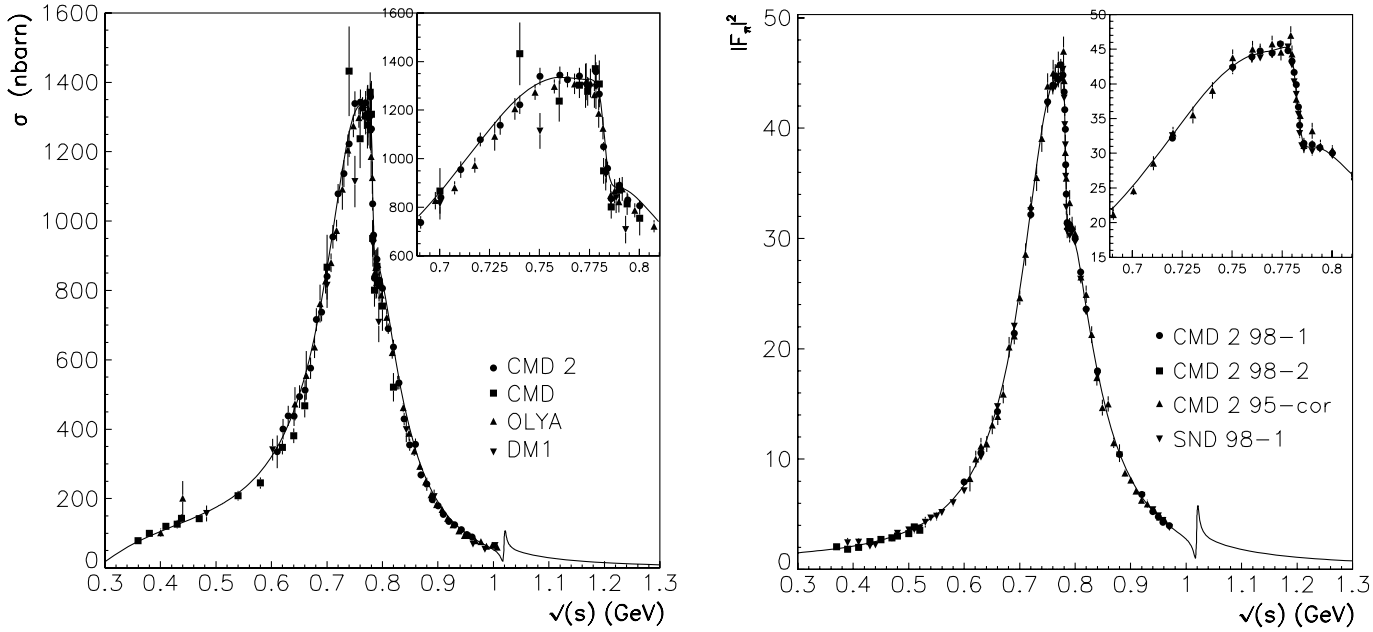

Fig. 2. Data and fits for the pion form factor in the e^+e^- timelike data. The *left figure* gives the fit cross section with, superimposed, the data from the OLYA and CMD collaborations [75], the data set [76] from the DM1 collaboration and the first (corrected) data from CMD2 [27]. The *right figure* shows the form factor curve with superimposed all data sets collected recently at Novosibirsk [27–30]. The ϕ region is commented upon in the body of the text

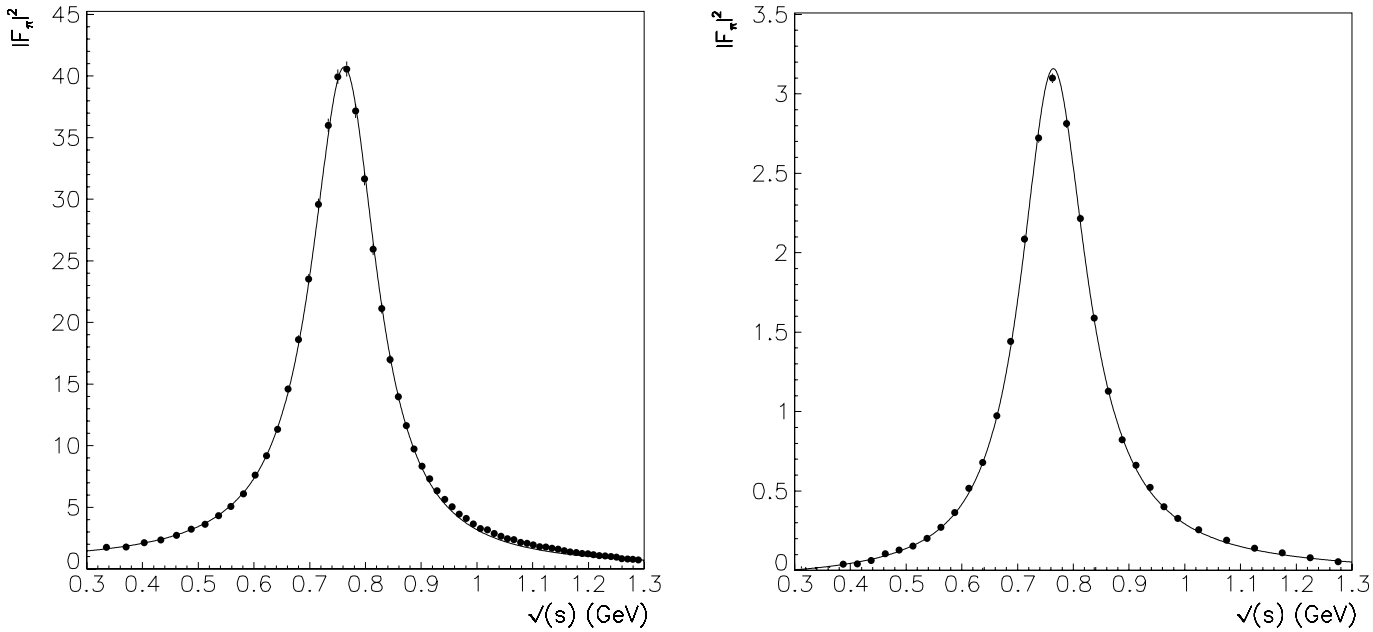

Fig. 3. Data and fits for the pion form factor in τ decay. The *left figure* shows the case for the ALEPH data [31], the *right figure* shows the case for the CLEO data [33]

ρ^0–ω–ϕ mixing scheme produced by breaking isospin symmetry, this figure can be compared with Fig. 1 in [26] or Fig. 9 in [36], where a systematic s-dependent effect was pointing towards a consistency problem between e^+e^- and τ data; such an effect is no longer observed, pointing to a presently more adequate manner of performing the breaking of isospin symmetry. One may possibly note that the dispersion of the residuals is very small everywhere for the 1998 CMD2 data [28, 29], while it is larger for the 1995 CMD2 [27] and SND [30] data, which additionally are moved in opposite directions in the ω mass region. This indicates that our fit parameter values are dominated by the 1998 CMD2 data.

The residual distributions for τ data – the upper plots in Fig. 6 – look more interesting. The arrows indicate the limit of the fit regions. The errors plotted are certainly

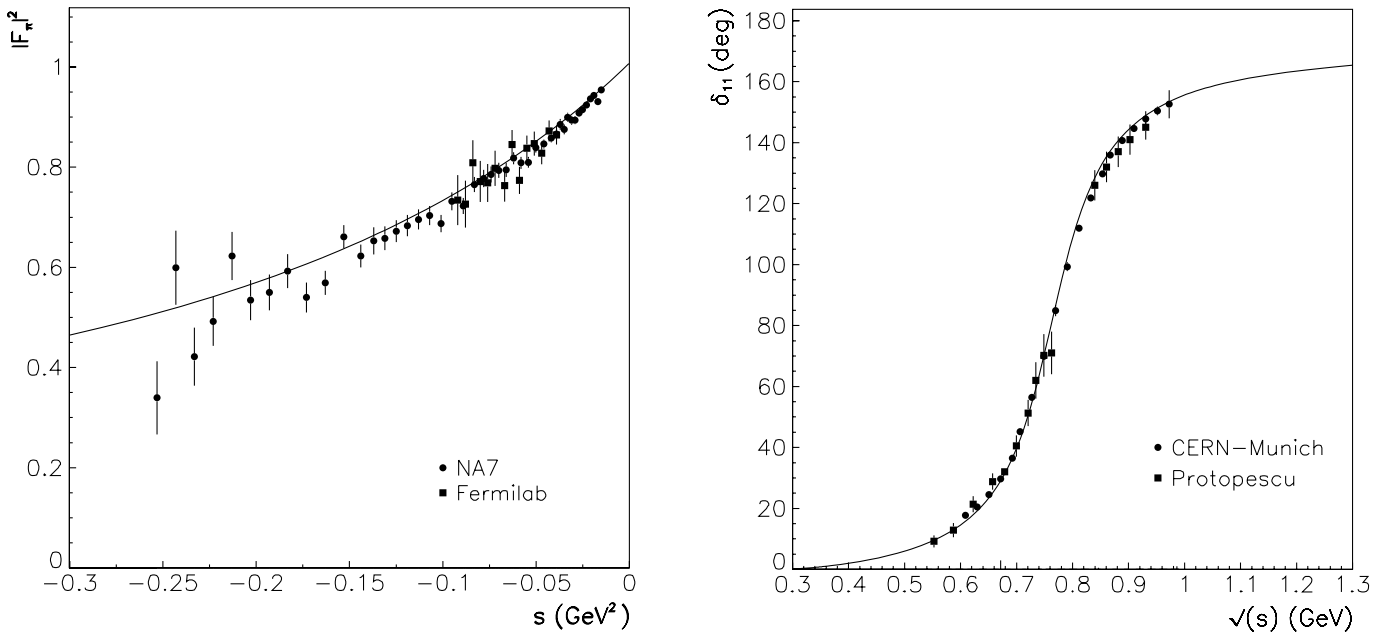

Fig. 4. The *left figure* shows the fit in the spacelike region close to $s = 0$ together with the data from NA7 [59] and Fermilab [80]; fit scale factors (1.008 and 1.006 respectively) have been applied. The *right-hand side figure* shows the prediction for the P_{11} phase shift with the Cern–Munich data [82] and the data from [83] superimposed

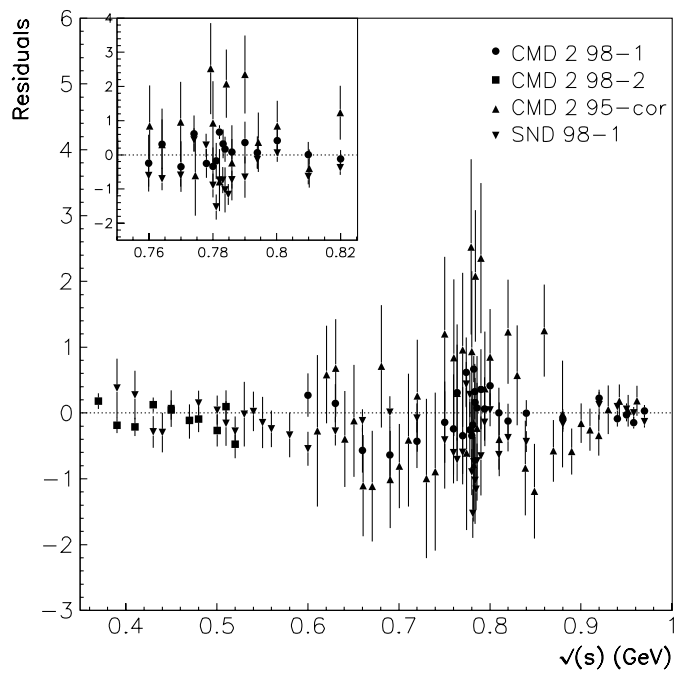

Fig. 5. Residual distribution for all the e^+e^- new timelike data over the whole invariant mass interval. The *inset* magnifies the ρ peak invariant mass region

underestimated, as the bin-to-bin correlations are not accounted for in the drawings; moreover, the errors produced by identifying invariant mass coordinate and central bin value also are not considered.

One now observes a small but clear s-dependent structure above the ρ peak location (more precisely above $s \simeq$ 850 MeV), which certainly reflects the influence of the unaccounted for higher mass vector mesons. One has also examined the effect of removing the parameter δm^2 by fixing it identically to zero while fitting. The τ data residuals are given by the lower plots in Fig. 6. One clearly observes the rise of a structure at the ρ peak location in the ALEPH data, which is therefore a clear signal of a ρ^0–$\rho^\pm$ mass difference. The mass shift observed is

$$m^2_{\rho^0} - m^2_{\rho^\pm} = -\delta m^2 = (0.27 \pm 0.10) \times 10^{-2}\,\mathrm{GeV}^2$$
$$\Longleftrightarrow m_{\rho^0} - m_{\rho^\pm} = 1.73 \pm 0.60\,\mathrm{MeV}\,, \qquad (48)$$

in good agreement with several other reported values [54]. This question will be discussed with more details in the subsection devoted the ρ meson parameters.

In contrast, the shape of the CLEO residual distribution rather indicates a systematic effect in CLEO data located only in the ρ peak region. The global CLEO energy shift of 0.9 MeV serves to recover from the disagreement with the ALEPH data. However, these plots clearly show that the problem of systematics is not global but local and that there is no evidence for a significant global invariant mass shift within the CLEO data in our fit range. As this residual behavior is also observed in the stand-alone fit performed in [33] (see Fig. 10 therein), it should not follow from the constraints specific to our model.

Actually, there is a correlation between δm^2 and the CLEO energy shift ε, which vanishes when performing a simultaneous fit of ALEPH and CLEO data. In order to check this statement, we have removed the ALEPH data from the fit data set. Then, fixing $\delta m^2 \equiv 0$, we get $\varepsilon = 1.57 \pm 0.40$ MeV and, conversely, fixing $\varepsilon \equiv 0$ results in $-\delta m^2 = (0.36 \pm 0.08) \times 10^{-2}\,\mathrm{GeV}^2$, with no change in the χ^2 value and always the same residual shape as shown

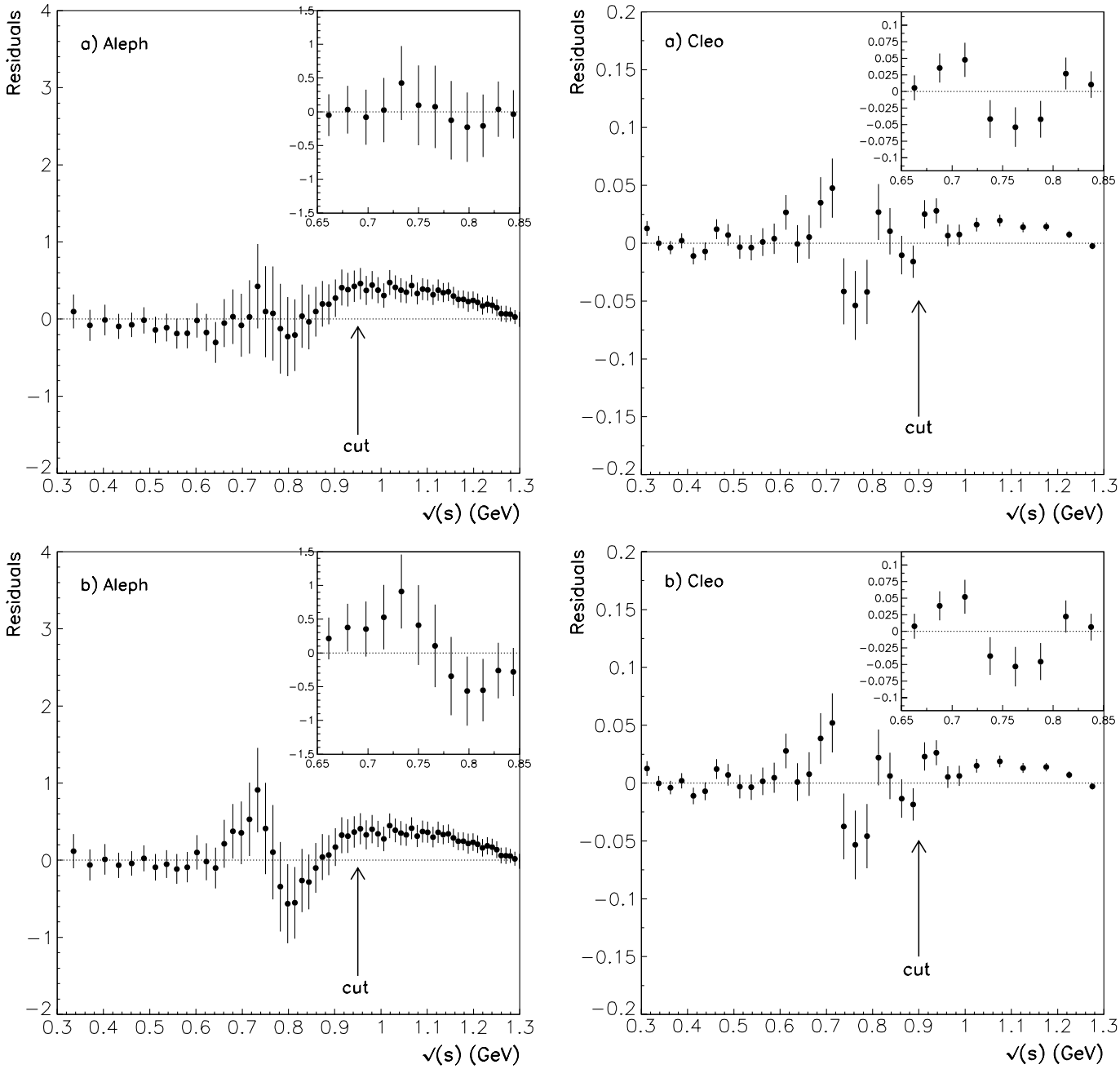

Fig. 6. Distribution of fit residuals for the τ data. The *upper* two plots give the residuals for ALEPH and CLEO data within the model presented. The *lower plots* show the τ data residuals when fitting without a ρ^0–$\rho^\pm$ mass shift (i.e. $\delta m^2 \equiv 0$ is required); one should note the vanishing of the structure around the ρ peak in ALEPH data produced by the ρ^0–$\rho^\pm$ mass shift. One should also note that the CLEO residual is not modified

in Fig. 6. Therefore, the value for δm^2 is set by the ALEPH data and should be confirmed by forthcoming data sets. Correspondingly, it is the use of the ALEPH data that indicates that the CLEO energy shift could well be consistent with zero.

All the reported exercises also show, as is clear from Tables 2 and 3, that the fit parameter values are stable (with the exception already mentioned). This means that our model is overconstrained and that, practically, only the fit quality (i.e. the height of the minimum) is affected by the various conditions we have imagined. We were also aware of possible correlations between the subtraction polynomials. Looking at the fit error covariance matrix, we did not observe strong correlations between the parameters belonging to different polynomials, which seems to indicate that they are indeed independent.

Therefore, one may consider that the description of all form factor data supports our mixing model, as reflected by the statistical fit qualities reported in Table 1 under various conditions.

Finally, the right-hand side of Fig. 4 shows the *predicted* phase of the $I = 1$ part of the pion form factor together with the measured P_{11} $(\pi\pi)$ phase data from [82, 83]. Clearly, the description is good, keeping in mind that some contributions have not been included, especially the exchange of a spacelike ρ. Therefore, this figure indicates that the neglected diagrams should contribute not more than a few degrees to the phase.

Therefore, the description of all form factor data can be considered as satisfactory and provides a solid ground to our main assumptions:

- **j/** The bulk of the isospin symmetry effects that create the difference between the e^+e^- and τ form factor line shapes is a ρ^0–ω–ϕ mixing scheme of dynamical (i.e. s-dependent) structure.
- **jj/** An appropriate subset of meson partial width decays and the e^+e^- form factor data mostly suffice to set up a ρ^0–ω–ϕ mixing scheme able to derive the τ spectrum with good precision.
- **jjj/** The effects of higher mass vector mesons in the mass region below 1.0 GeV, even if somewhat visible on the upper wing of the ρ peak, are negligible.
- **jv/** The (observed) ρ^0–$\rho^\pm$ mass shift is very small and of negligible effect. New τ data may confirm its relevance, as this follows only from the ALEPH data.

In view of the residuals shown in Fig. 5 and, even more clearly in Fig. 6, the statement in **jjj/** can be precisely commented upon. Because of their statistical accuracy, the Novosibirsk data do not exhibit any effect beyond doubt of higher mass resonances within the whole fit range; one may possibly guess a dip (of small significance) in the region between 850 and 900 MeV. In the CLEO data (right plots in Fig. 6), the residual structure is unclear in the region between $\simeq 700$ and $\simeq 950$ MeV, while in the region above $\simeq 1$ GeV, there is without doubt a missing structure, which can reasonably be attributed to the $\rho(1450)$ meson low mass tail. If one relies on the ALEPH data (left plots in Fig. 6), one is instead tempted to state that higher mass vector meson effects have influence down to $\simeq 850$ MeV (i.e. deep inside the high mass wing of the $\rho(770)$ meson). Additional τ data sets and large statistics e^+e^- data sets (collected through the radiative return method) are expected in the near future from B-factories and from DAPHNE, hopefully with controlled systematics. One may imagine that they should allow one to clarify the situation in the region from the ω to φ peak.

12.3 Light meson decays

As a preliminary remark, when fitting partial widths (actually coupling constants), the recommended data used are the partial widths taken from the RPP [54], when available. If not, they are derived from the branching ratios and the full widths. Sometimes, this procedure reveals surprising information. For instance, for $\eta \to \gamma\gamma$, the ratio of the "fit" partial width error to the corresponding central value is $0.026/0.51 = 0.05$, while the corresponding information derived from the quoted "fit" branching fraction is $0.26/39.98 = 0.007$, which might look somewhat optimistic.

Table 4. Reconstructed branching fractions for radiative and leptonic decays using any of the various fit strategies. The reported values are the mean value and the rms of the simulated distributions. The last column displays the recommended branching ratios [54]. The symbol $(*)$ indicates data commented upon in the text, $(**)$ indicates data that are not introduced in the fit procedure

Decay mode	Fit value	PDG/Reference
$\rho \to \pi^0\gamma$ $[\times 10^4]$	5.17 ± 0.04	6.0 ± 0.8
$\rho \to \pi^\pm\gamma$ $[\times 10^4]$	5.03 ± 0.03	4.5 ± 0.5
$\rho \to \eta\gamma$ $[\times 10^4]$	3.05 ± 0.04	2.95 ± 0.30
$\eta' \to \rho\gamma$ $[\times 10^2]$	33.3 ± 1.0	29.4 ± 0.9
$K^{*\pm} \to K^\pm\gamma$ $[\times 10^4]$	9.8 ± 0.9	9.9 ± 0.9
$K^{*0} \to K^0\gamma$ $[\times 10^3]$	2.26 ± 0.02	2.31 ± 0.20
$\omega \to \pi^0\gamma$ $[\times 10^2]$	8.23 ± 0.04	$8.9^{+0.27}_{-0.23}$ $(*)$
$\omega \to \eta\gamma$ $[\times 10^4]$	6.60 ± 0.09	4.9 ± 0.5 $(*)$
$\eta' \to \omega\gamma$ $[\times 10^2]$	3.14 ± 0.10	3.03 ± 0.31
$\phi \to \pi^0\gamma$ $[\times 10^3]$	1.24 ± 0.07	1.25 ± 0.07
$\phi \to \eta\gamma$ $[\times 10^2]$	1.292 ± 0.025	1.301 ± 0.024
$\phi \to \eta'\gamma$ $[\times 10^4]$	0.60 ± 0.02	0.62 ± 0.07
$\eta \to \gamma\gamma$ $[\times 10^2]$	35.50 ± 0.56	39.38 ± 0.26
$\eta' \to \gamma\gamma$ $[\times 10^2]$	2.10 ± 0.06	2.12 ± 0.14
$\rho \to e^+e^-$ $[\times 10^5]$	5.56 ± 0.06	4.70 ± 0.08 $(**)$
$\omega \to e^+e^-$ $[\times 10^5]$	7.15 ± 0.13	7.18 ± 0.12
$\phi \to e^+e^-$ $[\times 10^4]$	2.98 ± 0.05	2.97 ± 0.04
$\omega \to \pi^+\pi^-$ $[\times 10^2]$	1.13 ± 0.08	1.70 ± 0.27 $(**)$
$g_{\omega\pi^+\pi^-}$ phase [degr]	101.2 ± 1.6	104.7 ± 4.1 $(**)$ [50]
$\phi \to \pi^+\pi^-$ $[\times 10^5]$	7.14 ± 1.7	7.3 ± 1.3
$g_{\phi\pi^+\pi^-}$ phase [degr]	-27.0 ± 0.5	-34 ± 5 [71]
$\phi \to K^+K^-$ $[\times 10^2]$	50.3 ± 1.0	49.2 ± 0.6 $(**)$
$\phi \to K^0_S K^0_L$ $[\times 10^2]$	33.0 ± 0.7	34.0 ± 0.5 $(**)$

The numerical estimates of branching fractions have been calculated using the information returned by the MINOS program and taking into account the parameter error covariance matrix in the standard way (as recalled in Sect. 7.3 of [16], for instance). This is mandatory as some error correlation coefficients are very large, namely those among the two fit parameters hidden inside $\epsilon_1(s)$, or inside $\epsilon_2(s)$ are about 95%. Most other error correlation matrix elements are below the 10% level. We therefore consider that our error estimates are accurate.

On the other hand, all partial width results we compute have been derived using the accepted values for all vector and pseudoscalar meson masses [54]. In order to produce the branching ratios as given in Table 4, we have also divided these partial widths by the accepted total widths reported in the latest issue of the Review of Particle Properties [54]. The errors on masses and widths have been taken into account in the computer code used in order to derive the reconstructed branching ratios.

12.3.1 Radiative decays of light mesons

The fit values for the branching fractions of light mesons radiative decays are displayed on top of Table 4. Most de-

cay modes involving vector mesons are in nice correspondence with their recommended values [54].

The value returned for the $\omega \to \pi^0\gamma$ branching ratio is about 3σ from the presently recommended value [54], but is in good agreement with the former recommended value ($(8.5 \pm 0.5) \times 10^{-2}$) as well as the value found in the fit of the $e^+e^- \to \pi^0\gamma$ reported in [74] ($(8.39 \pm 0.25) \times 10^{-2}$). This indicates that the recommended central value for this decay mode can be questioned.

On the other hand, as already commented upon, the branching fraction found for $\omega \to \eta\gamma$ is in much better agreement with the average value proposed by the PDG in [54] ($(6.3 \pm 1.3) \times 10^{-4}$) than their so-called fit value reported in Table 4; this result is also in perfect agreement with the Crystal Barrel [87] measurement ($(6.6 \pm 1.7) \times 10^{-4}$) as well as the measurement obtained in a fit to the $e^+e^- \to \eta\gamma$ cross section [74] ($(6.56 \pm 2.5) \times 10^{-4}$). We also consider confidently our result for this decay mode.

The ratio

$$\frac{\Gamma(\omega \to \eta\gamma)}{\Gamma(\omega \to \pi^0\gamma)} = (0.802 \pm 0.011) \times 10^{-2} \qquad (49)$$

only weakly depends on the mass and width definitions of the ω meson and is in agreement with all reported direct measurements in the RPP [54]. This also gives support to both fit results.

The contribution of the $\eta' \to \rho^0\gamma$ mode to the χ^2 is 2.23, while all others are smaller or of order 1. This may indicate that the box anomaly [85, 88] shows up and might have been accounted for.

The only difficult point of the model is the $\simeq 1.9\sigma$ departure of the partial width for $\eta \to \gamma\gamma$ from the expected value commented upon at the beginning of this section. Whether this could be due to our assuming that the pion decay constant is not affected by isospin symmetry breaking effects is an open possibility. Instead, the partial width for $\eta' \to \gamma\gamma$ fits nicely its expected value, possibly because of its larger experimental uncertainty[26].

Finally, we should note that our model gives a precise indirect measurement of f_K/f_π:

$$\left[\frac{f_K}{f_\pi}\right]^2 = 1.503 \pm 0.010_{\rm stat} \pm 0.002_{\rm model} \Longrightarrow$$
$$\frac{f_K}{f_\pi} = 1.226 \pm 0.004_{\rm stat} \pm 0.001_{\rm model}\,, \qquad (50)$$

where the second quoted uncertainty reflects details of the model together with the effects of including the spacelike data in the fit. This is in balance with the corresponding quantity that can be derived from the reported world average data [54] as $f_K/f_\pi = 1.223 \pm 0.010$, assuming that the errors on f_π and f_K are uncorrelated.

[26] In order to test this assumption, we have left f_{π^0} free in our fits and, for $f_{\pi^0} = 87.9 \pm 2.4$ MeV, we have reached a probability slightly above 80%, with $\Gamma(\eta \to \gamma\gamma)$ at 0.55σ from its recommended value [54] and $\Gamma(\eta' \to \gamma\gamma)$ at only 0.37σ. This has to be compared with the reported value extracted from $\Gamma(\pi^0 \to \gamma\gamma)$, which provides $f_{\pi^0} = 91.92 \pm 3.54$ MeV.

12.3.2 Leptonic decays of light vector mesons

Table 4 indicates that our model nicely accommodates the $\omega \to e^+e^-$ and $\phi \to e^+e^-$ partial widths, giving values that coincide with their recommended values [54].

Our result for $\rho^0 \to e^+e^-$ is derived from the same data as the ones that underlie the other proposed values [54] and has been obtained with a careful account of all statistical and systematic reported errors. Therefore, this value can be confidently considered; one should note that it exhibits a $\simeq 10\sigma$ distance to the presently accepted branching fraction [54]. More straightforward information coming out of our fits is the corresponding partial width:

$$\Gamma(\rho \to e^+e^-) = (8.34 \pm 0.10 \pm 0.31) \times 10^{-3}\,\text{MeV}\,, \qquad (51)$$

where the first error merges all statistical and systematic uncertainties commented upon in the body of the text; the second error takes into account the real uncertainty affecting the ρ mass used in order to derive the partial width from the coupling. It has conservatively been fixed to 10 MeV for reasons that will become clearer shortly. The corresponding partial width as given in [54] is $(7.02 \pm 0.11) \times 10^{-3}$ MeV.

12.3.3 The $\omega/\phi \to \pi^+\pi^-$ decays

The value found for the $\phi \to \pi^+\pi^-$ partial width compares well with its measured value [71]. Actually, one may suspect that this datum prominently influences some of our free parameters; certainly those in the expression for $\epsilon_1(s)$. The phase of the corresponding coupling constant being close enough (1.4σ) to expectation [71] might indicate that the data (modulus and phase) for this mode carry small systematic uncertainties.

The branching fraction we get for the $\omega \to \pi^+\pi^-$ mode is more appealing. It is derived from all data involved in this measurement with a precise account of all systematic uncertainties. In addition, the quality of the measurement we propose probably does not suffer from significant model uncertainties, as the ρ–ω interference region is quite well described (see the insets in Fig. 2). Therefore, our conclusion for this decay mode is either of

$$\text{Br}(\omega \to \pi^+\pi^-) = (1.13 \pm 0.08)\,\%\,,$$
$$\Gamma(\omega \to \pi^+\pi^-) = (9.59 \pm 0.80) \times 10^{-2}\,\text{MeV}\,, \qquad (52)$$

using the recommended value for width and the mass of the ω meson [54].

This new datum may influence the global fit of all the ω decay modes in isolation. This is of concern for our purpose, as one has noticed that the disagreements observed between the PDG recommended values [54] and our results for the $VP\gamma$ modes refer mostly to the $\omega \to (\eta/\pi^0)\gamma$ branching ratios. Along this line, our fit solution yields

$$\frac{\Gamma(\omega \to \pi^+\pi^-)}{\Gamma(\omega \to \pi^0\gamma)} = 0.14 \pm 0.01\,, \qquad (53)$$

to be compared with the single existing measurement by KLOE [89], which provided 0.20 ± 0.04 and a 1.5σ distance. Therefore, our surprising estimate of the two pion mode together with radiative decays is in accord with experimental expectations.

Finally, the unfit Orsay phase for the coupling $\omega \to \pi^+\pi^-$ is found to be close to its expected value from a stand-alone fit to the so-called old timelike data [50], while our fit for the phase of the $\phi \to \pi^+\pi^-$ coupling is in good agreement with its measured value [71].

12.3.4 The $\phi \to K\overline{K}$ decays

As explained in the body of the text, we have been led to leave both $\phi \to K\overline{K}$ decay widths outside our fit procedure, as there is some uncertainty with possible factors, like Coulomb corrections, which may affect the usual coupling constant contributions to both partial widths[72, 73, 90].

Therefore, the values reported in Table 4 are predictions only influenced by the other decay modes and without any additional correction factor to each of the $\phi \to K\overline{K}$ branching ratios. The numerical values found for these branching ratios clearly illustrate that our model is overconstrained and provides precise values for the coupling constants of both $\phi \to K\overline{K}$ modes.

The ratio of the prediction to the recommended central values is 1.022 for the charged mode (i.e. a 1.8σ distance) and 0.97 for the neutral decay mode (i.e. a 2.0σ distance). Taking into account the model uncertainty reported in Table 4, the agreement could be considered as satisfactory.

Now, if correction factors have to be applied, they are expected to improve the prediction for the rates. Therefore, they should be of the order 0.976 and 1.031 for, respectively, the charged and neutral decay widths. This clearly invalidates the traditional 1.042 correction factor proposed in order to account for Coulomb interaction among the charged kaons[27].

Correcting both modes as argued in [73], even if one is able to provide a good account for the ratio $\Gamma(\phi \to K^+K^-)/\Gamma(\phi \to K^0\overline{K}^0)$, this does not allow for a good account of both modes separately, as the corrections proposed turn out to increase the expected rate for both modes.

Within the framework of our model, if correction factors have to be applied, they should not increase the charged decay mode by more than $\simeq 1\%$. There is more freedom with the neutral decay mode. Therefore, in order to fix one's ideas, one has to vary only a correction factor for the neutral decay mode. In this case, of course, the correction factor ($= 1.047 \pm 0.024$) is found such that the neutral mode exactly coincides with its measured value, which could be expected beforehand. However, more interesting is that the χ^2 contribution of the charged decay mode (which does not explicitly depend on this factor) is only 0.3 (a 0.5σ effect). This indeed confirms that only the predicted neutral decay width might have to be corrected significantly. Taking into account that systematic effects are harder to estimate for the charged mode than for the neutral one (see footnote 16 in [16]), this may look like a physical effect. Whether the "mixed isoscalar and isovector source" scheme of [90] can account for such an effect would be interesting to explore.

As a summary, our analysis tends to disfavor a significant correction factor to the $\phi \to K^+K^-$ decay width (above the 1.01 level). It would rather favor a significant correction factor for only the neutral mode $\phi \to K^0\overline{K}^0$ (which could be as large as 1.047 for the rate). If the traditional scheme of Coulomb corrections should really apply, both measured widths for $\phi \to K\overline{K}$ are hard to understand, as already stated in [16, 72].

12.3.5 What are the ρ parameters?

For objects as broad as the ρ (or K^*) meson, the definition for mass and width (from experimentally accessible information) is not a trivial matter [53], and no physically motivated uniqueness statement can be formulated. Having defined in our model the ρ^0 and $\rho^\pm$ propagators as analytic functions (or rather meromorphic functions on a two-sheeted Riemann surface with branch point at threshold), one has at one's disposal the poles of the propagators. This has been shown to provide the most stable definition of the mass and width [53]. If one assumes that analyticity of the S-matrix elements is a basic principle, this is also the most model independent definition. Indeed, whatever are the working assumptions, the pole basically tells where the peak is really located and how wide is the invariant mass distribution around the peak (typically, close to the full width at half maximum). Obviously, any given model cannot successfully describe the relevant data without having the pole located at the place requested by the data. The specific character of a given model is basically concentrated in the regular part of the Laurent expansion of the amplitude. To be complete, departures from this statement may exist but (parameter, model) freedom is essentially governed by the magnitude of the experimental error bars.

However, based on the expectation that the mass difference between charged and neutral ρ mesons is only of the order of a few MeV at most (i.e. $\delta m_\rho \simeq$ a few $10^{-3} m_\rho$), one may guess that this difference could be less sensitive to the mass definitions.

Our final results for the complex s locations of the ρ meson poles can be derived from our fit parameter values. Sampling them by taking into account the parameter error covariance matrix, one gets

$$\begin{cases} s_{\rho^0} = (0.5782 - \mathrm{i}0.1099) \pm (0.9 + \mathrm{i}0.5) \times 10^{-3}\,(\mathrm{GeV}^2)\,, \\ s_{\rho^\pm} = (0.5760 - \mathrm{i}0.1095) \pm (1.0 + \mathrm{i}0.5) \times 10^{-3}\,(\mathrm{GeV}^2)\,, \\ s_{\rho^0} - s_{\rho^\pm} = (2.26 - \mathrm{i}0.38) \times 10^{-3} \\ \qquad\qquad \pm (0.83 + \mathrm{i}0.14) \times 10^{-3}\,(\mathrm{GeV}^2)\,, \end{cases} \tag{54}$$

with uncertainties folding all reported statistical and systematic errors.

[27] See [72] for a detailed account of the usual way to deal with Coulomb corrections and isospin symmetry breaking effects in ϕ decays.

In order to compare with related information available in the literature, one has to relate the ρ pole locations with the usual M_ρ and Γ_ρ.

Defining [56] $s_{\rm R} = M_{\rm R}^2 - {\rm i}M_{\rm R}\Gamma_{\rm R}$, one gets

$$\begin{cases} M_{\rho^0} = 760.4 \pm 0.6\,{\rm MeV}\,, \\ \Gamma_{\rho^0} = 144.6 \pm 0.6\,{\rm MeV}\,, \\ M_{\rho^\pm} = 758.9 \pm 0.6\,{\rm MeV}\,, \\ \Gamma_{\rho^\pm} = 144.3 \pm 0.5\,{\rm MeV}\,, \\ M_{\rho^0} - M_{\rho^\pm} = 1.51 \pm 0.53\,{\rm MeV}\,, \\ \Gamma_{\rho^0} - \Gamma_{\rho^\pm} = 0.22 \pm 0.08\,{\rm MeV}\,, \end{cases} \tag{55}$$

which for ρ^0 are slightly larger than those found by [56] using only the so-called old timelike data. One may note that the mass difference is affected by a smaller uncertainty than the masses separately; this effect is even much more pronounced for the width difference. This error shrinking reflects the correlations contained in the parameter error covariance matrix of our fit.

One may also choose [57] $s_{\rm R} = (M_{\rm R} - {\rm i}\Gamma_{\rm R}/2)^2$ and obtain slightly different values (not provided). Defining the mass by the location of the maximum of the distribution and the width by the full width at half maximum cannot be derived easily from (54); they are

$$\begin{cases} M_{\rho^0} = 762.1 \pm 0.6\,{\rm MeV}\,, \\ \Gamma_{\rho^0} = 144.5 \pm 0.6\,{\rm MeV}\,, \\ M_{\rho^\pm} = 760.8 \pm 0.6\,{\rm MeV}\,, \\ \Gamma_{\rho^\pm} = 144.5 \pm 0.5\,{\rm MeV}\,, \\ M_{\rho^0} - M_{\rho^\pm} = 1.22 \pm 0.53\,{\rm MeV}\,, \\ \Gamma_{\rho^0} - \Gamma_{\rho^\pm} = 0.02 \pm 0.08\,. \end{cases} \tag{56}$$

One may consider these values as they are to be in consistency with the way the mass and width for objects like the ω and ϕ mesons are usually defined [54]. The difference between these results and those in (55) could be attributed to the influence of the regular part of the invariant mass distribution, which distorts a little bit the distribution line shape. Finally, in view of (55) and (56), one cannot be really conclusive about the sign of the width difference central value, as it sensitively varies with the parameter definitions (see also footnote 6).

Our mass difference values can be compared with results from other reactions available in the literature [54]. Limiting oneself to the most recent estimates (all with large statistics), one has

$$\begin{cases} m_{\rho^0} - m_{\rho^\pm} = 0.4 \pm 0.7 \pm 0.6\,{\rm MeV} \\ \quad {\rm KLOE\ 2003\ [89],\ 1980\ Kevents}\,, \\ m_{\rho^0} - m_{\rho^\pm} = 1.3 \pm 1.1 \pm 2.0\,{\rm MeV} \\ \quad {\rm SND\ 2002\ [91],\ 500\ Kevents}\,, \\ m_{\rho^0} - m_{\rho^\pm} = 1.6 \pm 0.6 \pm 1.7\,{\rm MeV} \\ \quad {\rm Crystal\ Barrel\ 1999\ [92],\ 600\ Kevents}\,, \end{cases} \tag{57}$$

which compare satisfactorily with our fit results in either of (55) or (56). These experiments analyze the $\pi^+\pi^-\pi^0$ final state produced in e^+e^- annihilations at the ϕ mass [89, 91] or in $p\overline{p}$ annihilations at rest [92] using standard varying width Breit–Wigner shapes for both charged and neutral ρ meson distributions.

The ALEPH Collaboration has also performed a global fit [31] of the e^+e^- Novosibirsk data together with the ALEPH and CLEO τ data sets (as we did) and gets

$$m_{\rho^0} - m_{\rho^\pm} = -2.4 \pm 0.8\,{\rm MeV} \quad {\rm ALEPH\ 2005\ [31]}\,, \tag{58}$$

significantly different from our findings. However, their fit residuals show a s-dependence below $s \simeq 1\,{\rm GeV}^2$ that is absent from our data[28].

The fit results from other experiments shown in (57) are consistent with either sign for $m_{\rho^0} - m_{\rho^\pm}$; our own results favor $m_{\rho^0} - m_{\rho^\pm} > 0$ (with respectively 2.9σ and 2.3σ significance), while naively one may expect the opposite. However, Bijnens and Gosdzinsky [93], analyzing within the ChPT framework all contributions to this mass difference, concluded that

$$-0.4\,{\rm MeV} < m_{\rho^0} - m_{\rho^\pm} < +0.7\,{\rm MeV}\,. \tag{59}$$

All measurements given in (57) are consistent with this mass interval. The ALEPH mass difference is at a 2.5σ distance from the lower bound of (59). Concerning our results, our largest estimate of the mass difference (1.51 ± 0.53) is only at 1.5σ from the upper bound, while our smallest estimate (1.22 ± 0.53) is at 1.0σ from this upper bound[29]. Therefore, awaiting new measurements that may confirm the ALEPH spectrum at the peak location, one may conclude that our fit results are in good agreement with ChPT expectations. From a statistical point of view, this agreement has even been marginally improved compared with the ALEPH best fit result.

If one decides to parametrize the distributions with varying width Breit–Wigner shapes, one would recover more traditional mass values as tabulated in [54]. However, their model dependence (not only their definition dependence) should be stressed. Because of having intricate decay and pion form factor data, it is not easy to perform this check within the present context. However, a good approximation of using varying width Breit–Wigner expressions is to define the ρ masses by

$${\rm Re}\,\left(D_\rho^{-1}\left(M_\rho^2\right)\right) = 0\,, \tag{60}$$

which, by the way, is fulfilled by the standard Gounaris–Sakurai propagator [31, 94]. In this case we get

$$\begin{aligned} M_{\rho^0} &= 774.8 \pm 0.6\,{\rm MeV}\,, \\ M_{\rho^\pm} &= 773.3 \pm 0.7\,{\rm MeV}\,, \\ M_{\rho^0} - M_{\rho^\pm} &= 1.48 \pm 0.50\,{\rm MeV}\,, \end{aligned} \tag{61}$$

which can be compared with standard values for the masses and provide a mass difference in good agreement

[28] Reference [31] does not provide, strictly speaking, the fit residuals, but this can be guessed from Fig. 67 therein.

[29] Comparing with the upper limit is the most favorable case for our results, while comparing with the lower limit is the most favorable case for ALEPH.

with our results above. This definition of the ρ meson parameters is very close to the corresponding ones following from the Gounaris–Sakurai expressions. Then, comparing (61) with the corresponding ALEPH results [31] is a way to exhibit the effect of the additional isospin breaking mechanism we propose.

Going a step further along the same line, one may also choose to define masses by the HK mass values as they come from the Lagrangian[30] and our fit parameters. Then one gets

$$\begin{aligned} M_{\rho^0} &= 782.1 \pm 2.1\,\mathrm{MeV}\,, \\ M_{\rho^\pm} &= 780.4 \pm 2.2\,\mathrm{MeV}\,, \\ M_{\rho^0} - M_{\rho^\pm} &= 1.74 \pm 0.60\,\mathrm{MeV}\,. \end{aligned} \tag{62}$$

This result is also interesting. Indeed, as stated above (see footnote 6), a reasonable breaking of the isospin symmetry at Lagrangian level, while producing a (HK) mass difference between the ρ^0 and $\rho^\pm$ mesons returns $m_{\rho^0} = m_\omega$. As one may think that the HK ω mass is close to the tabulated value [54] ($m_\omega = 782.65 \pm 0.12\,\mathrm{MeV}$), it may have the meaning that the HK mass for the ρ^0 is consistent with the accepted ω mass. For this purpose, it should be noted that the ω mass value used in our fits was fixed at this accepted value and then cannot directly influence the HK value for m_{ρ^0}.

Defining the width using (E.13) and using[31] the HK ρ masses given in (61) one derives the following information for the ρ widths[32]:

$$\begin{aligned} \Gamma_{\rho^0} &= 174.3 \pm 2.0\,\mathrm{MeV}\,, \\ \Gamma_{\rho^\pm} &= 175.0 \pm 2.0\,\mathrm{MeV}\,, \\ \Gamma_{\rho^0} - \Gamma_{\rho^\pm} &= -0.7 \pm 0.2\,\mathrm{MeV}\,, \end{aligned} \tag{63}$$

which are substantially larger than all other definitions and with a difference going in the opposite way compared with above; however, this follows from the most usually employed formula for the two-body decay widths of the ω and ϕ mesons. One may argue that the larger mass and width exhibited by (62) and (63) compared with the usual case is related with our having the HLS parameter a significantly different from 2 (a 3σ effect).

In summary, as far as the ρ meson parameters are concerned, we consider the most relevant information to be the s locations of the poles as given by (54); the definitions of the mass and width using $s_\mathrm{R} = M_\mathrm{R}^2 - \mathrm{i}M_\mathrm{R}\Gamma_\mathrm{R}$, or $s_\mathrm{R} = (M_\mathrm{R} - \mathrm{i}\Gamma_\mathrm{R}/2)^2$, or something else, can be derived algebraically and in some cases have been given.

[30] This has a clear physical meaning: it is the mass of the ρ meson while working at tree level (when possible, as maybe farther inside the spacelike region than we have gone). However, one should keep in mind that, numerically, they are derived from fits using expressions containing the unavoidable self-mass corrections.

[31] We have averaged the pion masses used for the charged ρ width computation.

[32] We tried to decouple $g_{\rho^0\pi\pi}$ from $g_{\rho^\pm\pi\pi}$ by defining $g_{\rho^\pm\pi\pi} = g_{\rho^0\pi\pi} + \delta g$ with δg submitted to the fit. The minimization procedure returned $\delta g = -0.018 \pm 0.014$ and an improvement of the χ^2 of the order 0.5, quite unsignificant.

12.4 A few more comments on the model

In order to justify the change from ideal to physical fields, one should check that the functions in the non-diagonal elements of the R matrix in (17) are small compared to 1 in the relevant invariant mass range. For this purpose, we have had a closer look at the functions

$$\begin{cases} F_{\rho\omega}(s) = \dfrac{\epsilon_1(s)}{\Pi_{\pi\pi}(s) - \epsilon_2(s)}\,, \\ F_{\rho\phi}(s) = \dfrac{\mu\epsilon_1(s)}{(1-z_V)m^2 + \Pi_{\pi\pi}(s) - \mu^2\epsilon_2(s)}\,, \\ F_{\omega\phi}(s) = \dfrac{\mu\epsilon_2(s)}{(1-z_V)m^2 + (1-\mu^2)\epsilon_2(s)}\,, \end{cases} \tag{64}$$

computed with the fit parameter values. These are the entries of the $R(s)$ matrix that defines our transformation from ideal (bare) fields to physical fields.

Figure 7 shows the real and imaginary parts of these functions. They are all small compared to 1 all along the physical region: $|F_{\rho\omega}(s)| \simeq \mathcal{O}(10^{-2})$, $|F_{\rho\phi}(s)| \simeq \mathcal{O}(10^{-2})$ and $|F_{\omega\phi}(s)| \simeq \mathcal{O}(10^{-1})$. As expected, $F_{\omega\phi}(s)$, which does not vanish in the isospin symmetry limit, is larger, and one observes an order of magnitude difference.

$F_{\rho\omega}(s)$ represents the traditional ρ–ω mixing and its behavior translates in our modeling the known large (Orsay) phase by the quasi-vanishing of its real part around m_ω^2. It exhibits around $\sqrt{s} \simeq 0.3\,\mathrm{GeV}$ the two-pion threshold, an unexpected behavior that is actually too small to influence numerically the pion form factor. Whether this local effect should be considered seriously is unclear, taking into account the approximations done in order to work out the model[33]. The important point here is that, even if narrow, the amplitude does not exceed a 10% level there and a few percents all along the physical region (namely the ρ/ω and ϕ peak locations).

$F_{\rho\phi}(s)$ is of the same order of magnitude as $F_{\rho\omega}(s)$ but much smoother all along the physical region; its real and imaginary parts around the ϕ meson mass are comparable ($\simeq 1\%$).

$F_{\omega\phi}(s)$ is more interesting as it represents what is traditionally attributed to a constant mixing angle of a few degrees [8]. It is indeed what is exhibited, as this function is real at m_ω^2 and close to real at m_ϕ^2. However, the numerical values of the mixing angle vary significantly: at the ω mass the angle is 0.45°, while it is 4.64° at the ϕ mass. This tends to indicate that the notion of mixing angle has to be readdressed.

As explained above, the (not too small) magnitude of $F_{\omega\phi}(s)$ could have been inferred from the HLS model, as the transitions between ω_I and ϕ_I follow from (kaon, K^*K and $K^*\overline{K}^*$) loop effects and not from supplementing them with isospin symmetry breaking effects.

[33] This goes along with the remark that one would have preferred a solution for $F_{\rho\omega}(s)$ that vanishes at $s = 0$ as $F_{\rho\phi}(s)$ and $F_{\omega\phi}(s)$ do, even for non-identically vanishing of ϵ_1. This could also be a consequence of working at first order in ϵ_1 and ϵ_2. However, the neglecting of the anomalous loop effects may play some role near $s = 0$.

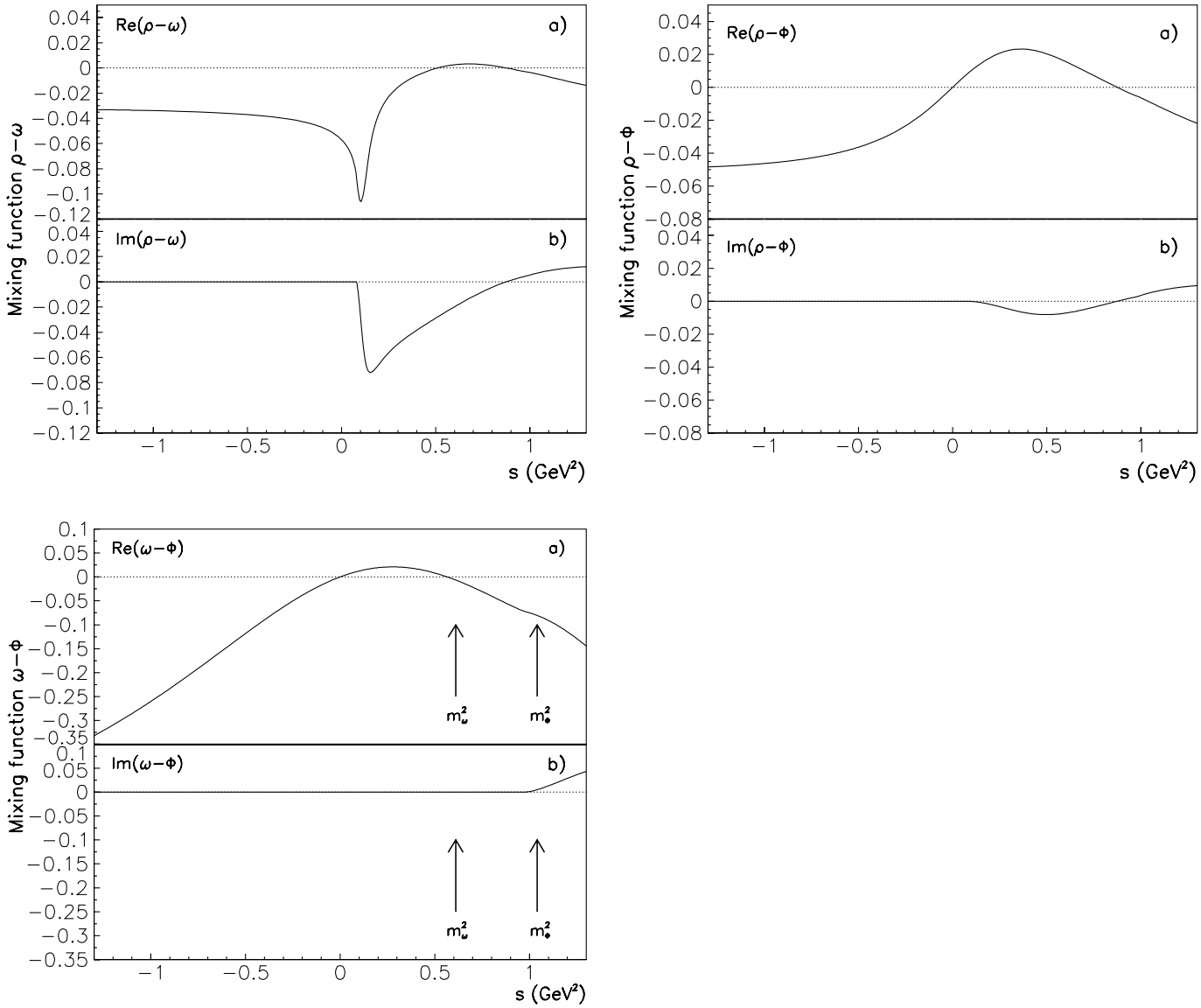

Fig. 7. Matrix elements producing the neutral vector meson mixing. The functions shown are those given in (64) with their name recalled in each figure. The *upper part* of each plot gives the real part of the function, the *lower part* its imaginary part

Figure 8 emphasizes the important features of our model for the pion form factor. The upper plot shows the function

$$H(s) = \frac{|F_\pi^e(s)|^2 - |F_\pi^\tau(s)|^2}{|F_\pi^\tau(s)|^2}\,, \tag{65}$$

which summarizes the breaking of isospin symmetry all along the physical region. The strong effects at the ω and ϕ mass locations could have been expected. However, one clearly sees a non-zero "background" contribution extending down to threshold (and even below) and beyond the ϕ mass. This simply illustrates that our ρ–ω–ϕ mixing scheme is really invariant mass dependent. This is why it can suppress the unwanted effects exhibited by residuals in more standard approaches (see for instance [26, 35, 36]).

The lower plot instead shows

$$H_1(s) = \frac{|F_{\pi,I=1}^e(s)|^2 - |F_\pi^\tau(s)|^2}{|F_\pi^\tau(s)|^2}\,, \tag{66}$$

where $F_{\pi,I=1}^e(s)$ is identified with the ρ^0 part of the pion form factor, as traditionally is done. It clearly exhibits that the ρ^0 and $\rho^\pm$ mesons are different kinds of objects in our modeling. We indeed observe[34] an effect of several percents and functionally s-dependent.

Stated otherwise, the $\rho^\pm$ is indeed a pure isospin 1 meson, while the ρ^0 meson is actually a mixture of isospin 1

[34] The local minimum just above threshold, which reflects the structure of $F_{\rho\omega}(s)$ we discussed, may be an artifact of the model. Its numerical value at this location makes it however totally invisible.

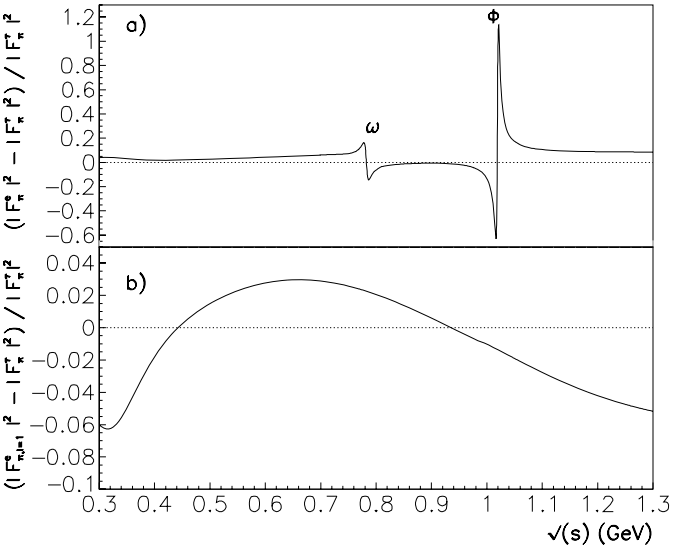

Fig. 8. Isospin symmetry breaking effects following from the ρ^0–ω–ϕ mixing scheme. The *upper plot* shows the difference between $|F_\pi^e(s)|^2$ and $|F_\pi^\tau(s)|^2$ normalized to the latter. The *lower plot* instead shows the ρ part of $|F_\pi^e(s)|^2$

$(\rho_{\rm I}^0)$ and isospin 0 states ($\omega_{\rm I}$ and $\phi_{\rm I}$). A real extraction of the isospin 1 component of $F_\pi^e(s)$ should isolate the isospin 1 part of the ρ, ω, and ϕ amplitudes, which is exactly what our model does, by construction. This allows us to agree with the analysis by Maltman [48, 49], concluding that the ρ part of the pion form factor in the e^+e^- data does not behave as being isospin 1; however, this does not invalidate the e^+e^- data.

Therefore, the single departure from CVC one observes is simply the tiny shift between the ρ^0 and $\rho^\pm$ masses that follows from the ALEPH data.

It also follows from our model that using the τ data in order to reconstruct the equivalent e^+e^- spectrum is not straightforward and requires a non-trivial physics input as shown by both plots in Fig. 8.

One is tempted to think of extending the model in order to include higher mass vector meson nonets. In order to do it properly within the HLS context, one may change in the covariant derivative (see (A.7)) the (presently) single vector term gV to $\sum g_i V_i$. This induces further transition amplitudes like, for instance, $\rho^0(770) \longleftrightarrow \rho^0(1450)$, which may sharply complicate the model. It is not easy to have a feeling for the numerical magnitude of the inter-nonet transitions, as now pion and kaon loops contribute. Moreover, the higher mass vector mesons are in the region where all the thresholds of the VP channels are open. Therefore, one may also have to include the corresponding loops explicitly. Whether the problem will not become numerically intractable is therefore unclear.

For this purpose, one has certainly to notice that the problem we have examined is highly non-linear in the parameters. This makes the search for solutions highly dependent on getting a starting point (in the parameter phase-space) reasonably close to the final solution that the fit procedure may succeed. In the present case, it was already a non-trivial (and highly time consuming) task.

Finally, as is clear from the down most part of Fig. 8, our model predicts a few percent effect for isospin breaking in the resonance region as well as in the low energy region where ChPT applies. Although our pion form factor fit results are good down to the lowest energy points in e^+e^- data (about 360 MeV), it would be interesting to compare with ChPT estimates in this region. Examining this question, the authors of [23] argued that a reliable answer may call for a $\mathcal{O}(p^6)$ estimate, which presently is still missing.

13 Conclusion

Within the context of the HLS model, as for other models, at tree level the so-called ideal fields ($\rho_{\rm I}$, $\omega_{\rm I}$, $\phi_{\rm I}$) are mass eigenstates. This simple picture vanishes at one-loop order. In this case, kaon loops generate non-zero amplitudes allowing $\omega_{\rm I} \longleftrightarrow \phi_{\rm I}$ transitions. Breaking of isospin symmetry in the pseudoscalar sector generates a mass difference between the kaons and, besides, the transition amplitudes $\omega_{\rm I} \longleftrightarrow \rho_{\rm I}$ and $\phi_{\rm I} \longleftrightarrow \rho_{\rm I}$, even if of small magnitude, are no longer vanishing. In addition, these amplitudes exhibit a dependence on s, the square of the momentum flowing through the vector meson lines. As the physical fields ρ, ω and ϕ are expected to be eigenstates of the squared mass matrix, this unavoidably leads one to define them as linear combinations of their ideal partners. However, as the transition amplitudes are s-dependent, it is clear that these combinations should also be s-dependent.

We substantiate these considerations starting from the HLS Lagrangian, modified by including in the squared mass matrix of the neutral vector mesons all self-energies and transition amplitudes. Making the assumption that the physical neutral vector fields should be eigenstates of the loop modified squared mass matrix of the (ideal) neutral vector meson, we solve the eigenvalue problem perturbatively. This leads to physical vector meson fields expressed as linear combinations of their ideal partners with definite s-dependent coefficients, which are actually analytic – or, rather, meromorphic – functions of s. Of course, this algebra leaves unchanged the charged and/or open strangeness sector, as the starting fields acquire a running mass but no transition from one to another meson field.

The main mechanism producing the vector meson field mixing is the occurrence of neutral and charged kaon loops in the transitions between the ideal neutral vector meson fields. We have also shown that the anomalous HLS-FKTUY sector and the Yang–Mills Lagrangian piece provide as supplementing mechanisms the K^*K and $K^*\overline{K}^*$ loops, occurring in transitions in nice correspondence with kaon loops. Within this framework, the $\omega\phi$ mixing has been shown to proceed from quantum (loop) effects, while the $\rho^0\omega$ and $\rho^0\phi$ mixings follow from isospin symmetry breaking effects and vanish when this symmetry is restored. From a numerical point of view, the bulk of the effect is carried more by the subtraction polynomials

than the loop expression themselves, as these are logarithmic functions of small amplitude in the physics region of interest.

The vector meson mixing allows one to dynamically generate isospin violating couplings $\phi\pi^+\pi^-$ and $\omega\pi^+\pi^-$ at the (modified HLS) Lagrangian level. With this at hand, we have been able to construct the pion form factor expression at one-loop order modified in order to account for isospin symmetry breaking through only a dynamically generated $\rho_{\rm I}$–$\omega_{\rm I}$–$\phi_{\rm I}$ mixing scheme. A priori, this fully affects the e^+e^- physics but in no way the τ physics; in this sector, as a second order refinement, we have been led to accept shifting with respect to each other the Higgs–Kibble masses of the ρ^0 and $\rho^\pm$ mesons. This provides a tiny effect; one nevertheless clearly visible in the ALEPH τ data, but not obvious in the CLEO data. New data expected from B-factories may confirm the need for this mass shift. As a final result, we end up with structureless residuals in the fit regions, which confirm that our dynamical mixing scheme is appropriate.

The mixing properties have been introduced in the anomalous decay amplitudes $V \to P\gamma$ and $P \to V\gamma$. These processes actually represent our main lever arm, while defining numerically our isospin breaking scheme.

Beside a good description of the $V \to P\gamma$ and $P \to V\gamma$ decay data, this allows for a very good simultaneous description of all pion form factor data from the close spacelike region to the ϕ mass, in e^+e^- annihilations as well as in τ decays. The physical ground of this result can be traced back to the fact that the ρ^0 meson is a mixture of isospin 0 and 1 states (as the ϕ and ω meson), in contrast to the $\rho^\pm$ meson, which is purely isospin 1. Actually, extracting the isospin 1 part of the pion form factor in e^+e^- annihilations requires one to split up the ρ^0, ϕ and ω contributions. This is done automatically by our model, and one can claim that such a splitting cannot be done without some model.

The net result of this model is the proof that the line shapes for the pion form factor in e^+e^- annihilations and in τ decays are perfectly consistent with each other, without any further breaking of CVC but a possible tiny ρ^0–$\rho^\pm$ mass difference. In a further step, one may include the data from KLOE as well as data expected to come from BaBar and Belle concerning the τ spectrum on the one hand and the e^+e^- initial state radiation samples on the other hand. However, our comparison of the e^+e^- and τ data does not seem to leave room for any kind of new physics.

On the other hand, we have shown that this model allows for a good account of all decays of the form $V \to P\gamma$ and $P \to V\gamma$. The case of the $\omega \to \eta\gamma$ and $\omega \to \pi^0\gamma$ partial widths, where some disagreement is observed with the so-called "fit" values proposed by the PDG, has been discussed and we have argued that the real situation is somewhat unclear.

Our dealing with the pion form factor data has led us to propose improved values for data sharply related with the $e^+e^- \to \pi^+\pi^-$ annihilation process, namely the $\rho^0 \to e^+e^-$ and $\omega \to \pi^+\pi^-$ partial width decays. In both cases, we find that the reference values should be significantly modified and we propose for these cases new reference data.

Finally, we have briefly commented upon the mass and width of the ρ^0 and $\rho^\pm$ mesons and argued that the best motivated definition should rely on the pole position in the complex s-plane and related definitions.

Having shown that the e^+e^- data and τ data are perfectly consistent with each other provided one uses an appropriate model of isospin symmetry breaking, we can conclude that there is no reason to question the e^+e^- data. This result is important as these data serve to estimate numerically the hadronic photon vacuum polarization used in order to predict the value of the muon anomalous magnetic moment $g-2$. Therefore our model indirectly confirms the 3.3σ discrepancy between the BNL direct measurement of the muon anomalous magnetic moment and its theoretical estimate.

Acknowledgements. We gratefully acknowledge S. Eidelman (Budker Institute, Novosibirsk) for information on the Novosibirsk data and their systematics and for several useful and friendly discussions and comments. We also benefited from useful information in order to deal in the most appropriate way with the ALEPH data from A. Höcker (CERN, Geneva) and with the CLEO data from J. Urheim (Indiana University, Bloomington) who also made valuable remarks. We also acknowledge B. Pietrzyk (LAPP, Annecy) and A. Vainshtein (University of Minnesota, Minneapolis) for interesting discussions and comments. M. Davier (LAL, Orsay) has drawn our attention on the photon vacuum polarization effects, we first neglected; we are indebted to him of having provided us with his code for calculating the hadronic photon vacuum polarization in the timelike region before publication. We finally are thankful to H. Burkhardt (CERN, Geneva) for having provided us with the hadronic photon vacuum polarization in the close spacelike region. Both pieces of information have been quite useful to the present work.

Appendix A: The full HLS non-anomalous Lagrangian

The construction of the non-anomalous Lagrangian of the hidden local symmetry (HLS) model has been presented in great detail several times by its authors (see for instance [1] or more recently [2]). Let us simply outline the main steps of the construction procedure.

The HLS model allows one to produce a theory with vector mesons as gauge bosons of a hidden local symmetry. These acquire a mass because of the spontaneous breakdown of a global chiral symmetry $G_{\rm global} = {\rm U}(3)_{\rm L} \otimes {\rm U}(3)_{\rm R}$. The chiral Lagrangian is written

$$\mathcal{L}_{\rm chiral} = \frac{f_\pi^2}{4} {\rm Tr}\left[\partial_\mu U \partial^\mu U\right] , \qquad (A.1)$$

where $U(x) = \exp\left[2{\rm i}P(x)/f_\pi\right]$; here f_π is identified with the pion decay constant ($f_\pi = 92.42\,{\rm MeV}$) and P is the matrix of the pseudoscalar mesons (the Goldstone bosons associated with the spontaneous breakdown of $G_{\rm global}$). The

matrix

$$P = P_8 + P_0 = \frac{1}{\sqrt{2}} \times \begin{pmatrix} \frac{1}{\sqrt{2}}\pi^0 + \frac{1}{\sqrt{6}}\eta_8 + \frac{1}{\sqrt{3}}\eta_0 & \pi^+ & K^+ \\ \pi^- & -\frac{1}{\sqrt{2}}\pi^0 + \frac{1}{\sqrt{6}}\eta_8 + \frac{1}{\sqrt{3}}\eta_0 & K^0 \\ K^- & \overline{K}^0 & -\sqrt{\frac{2}{3}}\eta_8 + \frac{1}{\sqrt{3}}\eta_0 \end{pmatrix} \tag{A.2}$$

contains a singlet term besides the octet term; appropriate combinations of η_8 and η_0 correspond to the physical pseudoscalar fields η and η'. Here and throughout this paper we restrict ourselves to three flavors.

However, besides the global symmetry $G_{\rm global}$, the chiral Lagrangian possesses a local symmetry $H_{\rm local} = {\rm SU}(3)_V$ which is included in the HLS approach by splitting up U as

$$U(x) = \xi_{\rm L}^\dagger \xi_{\rm R}\,, \tag{A.3}$$

where the ξ fields undergo the local transformation. These variables are parametrized as

$$\xi_{\rm R,L} = {\rm e}^{{\rm i}\sigma/f_\sigma} {\rm e}^{\pm {\rm i}P/f_\pi} \tag{A.4}$$

and the scalar field σ is usually eliminated through a gauge choice, and it can be considered absorbed into the gauge bosons and removed. However, the decay constant f_σ goes on appearing in the model through the HLS fundamental parameter $a = f_\sigma^2/f_\pi^2$. Using this parametrization, (A.1) can be rewritten

$$\mathcal{L}_{\rm chiral} = -\frac{f_\pi^2}{4}{\rm Tr}\left[\left(\partial_\mu \xi_{\rm L}\xi_{\rm L}^\dagger - \partial_\mu \xi_{\rm R}\xi_{\rm R}^\dagger\right)^2\right]. \tag{A.5}$$

This Lagrangian can be gauged for electromagnetism, the weak interaction and the hidden local symmetry by changing the usual derivatives ∂_μ to covariant derivatives D_μ [1, 2] and one then gets

$$\begin{cases} \mathcal{L}_{\rm HLS} = \mathcal{L}_A + a\mathcal{L}_V\,, \\ \mathcal{L}_A = -\dfrac{f_\pi^2}{4}{\rm Tr}\left[\left(D_\mu \xi_{\rm L}\xi_{\rm L}^\dagger - D_\mu \xi_{\rm R}\xi_{\rm R}^\dagger\right)^2\right] \equiv -\dfrac{f_\pi^2}{4}{\rm Tr}[L-R]^2\,, \\ \mathcal{L}_V = -\dfrac{f_\pi^2}{4}{\rm Tr}\left[\left(D_\mu \xi_{\rm L}\xi_{\rm L}^\dagger + D_\mu \xi_{\rm R}\xi_{\rm R}^\dagger\right)^2\right] \equiv -\dfrac{f_\pi^2}{4}{\rm Tr}[L+R]^2\,, \end{cases} \tag{A.6}$$

using obvious notation.

Now let us turn to the covariant derivatives. These are given by [2]

$$\begin{cases} D_\mu \xi_{\rm L} = \partial_\mu \xi_{\rm L} - {\rm i}gV_\mu \xi_{\rm L} + {\rm i}\xi_{\rm L}\mathcal{L}_\mu\,, \\ D_\mu \xi_{\rm R} = \partial_\mu \xi_{\rm R} - {\rm i}gV_\mu \xi_{\rm R} + {\rm i}\xi_{\rm R}\mathcal{R}_\mu \end{cases} \tag{A.7}$$

(where we have factored out the universal vector meson coupling constant), with

$$\begin{cases} \mathcal{L}_\mu = {\rm e}QA_\mu + \dfrac{g_2}{\cos\theta_{\rm W}}\left(T_z - \sin^2\theta_{\rm W}\right)Z_\mu \\ \qquad\quad + \dfrac{g_2}{\sqrt{2}}\left(W_\mu^+ T_+ + W_\mu^- T_-\right)\,, \\ \mathcal{R}_\mu = {\rm e}QA_\mu - \dfrac{g_2}{\cos\theta_{\rm W}}\sin^2\theta_{\rm W} Z_\mu\,. \end{cases} \tag{A.8}$$

Equations (A.7) and (A.8) introduce the matrix of the vector meson fields (the gauge bosons of the hidden local symmetry), which is

$$V = \frac{1}{\sqrt{2}}\begin{pmatrix} (\rho^{\rm I} + \omega^{\rm I})/\sqrt{2} & \rho^+ & K^{*+} \\ \rho^- & (-\rho^{\rm I} + \omega^{\rm I})/\sqrt{2} & K^{*0} \\ K^{*-} & \overline{K}^{*0} & \phi^{\rm I} \end{pmatrix} \tag{A.9}$$

in terms of the so-called ideal field combinations (indicated by the superscript I) for the neutral vector mesons, which should be distinguished from the physical fields introduced in the main text. A_μ is the electromagnetic field and e the unit electric charge, g_2 and $\theta_{\rm W}$ are respectively the gauge weak coupling constant and the weak (Weinberg) angle. Z_μ and $W_\mu^\pm$ are, of course the weak gauge boson fields. Q is the quark charge matrix and the T matrices are SU(3) matrices: $Q = 1/3{\rm Diag}(2,-1,-1)$ and $T_z = 1/2{\rm Diag}(1,-1,-1)$, while $T_+ = (T_-)^\dagger$, with

$$T_+ = \begin{pmatrix} 0 & V_{ud} & V_{us} \\ 0 & 0 & 0 \\ 0 & 0 & 0 \end{pmatrix}, \tag{A.10}$$

in terms of elements of the Cabibbo–Kobayashi–Maskawa matrix elements. In this work, the Z_μ terms do not have to be considered; they have been given for completeness. The HLS Lagrangian given above should be completed with the vector meson kinetic energy term [2] but also with the usual free Lagrangian for electromagnetic and weak boson fields. The leptonic sector also has to be added; it is written as per usual

$$\mathcal{L}_{\ell,\nu} = \sum_{\ell=(e,\mu,\tau)}\left[q_\ell \ell^- \gamma^\mu \ell^+ A_\mu - \frac{g_2}{2\sqrt{2}}\overline{\nu}_\ell \gamma^\mu (1-\gamma_5)\ell^- W^+ + \cdots\right]. \tag{A.11}$$

From a practical point of view, g_2 defined above is related with the Fermi constant $G_{\rm F}$ and the W boson mass by

$$g_2 = 2m_W\sqrt{G_{\rm F}\sqrt{2}}\,, \tag{A.12}$$

and it is useful to note that at the τ lepton mass scale one has [54]: $g_2 = 0.629$ (and $e = 0.30286$).

Appendix B: The HLS anomalous sector

QCD admits a non-abelian anomaly that explicitly breaks chiral symmetry. This anomaly is well reproduced by the Wess–Zumino–Witten Lagrangian [95, 96]; this has been incorporated within the HLS context by Fujiwara et al. along with the vector mesons [2, 3]. In this way, it becomes possible to provide a framework that allows one to describe most decays of vector mesons, and especially modes like $\omega \to \pi^+\pi^-\pi^0$ and others more relevant in the present context.

Let us briefly outline the derivation and its assumptions, which have been presented in comprehensive reviews [2, 7, 97]. The anomalous action can be cast in the form

$$\begin{aligned} \Gamma &= \Gamma_{\rm WZW} + \Gamma_{\rm FKTUY}\,, \\ \Gamma_{\rm FKTUY} &= \sum_{i=1}^{4} c_i \int {\rm d}^4x \mathcal{L}_i\,, \end{aligned} \tag{B.1}$$

where $\Gamma_{\rm WZW}$ is the original WZW Lagrangian. The Lagrangian pieces $\mathcal{L}_i$ were first given in [3] and each of them contains $APPP$ and AAP pieces that would contribute to the anomalous decays but are cancelled by APV terms. These Lagrangians contain also $VPPP$ and VVP pieces [2, 3]. A priori, the weighting coefficients c_i are arbitrary. However, in order to reconcile this Lagrangian with decay data, especially $\omega \to \pi^+\pi^-\pi^0$, FKTUY [2, 3] finally chose the following combination:

$$\mathcal{L}^{\rm FKUTY} = -\frac{3g^2}{4\pi^2 f_\pi}\epsilon^{\mu\nu\rho\sigma}{\rm Tr}[\partial_\mu V_\nu \partial_\rho V_\sigma P] - \frac{1}{2}\mathcal{L}_{\gamma PPP}\,, \tag{B.2}$$

which turns out to complement the usual WZW term for the γPPP interaction with only a VVP term. In this model, for instance the decay $\pi^0 \to \gamma\gamma$ occurs solely through $\pi^0 \to \omega\rho^0$ followed by the (non-anomalous) transitions $\omega \to \gamma$ and $\rho^0 \to \gamma$, and the partial width is identical to the current algebra prediction reproduced by $\mathcal{L}_{\gamma\gamma P}$:

$$\mathcal{L}_{\gamma\gamma P} = -\frac{N_{\rm c}e^2}{4\pi^2 f_\pi}\epsilon^{\mu\nu\rho\sigma}\partial_\mu A_\nu \partial_\rho A_\sigma {\rm Tr}[Q^2 P]\,. \tag{B.3}$$

The model given by (B.2) with

$$\mathcal{L}_{\gamma PPP} = -\frac{{\rm i}eN_c}{3\pi^2 f_\pi^3}\epsilon^{\mu\nu\rho\sigma}A_\mu {\rm Tr}[Q\partial_\nu P \partial_\rho P \partial_\sigma P] \tag{B.4}$$

($N_c = 3$) has also been shown [85] to perfectly reproduce the data on $\eta/\eta' \to \pi^+\pi^-\gamma$, especially the most precise ones [88]. Indeed, with no free parameter, the distortion of the ρ line shape is accurately accounted for and this can be considered as the signature for the box anomaly in the experimental data.

Accounting for the light meson radiative decays of the AVP or AAP forms is then a VVP coupling followed by one or two $V \to \gamma$ transition(s). From a practical point of view, it has also been shown [9] that the corresponding couplings can be directly derived from the following Lagrangian piece:

$$\begin{aligned} \mathcal{L} &= C\epsilon^{\mu\nu\rho\sigma}{\rm Tr}[\partial_\mu({\rm e}QA_\nu + gV_\nu)\partial_\rho({\rm e}QA_\sigma + gV_\sigma)P]\,, \\ C &= -\frac{3}{4\pi^2 f_\pi}\,. \end{aligned} \tag{B.5}$$

Let us note that in the meson decays we are interested in the weak boson sector is irrelevant. Finally, one can find the VVP Lagrangian expanded in [8], more precisely in Appendix 1 and 4 for respectively the fully flavor symmetric case and the SU(3)/U(3) broken case[35].

Appendix C: SU(3)/U(3) symmetry breaking of the HLS model

The HLS Lagrangian we are interested in is the lowest order expansion of (A.6) supplemented with (B.5). However, in order to use it with most real data, one cannot avoid defining an appropriate symmetry breaking mechanism. Several breaking schemes have been proposed [4–7] as there is no unique way to implement such a mechanism in the HLS model. We will prefer the method proposed in [6], which looks like the simplest one that automatically fulfills the hermiticity requirement. This symmetry breaking scheme turns out to modify the non-anomalous Lagrangian terms in (A.6) to

$$\begin{cases} \mathcal{L}_A = -\dfrac{f_\pi^2}{4}{\rm Tr}[(L-R)X_A]^2\,, \\ \mathcal{L}_V = -\dfrac{f_\pi^2}{4}{\rm Tr}[L+R)X_V]^2\,, \end{cases} \tag{C.1}$$

where the SU(3) symmetry breaking matrices X_A and X_V can be written

$$\begin{cases} X_A = {\rm Diag}(1, 1, z_A)\,, \\ X_V = {\rm Diag}(1, 1, z_V)\,. \end{cases} \tag{C.2}$$

As the parameter $z_A = [f_K/f_\pi]^2$ is fixed here by kaon decay data, it can hardly be considered as a truly free parameter, even if one allows it to vary within errors [54]: $z_A = 1.495 \pm 0.031$. As shown in the Lagrangian pieces given in the main text, the second breaking parameter, z_V, allows one to shift the ϕ meson mass away from those of the ρ and ω mesons; practically we have more freedom in varying it. The full SU(3) broken HLS Lagrangian produced by this mechanism (without $W^\pm$ interaction terms) has been given in [6]. Using this mechanism, however, the pseudoscalar kinetic energy term of the HLS Lagrangian is no longer canonical and a renormalization of the pseudoscalar fields is required [7]:

$$P' = X_A^{1/2} P X_A^{1/2}\,, \tag{C.3}$$

where P and P' stand respectively for the bare and renormalized pseudoscalar field matrices. With this redefinition, the kinetic energy term of the SU(3) broken Lagrangian is once again canonical. However, the coupling constants to the kaons have to be changed correspondingly by introducing renormalized fields.

With this symmetry breaking mechanism, the realm of practical relevance for the HLS model extends to pions and kaons, as far as pseudoscalar mesons are concerned. In

[35] In Appendix 4, the two breaking parameters ℓ_W and ℓ_T (denoted z_T in the present paper) have been found in this reference to fulfill $\ell_W \ell_T^2 = 1$.

order to bring η and η' mesons into the game, one needs first to define them in terms of the η_8 and η_0 fields, second to extend the breaking scheme from SU(3) to U(3).

We use the traditional one-angle mixing expression:

$$\begin{bmatrix}\eta\\ \eta'\end{bmatrix} = \begin{bmatrix}\cos\theta_P & -\sin\theta_P\\ \sin\theta_P & \cos\theta_P\end{bmatrix}\begin{bmatrix}\pi_8\\ \eta_0\end{bmatrix}. \tag{C.4}$$

It has been shown [11] that the one-angle description was equivalent at the first two leading orders to the two-angle, two-decay constant description, which is in favor since the extended chiral perturbation theory (EChPT) [13–15].

Now the question is how nonet symmetry breaking (NSB) can be incorporated within the (SU(3) broken) HLS Lagrangian already defined. This can be done by means of determinant terms [12] that break the $\mathrm{U}_A(1)$ symmetry:

$$\mathcal{L} = \mathcal{L}_{\mathrm{HLS}} + \frac{\mu^2 f_\pi^2}{12}\ln\det U \ln\det U^\dagger + \lambda\frac{f_\pi^2}{12}\ln\det\partial_\mu U \ln\det\partial^\mu U^\dagger\,, \tag{C.5}$$

where U is defined by (A.3) and (A.4) after removal of the σ field matrix. This can be rewritten more explicitly

$$\mathcal{L} = \mathcal{L}_{\mathrm{HLS}} + \mathcal{L}'_{\mathrm{HLS}} \equiv \mathcal{L}_{\mathrm{HLS}} + \frac{1}{2}\mu^2\eta_0^2 + \frac{1}{2}\lambda\partial_\mu\eta_0\partial^\mu\eta_0\,. \tag{C.6}$$

Therefore, in this manner, one provides both a mass to the singlet and a modification of the kinetic singlet term, which is thus no longer canonical and, then, calls for a renormalization. The exact renormalization relation is given in [11], where it has also been shown that, at leading order, this transformation is equivalent to using the HLS Lagrangian but replacing (C.3) by

$$P'_8 + xP'_0 = X_A^{1/2}(P_8 + P_0)X_A^{1/2} \tag{C.7}$$

(with obvious notation). The nonet symmetry breaking (NSB) mechanism introduces a parameter x that can be related [11] with λ by

$$x = 1 - \frac{\lambda}{2}B^2 \simeq \frac{1}{\sqrt{1+\lambda B^2}} \Longrightarrow \lambda \simeq 0.20\text{–}0.25 \tag{C.8}$$

($B = (2z_A+1)/3z_A$) with a precision better than $\simeq 5\%$.

Therefore one has only to equip the SU(3) broken HLS Lagrangian with the U(3) broken renormalization condition given by (C.7). Reference [11] showed that, at leading order in the breaking parameters one recovers the ChPT expectations.

In order to achieve this general presentation of the broken HLS model, we recall in a few words the breaking procedure of the anomalous Lagrangian. A priori, the transformation to renormalized fields given by (C.7) induces a breaking mechanism into the anomalous HLS Lagrangian given by (B.2) and (B.4). It has been shown [8, 9] that, alone, this breaking scheme (as well as no breaking at all, both) implies that the coupling constant ratio $G_{K^{*0}K^0\gamma}/G_{K^{*\pm}K^\pm\gamma}$ equals 0.5 in sharp disagreement with the experimental data [54]. Interestingly, the nonrelativistic quark model (NRQM) allows for more freedom by exhibiting a dependence of this ratio upon the ratio of the magnetic moments of the quark r [98]:

$$\frac{G_{K^{*0}K^0\gamma}}{G_{K^{*\pm}K^\pm\gamma}} = -\frac{1+r}{2-r}\,. \tag{C.9}$$

In [8, 9], it has been shown that this effect can be obtained by mixing the symmetry breaking scheme proposed by Bramon, Grau and Pancheri (BGP) [4, 5] with some sort of vector field renormalization. In the following appendix, we show that the guess expressed in [8, 9] that a vector field renormalization should take place is justified while having to perform the SU(3) symmetry breaking of the Yang–Mills piece in the HLS Lagrangian.

Numerical analysis implies that these two mechanisms (namely the BGP mechanism and the vector field renormalization) are highly correlated[36] with the neat result that the broken VVP Lagrangian in (B.5) becomes

$$\mathcal{L} = C\epsilon^{\mu\nu\rho\sigma}\mathrm{Tr}\big[X_T\partial_\mu(\mathrm{e}QA_\nu + gV_\nu)X_T^{-2}\partial_\rho(\mathrm{e}QA_\sigma + gV_\sigma) \times X_T P\big]\,, \tag{C.10}$$

with P being replaced by renormalized fields using (C.7) above and V being understood as already renormalized (as a consequence of breaking the SU(3) symmetry of $\mathcal{L}_{\mathrm{YM}}$).

Therefore, the Lagrangian we use in order to account for the anomalous decays is[37] (C.10) with

$$X_T = \mathrm{Diag}(1, 1, \sqrt{z_T})\,, \tag{C.11}$$

where z_T is a parameter to be fit. We should stress that this specific breaking, which allows one to recover (C.9), leaves all other couplings of physical interest (AVP and AAP) unchanged. One should note that, except for (conceptually unavoidable) mixing angles, the model we use introduces only two parameters z_A and z_T in the anomalous sector, the former being essentially fixed by pure kaon physics. Taking into account that our broken anomalous Lagrangian aims at accounting for 14 decay modes, the parameter freedom is actually very limited.

[36] Actually, as stated in [9], imposing that the two-photon decay widths of the η and η' mesons should remain as given by the original Wess–Zumino–Witten Lagrangian [95, 96] provides the functional correlation first found numerically.

[37] Equation (B.4) might also have to be broken similarly. However, the existing data on box anomalies allow for access only to the limited sector $\pi^0/\eta/\eta' \to \pi^+\pi^-\gamma$, not affected by more breaking than reflected by (C.7); it has been shown [85] that (B.4), as it already stands, suffices for satisfactorily accounting for the data. There is therefore no need to go beyond for this term.

Appendix D: The Yang–Mills term of the HLS Lagrangian

The HLS Lagrangian defined in the body of the text should be understood as supplemented with the Yang–Mills piece associated with the vector meson fields [2]. Defining the vector field matrix as given in (A.9) (see Appendix A), this reads [2]

$$\begin{cases} \mathcal{L}_{\rm YM} = -\dfrac{1}{2}{\rm Tr}\left[F_{\mu\nu}F^{\mu\nu}\right] , \\ F_{\mu\nu} = \partial_\mu V_\nu - \partial_\nu V_\mu - {\rm i}g[V_\mu, V_\nu] . \end{cases} \tag{D.1}$$

The square of the abelian part provides the usual kinetic energy term of the vector meson fields and is certainly canonical while working with ideal fields. When performing the field transformation defined by (16) and (17), this piece remains canonical in terms of physical fields, as a trivial consequence of the orthogonality property of the matrix R: $R(s)\widetilde{R}(s) = 1$.

The mixed abelian–non-abelian term contributes to all vector meson self-energies. In addition, it also provides transition amplitudes among the ideal ρ^0, ω and ϕ fields. One can check that these additional contributions to the transition amplitudes only involve $K^*\overline{K}^*$ loops and contribute in the following way to the right-hand sides of (8):

$$\begin{cases} \Pi_{\omega\phi}(s) = \cdots + g_{\phi K^*\overline{K}^*}g_{\omega K^*\overline{K}^*} \\ \qquad\qquad \times \left[\Pi_{K^{*\pm}\overline{K}^{*\mp}}(s) + \Pi_{K^{*0}\overline{K}^{*0}}(s)\right] , \\ \Pi_{\rho\omega}(s) = \cdots + g_{\rho K^*\overline{K}^*}g_{\omega K^*\overline{K}^*} \\ \qquad\qquad \times \left[\Pi_{K^{*\pm}\overline{K}^{*\mp}}(s) - \Pi_{K^{*0}\overline{K}^{*0}}(s)\right] , \\ \Pi_{\rho\phi}(s) = \cdots + g_{\rho K^*\overline{K}^*}g_{\phi K^*\overline{K}^*} \\ \qquad\qquad \times \left[\Pi_{K^{*\pm}\overline{K}^{*\mp}}(s) - \Pi_{K^{*0}\overline{K}^{*0}}(s)\right] , \end{cases} \tag{D.2}$$

still using obvious notation. Quite interestingly, one sees that the transition amplitudes $\Pi_{\omega\phi}(s)$, $\Pi_{\rho\omega}(s)$ and $\Pi_{\rho\phi}(s)$ are modified in such a way that $\omega\phi$ always receives an additional non-vanishing contribution, while the $\rho\omega$ and $\rho\phi$ transitions receive non-vanishing contributions only if isospin symmetry is broken ($m_{K^{*\pm}} \neq m_{K^{*0}}$). One may note the striking correspondence between the Yang–Mills contributions to the transition amplitudes and those already given in (8).

Moreover, taking into account the threshold value of the $K^*\overline{K}^*$ loops, these are certainly real below 1 GeV and their effects can be considered numerically absorbed in the subtraction polynomials we already use. Denoting by M the K^* mass, the amputated $K^*\overline{K}^*$ loop obeys

$${\rm Im}\,\Pi(s) = -\frac{1}{48\pi}\frac{s+3M^2}{M^2}\frac{(s-4M^2)^{3/2}}{s^{1/2}} , \tag{D.3}$$

above the two-K^* threshold. This function can be algebraically derived from the two-pion loop (see Appendix E) and undergoes the same minimum number of subtractions as this.

If no SU(3) breaking is implemented inside $\mathcal{L}_{\rm YM}$, the relevant coupling constants are

$$\begin{cases} G_{\omega K^{*+}K^{*-}} = G_{\rho K^{*+}K^{*-}} = -\sqrt{2}G_{\phi K^{*+},K^{*-}} = -\dfrac{g}{2} , \\ G_{\omega K^{*0}\overline{K}^{*0}} = -G_{\rho K^{*0}\overline{K}^{*0}} = -\sqrt{2}G_{\phi K^{*0}\overline{K}^{*0}} = -\dfrac{g}{2} . \end{cases} \tag{D.4}$$

Finally, tadpole terms may also contribute to the transition amplitudes; they are generated by the non-abelian term squared. One can prove that they follow the same pattern as shown in (D.2) above, namely still contributing to $\Pi_{\omega\phi}(s)$, while contributing to $\Pi_{\rho\omega}(s)$ and $\Pi_{\rho\phi}(s)$ only if isospin symmetry is broken.

Another remark is of interest and concerns the flavor SU(3) symmetry breaking of the Yang–Mills piece. Indeed, as we already performed the flavor SU(3) symmetry breaking of the $\mathcal{L}_A$ and $\mathcal{L}_V$ pieces of the HLS Lagrangian (see (C.1) and (C.2)), we should perform this likewise with $\mathcal{L}_{\rm YM}$. In consistency with our SU(3) symmetry breaking scheme, this should be done as follows:

$$\begin{cases} \mathcal{L}_{\rm YM} = -\dfrac{1}{2}{\rm Tr}[F_{\mu\nu}X_{\rm YM}F^{\mu\nu}X_{\rm YM}] , \\ X_{\rm YM} = {\rm Diag}(1, 1, z_{\rm YM}) . \end{cases} \tag{D.5}$$

It is easy to check that, in order to restore the canonical form of the vector meson kinetic energy term, one has to renormalize the vector fields and define

$$V_\mu = X_{\rm YM}^{-1/2}V_\mu^{\rm Ren}X_{\rm YM}^{-1/2} . \tag{D.6}$$

This change of fields should be propagated to the anomalous Lagrangian. Proceeding in this way and introducing the breaking procedure proposed by Bramon, Grau and Pancheri [5], one indeed ends up with (C.10) in Appendix C [8, 9] with

$$X_T = X_{\rm YM}^{-1/2} . \tag{D.7}$$

In this renormalization, (D.4) remains valid with replacing each $G_{\phi K^*\overline{K}^*}$ by $G_{\phi K^*\overline{K}^*}/z_T$. However, it is interesting to note that the single piece of information in our global data set that is really sensitive to this renormalization is the (charged and neutral) K^* radiative decay. Actually, the vector field renormalization also affects the ideal ϕ meson decay to the $K\overline{K}$ and e^+e^- modes; because of mixing among the ideal fields, this also affects the ω and ρ decays to e^+e^-. However, one can easily convince oneself that the influence of this renormalization is absorbed numerically in the fit value for the parameter z_V.

Appendix E: Radiative and leptonic coupling constants

In order to simplify the main text we prefer to list here the coupling constants entering the decay widths expression that will be treated in this paper. Most of them can be derived trivially from the expressions already given in Appendix E in [9].

E.1 Radiative decays

Starting from the Lagrangian in (C.10), and using the breaking procedure as defined by (C.7), one can compute the coupling constants for all radiative decays of relevance. Let us define

$$G=-\frac{3eg}{8\pi^2 f_\pi}\,,\quad G'=-\frac{3eg}{8\pi^2 f_K}\,,\quad Z=\left[\frac{f_\pi}{f_K}\right]^2=\frac{1}{z_A}\,,$$
$$\delta_P=\theta_P-\theta_0\quad(\tan\theta_0=1/\sqrt{2})\,. \tag{E.1}$$

Some $VP\gamma$ coupling constants are not affected by isospin symmetry breaking:

$$\begin{cases} G_{\rho^\pm\pi^\pm\gamma}=\dfrac{1}{3}G\,,\\ G_{K^{*0}K^0\gamma}=-\dfrac{G'}{3}\sqrt{z_T}\left(1+\dfrac{1}{z_T}\right)\,,\\ G_{K^{*\pm}K^\pm\gamma}=\dfrac{G'}{3}\sqrt{z_T}\left(2-\dfrac{1}{z_T}\right)\,. \end{cases} \tag{E.2}$$

The $\rho_{\rm I}P\gamma$ coupling constants are

$$\begin{cases} G_{\rho_{\rm I}\pi^0\gamma}=\dfrac{1}{3}G\,,\\ G_{\rho_{\rm I}\eta\gamma}=\dfrac{1}{3}G\left[\sqrt{2}(1-x)\cos\delta_P-(2x+1)\sin\delta_P\right]\,,\\ G_{\rho_{\rm I}\eta'\gamma}=\dfrac{1}{3}G\left[\sqrt{2}(1-x)\sin\delta_P+(2x+1)\cos\delta_P\right]\,. \end{cases} \tag{E.3}$$

The other single photon radiative modes provide the following coupling constants:

$$\begin{cases} G_{\omega_{\rm I}\pi^0\gamma}=G\,,\\ G_{\phi_{\rm I}\pi^0\gamma}=0\,,\\ G_{\omega_{\rm I}\eta\gamma}=\dfrac{1}{9}G\left[\sqrt{2}(1-x)\cos\delta_P-(1+2x)\sin\delta_P\right]\,,\\ G_{\omega_{\rm I}\eta'\gamma}=\dfrac{1}{9}G\left[(1+2x)\cos\delta_P+\sqrt{2}(1-x)\sin\delta_P\right]\,,\\ G_{\phi_{\rm I}\eta\gamma}=\dfrac{2}{9}G\left[Z(2+x)\cos\delta_P-\sqrt{2}Z(1-x)\sin\delta_P\right]\,,\\ G_{\phi_{\rm I}\eta'\gamma}=\dfrac{2}{9}G\left[\sqrt{2}Z(1-x)\cos\delta_P+Z(2+x)\sin\delta_P\right]\,. \end{cases} \tag{E.4}$$

In order to go from ideal field couplings to physical vector field couplings, one has to use linear combinations of the couplings in (E.3) and (E.4) weighted by the elements of the transformation matrix $R(s)$ given in the body of the paper.

E.2 $P\gamma\gamma$ and V–γ modes

The two-photon decay modes are not affected by isospin symmetry breaking in the vector sector and keep their usual form within the HLS model [8, 9, 11]:

$$\begin{cases} G_{\eta\gamma\gamma}=-\dfrac{\alpha_{em}}{\pi\sqrt{3}f_\pi}\left[\dfrac{5-2Z}{3}\cos\theta_P-\sqrt{2}\dfrac{5+Z}{3}x\sin\theta_P\right]\,,\\ G_{\eta'\gamma\gamma}=-\dfrac{\alpha_{em}}{\pi\sqrt{3}f_\pi}\left[\dfrac{5-2Z}{3}\sin\theta_P+\sqrt{2}\dfrac{5+Z}{3}x\cos\theta_P\right]\,,\\ G_{\pi^0\gamma\gamma}=-\dfrac{\alpha_{em}}{\pi f_\pi}\,. \end{cases} \tag{E.5}$$

As stated in the text, we actually replace this last coupling by using the world average value for f_π as given in the RPP [54].

Finally, in the non-anomalous sector, the leptonic decay widths of the vector mesons depend on the HLS V–γ couplings. For the ideal combinations, we have

$$\begin{cases} f_{\rho_{\rm I}\gamma}=af_\pi^2 g\,,\\ f_{\omega_{\rm I}\gamma}=\dfrac{f_{\rho_{\rm I}\gamma}}{3}\,,\\ f_{\phi_{\rm I}\gamma}=-\dfrac{f_{\rho_{\rm I}\gamma}}{3}\sqrt{2}z_V\,. \end{cases} \tag{E.6}$$

It was shown in [11] that the pseudoscalar mixing angle is not a free parameter but is related with the SU(3) breaking parameter $Z(=1/z_A)$ and the nonet symmetry breaking parameter x by

$$\tan\theta_P=\sqrt{2}\frac{Z-1}{2Z+1}x\,, \tag{E.7}$$

with a very good accuracy. This relation is used in our fits as a constraint.

E.3 Partial widths

We list for completeness in this section the expressions for the partial widths in terms of the coupling constants for the various cases examined in the text.

The two-photon partial widths are

$$\Gamma(P\to\gamma\gamma)=\frac{m_P^3}{64\pi}|G_{P\gamma\gamma}|^2\,,\quad P=\pi^0,\eta,\eta'\,. \tag{E.8}$$

The leptonic partial widths are

$$\Gamma(V\to e^+e^-)=\frac{4\pi\alpha^2}{3m_V^3}|f_{V\gamma}|^2\,. \tag{E.9}$$

The radiative widths are

$$\Gamma(V\to P\gamma)=\frac{1}{96\pi}\left[\frac{m_V^2-m_P^2}{m_V}\right]^3|G_{VP\gamma}|^2\,, \tag{E.10}$$

where V is either of ρ^0, ω, ϕ and P is either of π^0, η, η', and

$$\Gamma(P\to V\gamma)=\frac{1}{32\pi}\left[\frac{m_P^2-m_V^2}{m_P}\right]^3|G_{VP\gamma}|^2\,. \tag{E.11}$$

The decay width for a vector meson decaying to $V+P$ is

$$\Gamma(V'\to VP) = \frac{1}{96\pi} \times \left[\frac{\sqrt{\left[m_{V'}^2-(m_V+m_P)^2\right]\left[m_{V'}^2-(m_V-m_P)^2\right]}}{m_{V'}}\right]^3 \times |G_{V'VP}|^2 \,. \quad \text{(E.12)}$$

Finally, the partial width for a vector meson decaying into two pseudoscalar mesons of equal masses is

$$\Gamma(V\to PP) = \frac{1}{48\pi}\frac{\left[m_V^2-4m_P^2\right]^{3/2}}{m_V^2}|G_{VPP}|^2 \,. \quad \text{(E.13)}$$

Appendix F: The loop functions

The loop functions can be written quite generally as

$$\Pi(s) = f(s)K(s)+P(s)\,, \quad \text{(F.1)}$$

where $f(s)$ is a polynomial $Q(s)$ divided by some power of s. The degree of the polynomial $P(s)$ is fixed always at second degree and we require $P(0)=0$. We have

$$\begin{cases} \mathrm{Im}\,K(s) = -(s-s_\mathrm{c})^{1/2}(s-s_0)^{1/2} \quad (s\geq s_0)\,, \\ K(s) = c_0+c_1 s+c_2 s^2+\dfrac{s^3}{\pi}\displaystyle\int_{s_0}^{\infty}\frac{\mathrm{Im}\,K(z)}{z^3(z-s+\mathrm{i}\epsilon)}\,\mathrm{d}z\,, \end{cases} \quad \text{(F.2)}$$

where s_0 is the (direct) threshold mass squared, while s_c is the (crossed) threshold mass squared.

F.1 The PP loop

In the case of equal masses, $s_\mathrm{c}=0$ and we have [9]

$$\Pi(s) = \frac{g_{VP\overline{P}}^2}{48\pi}\frac{s-s_0}{s}K(s)+P(s) \quad \text{(F.3)}$$

and the solution is

$$\begin{cases} & \Pi(s) = d_0+d_1 s+Q(s)\,, \\ & Q(s) = \frac{g_{VP\overline{P}}^2}{24\pi^2}\left[G(s)+s_0\right]\,, \\ s\leq 0: & G(s) = \frac{1}{2}\frac{(s_0-s)^{3/2}}{(-s)^{1/2}}\ln\frac{(s_0-s)^{1/2}-(-s)^{1/2}}{(s_0-s)^{1/2}+(-s)^{1/2}}\,, \\ 0\leq s\leq s_0: & G(s) = -\frac{(s_0-s)^{3/2}}{s^{1/2}}\arctan\sqrt{\frac{s}{(s_0-s)}}\,, \\ s\geq s_0: & G(s) = -\frac{1}{2}\frac{(s-s_0)^{3/2}}{s^{1/2}}\left[\ln\frac{s^{1/2}-(s-s_0)^{1/2}}{s^{1/2}+(s-s_0)^{1/2}}\right] \\ & \quad -\frac{\mathrm{i}\pi}{2}\frac{(s-s_0)^{3/2}}{s^{1/2}}\,. \end{cases} \quad \text{(F.4)}$$

The behavior of $\Pi(s)$ near $s=0$ is simply $\mathcal{O}(s)$, and $Q(s)$ behaves like $\mathcal{O}(s)$ near the origin. This result coincides with the one of [9, 52]. By performing more subtractions, one could choose to fix externally the actual s^n behavior of the loop near the origin.

F.2 The PP' loop

In this case, we have

$$\Pi(s) = \frac{g_{VP\overline{P}}^2}{48\pi}\frac{(s-s_0)(s-s_\mathrm{c})}{s^2}K(s)+P(s)\,. \quad \text{(F.5)}$$

Let us define

$$\begin{cases} s\leq s_\mathrm{c}: & \varphi(s) = \frac{1}{\pi}(s_0-s)^{1/2}(s_\mathrm{c}-s)^{1/2} \\ & \quad \times\ln\frac{(s_0-s)^{1/2}-(s_\mathrm{c}-s)^{1/2}}{(s_0-s)^{1/2}+(s_\mathrm{c}-s)^{1/2}}\,, \\ s_\mathrm{c}\leq s\leq s_0: & \varphi(s) = \frac{2}{\pi}(s_0-s)^{1/2}(s-s_\mathrm{c})^{1/2} \\ & \quad \times\arctan\sqrt{\frac{s-s_\mathrm{c}}{s_0-s}}\,, \\ s\geq s_0: & \varphi(s) = \frac{-1}{\pi}(s-s_0)^{1/2}(s-s_\mathrm{c})^{1/2} \\ & \quad \times\left[\ln\frac{(s-s_\mathrm{c})^{1/2}-(s-s_0)^{1/2}}{(s-s_\mathrm{c})^{1/2}+(s-s_0)^{1/2}}\right] \\ & \quad -\mathrm{i}(s-s_0)^{1/2}(s-s_\mathrm{c})^{1/2}\,. \end{cases} \quad \text{(F.6)}$$

The solution for K is obtained by subtracting a polynomial in such a way that the behavior of (F.5) is not singular at the origin:

$$K(s) = \varphi(s)-\left[c_0+c_1 s+c_2 s^2\right]\,, \quad \text{(F.7)}$$

with ($s_0=m_0^2$ and $s_\mathrm{c}=m_c^2$)

$$\begin{cases} c_0 = \dfrac{m_0 m_c}{\pi}\ln\dfrac{m_0-m_c}{m_0+m_c}\,, \\ c_1 = -\dfrac{1}{2\pi}\ln\dfrac{m_0-m_c}{m_0+m_c}\dfrac{(m_0-m_c)^2}{m_0 m_c}\,, \\ c_2 = -\dfrac{1}{8\pi}\left[\dfrac{(m_0^2-m_c^2)^2}{m_0^3 m_c^3}\ln\dfrac{m_0-m_c}{m_0+m_c}+2\dfrac{m_0^2+m_c^2}{m_0^2 m_c^2}\right]\,. \end{cases} \quad \text{(F.8)}$$

The exact behavior for $\Pi(s)$ at the origin is then determined by the choice of $P(s)$.

F.3 The PP' loop in the complex s-plane

The expressions in the two subsections above give the value of the loop functions for any real values of s. It is interesting to know how these functions extend into the complex s-plane, i.e. for complex values of s. It is actually in this manner that the expressions above have been derived. One can check that

$$\varphi(z) = -\frac{\mathrm{i}}{\pi}(z-s_\mathrm{c})^{1/2}(s_0-z)^{1/2} \times\ln\frac{(s_0-z)^{1/2}+\mathrm{i}(z-s_\mathrm{c})^{1/2}}{(s_0-z)^{1/2}-\mathrm{i}(z-s_\mathrm{c})^{1/2}} \quad \text{(F.9)}$$

is – up to a polynomial with real coefficients – the (single) analytic function of z real for $s_c < z < s_0$, having as imaginary part, for real $s > s_0$, $\mathrm{Im}\, K(s)$, which is given by (F.2). The most general solution to (F.2) is then written

$$K(z) = \varphi(z) + P_n(z)\,, \tag{F.10}$$

with a polynomial, $P_n(z)$, with real coefficients chosen in such a way that the behavior at $z = 0$ is the required one. The other coefficients have to be fixed by other external (renormalization) conditions. Equation (F.9) gives the loop function on the so-called physical sheet of the Riemann surface. The expression for $\varphi(z)$ on the unphysical sheet close to the physical region $s > s_0$ is obtained by a winding of 2π radians around the threshold (branch point) $s = s_0$.

F.4 The leptonic loop

In order to compute the photon vacuum polarization, one needs to have at one's disposal the analytic expression of the $\ell^+\ell^-$ loop. More precisely, one needs the ratio of this loop (lepton contribution to the photon self-energy) divided by s, the off-shell photon invariant mass. This can easily be derived from the function $\Pi^0(s)$ given in [99][38] or computed from detailed information from [100]:

$$\Pi(s) = \frac{\alpha}{4\pi}\left[\frac{20}{9} + \frac{4}{3z} - \frac{4(1-z)(1+2z)}{3z}G(z)\right]\,, \tag{F.11}$$

where

$$G(z) = \frac{2u\ln u}{u^2-1}\,, \quad u = \frac{\sqrt{1-1/z}-1}{\sqrt{1-1/z}+1}\,, \quad z = \frac{s}{4m_\ell^2}\,, \tag{F.12}$$

and m_ℓ is the lepton mass and α the fine structure constant.

However, for explicit computation in a minimization code, one needs the explicit expression along the real axis. This is

$$\begin{cases} & \Pi(z) = \frac{\alpha}{4\pi}\left[\frac{20}{9} + \frac{4}{3z} + Q(z)\right]\,, \\ z \le 0: & Q(z) = -\frac{2}{3}\frac{1+2z}{z^2}[-z(1-z)]^{1/2} \\ & \quad \times \ln\frac{(1-z)^{1/2}-(-z)^{1/2}}{(1-z)^{1/2}+(-z)^{1/2}}\,, \\ 0 \le z \le 1: & Q(z) = -\frac{4}{3}\frac{1+2z}{z^2}[z(1-z)]^{1/2} \\ & \quad \times \arctan\sqrt{\frac{z}{1-z}}\,, \\ z \ge 1: & Q(z) = \frac{2}{3}\frac{1+2z}{z^2}[z(z-1)]^{1/2} \\ & \quad \times \left[\ln\frac{z^{1/2}-(z-1)^{1/2}}{z^{1/2}+(z-1)^{1/2}} + \mathrm{i}\pi\right]\,. \end{cases} \tag{F.13}$$

[38] In this reference, the computed loop is actually the quark–antiquark one and therefore the color factor 3 has to be removed.

This function will be summed up with the (parametrized) hadronic vacuum polarization provided to us by Davier [68] and Burkhardt [69] for, respectively, the region above and below the two-pion threshold. The function $\Pi(z)$ just defined is analytic and vanishes at $z = 0$. The term of order α^2 can be derived from the function $\Pi^{(1)}$ given in [99] but is difficult to handle in fitting procedures. Other expressions for the function we use can be found in [62, 101]. Finally, even if possible in principle, we do not have the freedom of subtracting more the function $\Pi(z)$, as conditions at the Z boson mass for the full photon vacuum polarization seem to fix it at zero [65–67].

References

1. M. Bando, T. Kugo, K. Yamawaki, Phys. Rep. **164**, 217 (1988)
2. M. Harada, K. Yamawaki, Phys. Rep. **381**, 1 (2003) [hep-ph/0302103]
3. T. Fujiwara, T. Kugo, H. Terao, S. Uehara, K. Yamawaki, Prog. Theor. Phys. **73**, 926 (1985)
4. A. Bramon, A. Grau, G. Pancheri, Phys. Lett. B **345**, 263 (1995) [hep-ph/9411269]
5. A. Bramon, A. Grau, G. Pancheri, Phys. Lett. B **344**, 240 (1995)
6. M. Benayoun, H.B. O'Connell, Phys. Rev. D **58**, 074006 (1998) [hep-ph/9804391]
7. M. Bando, T. Kugo, K. Yamawaki, Nucl. Phys. B **259**, 493 (1985)
8. M. Benayoun, L. DelBuono, S. Eidelman, V.N. Ivanchenko, H.B. O'Connell, Phys. Rev. D **59**, 114027 (1999) [hep-ph/9902326]
9. M. Benayoun, L. DelBuono, P. Leruste, H.B. O'Connell, Eur. Phys. J. C **17**, 303 (2000) [nucl-th/0004005]
10. P.J. O'Donnell, Rev. Mod. Phys. **53**, 673 (1981)
11. M. Benayoun, L. DelBuono, H.B. O'Connell, Eur. Phys. J. C **17**, 593 (2000) [hep-ph/9905350]
12. G. 't Hooft, Phys. Rep. **142**, 357 (1986)
13. H. Leutwyler, Nucl. Phys. Proc. Suppl. **64**, 223 (1998) [hep-ph/9709408]
14. R. Kaiser, H. Leutwyler (1998) hep-ph/9806336, Pseudoscalar decay constants at large N_c
15. T. Feldmann, Int. J. Mod. Phys. A **15**, 159 (2000) [hep-ph/9907491]
16. M. Benayoun, H.B. O'Connell, Eur. Phys. J. C **22**, 503 (2001) [nucl-th/0107047]
17. H.B. O'Connell, B.C. Pearce, A.W. Thomas, A.G. Williams, Phys. Lett. B **336**, 1 (1994) [hep-ph/9405273]
18. H.B. O'Connell, B.C. Pearce, A.W. Thomas, A.G. Williams, Phys. Lett. B **354**, 14 (1995) [hep-ph/9503332]
19. H.B. O'Connell, B.C. Pearce, A.W. Thomas, A.G. Williams, Prog. Part. Nucl. Phys. **39**, 201 (1997) [hep-ph/9501251]
20. M.J. Iqbal, X.-M. Jin, D.B. Leinweber, Phys. Lett. B **367**, 45 (1996) [nucl-th/9504026]
21. K.L. Mitchell, P.C. Tandy, Phys. Rev. C **55**, 1477 (1997) [nucl-th/9607025]
22. S. Gardner, H.B. O'Connell, Phys. Rev. D **57**, 2716 (1998) [hep-ph/9707385]
23. H.B. O'Connell, K. Maltman, A.W. Thomas, A.G. Williams (1997) hep-ph/9707404, Near-threshold isospin vi-

olation in the pion form factor from chiral perturbation theory
24. M. Hashimoto, Phys. Rev. D **54**, 5611 (1996) [hep-ph/9605422]
25. Muon G-2 Collaboration, G.W. Bennett et al., Phys. Rev. D **73**, 072 003 (2006) [hep-ex/0602035]
26. M. Davier, Nucl. Phys. Proc. Suppl. **169**, 288 (2007) [hep-ph/0701163]
27. CMD-2 Collaboration, R.R. Akhmetshin et al., Phys. Lett. B **578**, 285 (2004) [hep-ex/0308008]
28. CMD-2 Collaboration, R.R. Akhmetshin et al., Phys. Lett. B **648**, 28 (2007) [hep-ex/0610021]
29. CMD-2 Collaboration, R.R. Akhmetshin et al., JETP Lett. **84**, 413 (2006) [hep-ex/0610016]
30. M.N. Achasov et al., J. Exp. Theor. Phys. **103**, 380 (2006) [hep-ex/0605013]
31. ALEPH Collaboration, S. Schael et al., Phys. Rep. **421**, 191 (2005) [hep-ex/0506072]
32. OPAL Collaboration, K. Ackerstaff et al., Eur. Phys. J. C **7**, 571 (1999) [hep-ex/9808019]
33. CLEO Collaboration, S. Anderson et al., Phys. Rev. D **61**, 112 002 (2000) [hep-ex/9910046]
34. M. Davier, S. Eidelman, A. Hocker, Z. Zhang, Eur. Phys. J. C **27**, 497 (2003) [hep-ph/0208177]
35. M. Davier, S. Eidelman, A. Hocker, Z. Zhang, Eur. Phys. J. C **31**, 503 (2003) [hep-ph/0308213]
36. M. Davier, A. Hocker, Z. Zhang, Rev. Mod. Phys. **78**, 1043 (2006) [hep-ph/0507078]
37. W.J. Marciano, A. Sirlin, Phys. Rev. Lett. **71**, 3629 (1993)
38. V. Cirigliano, G. Ecker, H. Neufeld, hep-ph/0109286 (2001)
39. V. Cirigliano, G. Ecker, H. Neufeld, Phys. Lett. B **513**, 361 (2001) [hep-ph/0104267]
40. V. Cirigliano, G. Ecker, H. Neufeld, JHEP **08**, 002 (2002) [hep-ph/0207310]
41. A. Flores-Tlalpa, F. Flores-Baez, G. Lopez Castro, G. Toledo Sanchez, Nucl. Phys. Proc. Suppl. **169**, 250 (2007) [hep-ph/0611226]
42. F. Flores-Baez, A. Flores-Tlalpa, G. Lopez Castro, G. Toledo Sanchez, Phys. Rev. D **74**, 071 301 (2006) [hep-ph/0608084]
43. A. Flores-Tlalpa, G. Lopez Castro, Phys. Rev. D **72**, 113 003 (2005) [hep-ph/0511315]
44. F. Jegerlehner, Acta Phys. Pol. B **38**, 3021 (2007) [hep-ph/0703125]
45. F. Jegerlehner, Nucl. Phys. Proc. Suppl. **131**, 213 (2004) [hep-ph/0312372]
46. F. Jegerlehner, Nucl. Phys. Proc. Suppl. **126**, 325 (2004) [hep-ph/0310234]
47. K. Maltman, C.E. Wolfe, Phys. Rev. D **73**, 013 004 (2006) [hep-ph/0509224]
48. K. Maltman, Phys. Lett. B **633**, 512 (2006) [hep-ph/0504201]
49. K. Maltman, Int. J. Mod. Phys. A **21**, 813 (2006) [hep-ph/0509249]
50. M. Benayoun et al., Eur. Phys. J. C **2**, 269 (1998) [hep-ph/9707509]
51. M. Benayoun, P. David, L. DelBuono, P. Leruste, H.B. O'Connell, Eur. Phys. J. C **29**, 397 (2003) [nucl-th/0301037]
52. F. Klingl, N. Kaiser, W. Weise, Z. Phys. A **356**, 193 (1996) [hep-ph/9607431]
53. M. Benayoun, H.B. O'Connell, A.G. Williams, Phys. Rev. D **59**, 074 020 (1999) [hep-ph/9807537]
54. Particle Data Group, W.M. Yao et al., J. Phys. G **33**, 1 (2006)
55. J.H. Kuhn, A. Santamaria, Z. Phys. C **48**, 445 (1990)
56. A. Bernicha, G. Lopez Castro, J. Pestieau, Phys. Rev. D **50**, 4454 (1994)
57. D. Melikhov, O. Nachtmann, V. Nikonov, T. Paulus, Eur. Phys. J. C **34**, 345 (2004) [hep-ph/0311213]
58. R. Eden, P. Landshoff, D. Olive, J. Polkinghorne, The Analytic S-Matrix (Cambridge Univ. Press, Cambridge, 1966)
59. NA7 Collaboration, S.R. Amendolia et al., Nucl. Phys. B **277**, 168 (1986)
60. F. Byron, R. Fuller, Mathematics of Classical And Quantum Physics (Addison-Wesley Publ. Company, Reading, 1965), Reedition Dover (1992)
61. D. Melikhov, O. Nachtmann, T. Paulus, hep-ph/0209151 (2002)
62. A. Hoefer, J. Gluza, F. Jegerlehner, Eur. Phys. J. C **24**, 51 (2002) [hep-ph/0107154]
63. J. Gluza, A. Hoefer, S. Jadach, F. Jegerlehner, Eur. Phys. J. C **28**, 261 (2003) [hep-ph/0212386]
64. KLOE Collaboration, A. Aloisio et al., Phys. Lett. B **606**, 12 (2005) [hep-ex/0407048]
65. H. Burkhardt, B. Pietrzyk, Phys. Lett. B **356**, 398 (1995)
66. H. Burkhardt, B. Pietrzyk, Phys. Lett. B **513**, 46 (2001)
67. H. Burkhardt, B. Pietrzyk, Phys. Rev. D **72**, 057 501 (2005)
68. M. Davier, private communication
69. H. Burkhardt, private communication
70. I.B. Vasserman et al., Phys. Lett. B **99**, 62 (1981)
71. M.N. Achasov et al., Phys. Lett. B **474**, 188 (2000) [hep-ex/0001048]
72. A. Bramon, R. Escribano, M. José Luis Lucio, G. Pancheri, Phys. Lett. B **486**, 406 (2000) [hep-ph/0003273]
73. E. Fischbach, A.W. Overhauser, B. Woodahl, Phys. Lett. B **526**, 355 (2002) [hep-ph/0112170]
74. M. Benayoun, S.I. Eidelman, V.N. Ivanchenko, Z. Phys. C **72**, 221 (1996)
75. L.M. Barkov et al., Nucl. Phys. B **256**, 365 (1985)
76. A. Quenzer et al., Phys. Lett. B **76**, 512 (1978)
77. S. Eidelman, private communication
78. CMD-2 Collaboration, R.R. Akhmetshin et al., Phys. Lett. B **527**, 161 (2002) [hep-ex/0112031]
79. P. Lichard, M. Vojik, hep-ph/0611163 (2006)
80. E.B. Dally et al., Phys. Rev. Lett. **48**, 375 (1982)
81. Jefferson Lab F(pi), V. Tadevosyan et al., Phys. Rev. C **75**, 055 205 (2007) [nucl-ex/0607007]
82. G. Grayer et al., Nucl. Phys. B **75**, 189 (1974)
83. S.D. Protopopescu et al., Phys. Rev. D **7**, 1279 (1973)
84. J. Urheim, private communication
85. M. Benayoun, P. David, L. DelBuono, P. Leruste, H.B. O'Connell, Eur. Phys. J. C **31**, 525 (2003) [nucl-th/0306078]
86. F. James, M. Roos, Comput. Phys. Commun. **10**, 343 (1975)
87. Crystal Barrel Collaboration, A. Abele et al., Phys. Lett. B **411**, 361 (1997)
88. Crystal Barrel Collaboration, A. Abele et al., Phys. Lett. B **402**, 195 (1997)
89. KLOE Collaboration, A. Aloisio et al., Phys. Lett. B **561**, 55 (2003) [hep-ex/0303016]

90. S. Dubynskiy, A. Le Yaouanc, L. Oliver, J.C. Raynal, M.B. Voloshin, Phys. Rev. D **75**, 113 001 (2007)
91. SND Collaboration, M.N. Achasov et al., Phys. Rev. D **65**, 032 002 (2002) [hep-ex/0106048]
92. Crystal Barrel Collaboration, A. Abele et al., Phys. Lett. B **469**, 270 (1999)
93. J. Bijnens, P. Gosdzinsky, Phys. Lett. B **388**, 203 (1996) [hep-ph/9607462]
94. G.J. Gounaris, J.J. Sakurai, Phys. Rev. Lett. **21**, 244 (1968)
95. J. Wess, B. Zumino, Phys. Lett. B **37**, 95 (1971)
96. E. Witten, Nucl. Phys. B **223**, 422 (1983)
97. U.G. Meissner, Phys. Rep. **161**, 213 (1988)
98. G. Morpurgo, Phys. Rev. D **42**, 1497 (1990)
99. K.G. Chetyrkin, J.H. Kuhn, M. Steinhauser, Nucl. Phys. B **482**, 213 (1996) [hep-ph/9606230]
100. G. Burgers, W. Hollik, CERN 88-06 (Yellow Report) **1**, 136 (1988) [CERN-TH-5131/88]
101. A.B. Arbuzov et al., JHEP **10**, 006 (1997) [hep-ph/9703456]